



Quantification of margins and uncertainties: Conceptual and computational basis

Jon C. Helton*

Department of Mathematics and Statistics, Arizona State University, Tempe, AZ 85287-1804, USA

ARTICLE INFO

Article history:

Received 9 April 2010

Received in revised form

27 January 2011

Available online 14 April 2011

Keywords:

Aleatory uncertainty

Epistemic uncertainty

Performance assessment

Quantification of margins and uncertainties

Risk assessment

Sensitivity analysis

Uncertainty analysis

ABSTRACT

In 2001, the National Nuclear Security Administration of the U.S. Department of Energy in conjunction with the national security laboratories (i.e., Los Alamos National Laboratory, Lawrence Livermore National Laboratory and Sandia National Laboratories) initiated development of a process designated Quantification of Margins and Uncertainties (QMU) for the use of risk assessment methodologies in the certification of the reliability and safety of the nation's nuclear weapons stockpile. This presentation discusses and illustrates the conceptual and computational basis of QMU in analyses that use computational models to predict the behavior of complex systems. The following topics are considered: (i) the role of aleatory and epistemic uncertainty in QMU, (ii) the representation of uncertainty with probability, (iii) the probabilistic representation of uncertainty in QMU analyses involving only epistemic uncertainty, and (iv) the probabilistic representation of uncertainty in QMU analyses involving aleatory and epistemic uncertainty.

© 2011 Elsevier Ltd. All rights reserved.

1. Introduction

In 2001, the National Nuclear Security Administration (NNSA) of the U.S. Department of Energy (DOE) in conjunction with the national security laboratories (i.e., Los Alamos National Laboratory, Lawrence Livermore National Laboratory and Sandia National Laboratories) initiated development of a process designated Quantification of Margins and Uncertainties (QMU) for the use of risk assessment methodologies in the certification of the reliability and safety of the nation's nuclear weapons stockpile [1–6]. Specifically, the following requirements have been proposed [7]:

Design agency assessments shall incorporate QMU methodologies as an essential part of the framework necessary for the evaluation of the performance of warhead and warhead components. QMU can be used as one of the tools for identification and prioritization of actions required for a component or system. Issues that require immediate attention must be raised to the NNSA Office of Stockpile Assessments and Certification. The design agency laboratories shall develop site-appropriate QMU implementation plans. (NNSA-1)

Certification, qualification, and significant finding investigations closure plans shall include QMU methodologies where applicable. Results of assessments using QMU shall be included

in warhead certification documents, component qualification documents, annual assessment reports (AARs) and Significant Finding Investigation (SFI) closure documentation. (NNSA-2)

As indicated by the preceding statements, the NNSA intends for QMU to be an integral component of the assessment process for the nation's nuclear weapons stockpile. However, the preceding statements give no indication of what the NNSA envisions as the conceptual and computational basis for QMU. In this regard, some additional information with respect to the NNSA's intent for QMU is provided by the following definitions supplied in conjunction with the preceding statements [7]:

Quantification of Margins and Uncertainties is a scientific methodology that identifies relevant nuclear-warhead parameters and quantifies, using available experimental and computational tools, the margin of that parameter relative to its failure point and the uncertainties associated with the parameter and the failure point. An assessment of the relationship between the margin and uncertainties facilitates stockpile management decisions, resource allocation prioritization, and informed judgments on the safety, reliability and performance of nuclear warheads. (NNSA-3)

Uncertainty is a best estimate of the range of a particular metric which may derive from one or two broad sources. Uncertainties that reflect a lack of knowledge about the appropriate value to use for a quantity that is assumed to have (missing modifier: *a fixed?*) value in the context of a particular analysis are termed epistemic. Uncertainties that arise from an inherent

* Correspondence address: Department 1545, MS 0748, Sandia National Laboratories, Albuquerque, NM 87185-0748, USA. Tel.: +1 505 284 4808.
E-mail address: jchelto@sandia.gov

randomness in the behavior of the system under study are termed aleatoric. (NNSA-4)

Although designated as definitions, the statements in Quotes (NNSA-3) and (NNSA-4) are at a high level and lack specifics. For example, QMU is defined in Quote (NNSA-3) as a “scientific methodology” but no details are given with respect to what the conceptual basis and resultant computational implementation of this methodology should be. This lack of specificity is consistent with the requirement in Quote (NNSA-1) that “site-appropriate QMU implementation plans” should be developed and has the advantage of allowing QMU to be developed and implemented in manners appropriate for specific analysis contexts. However, this lack of specificity does not exempt individual analyses from a requirement to clearly define their conceptual basis and associated computational implementation. Such definitions are essential if a specific use of QMU is to be considered a “scientific methodology.”

What is unambiguous from Quote (NNSA-3) is that the appropriate treatment of uncertainty is to be an integral part of any implementation of QMU. The nature of uncertainty and the division of uncertainty into epistemic and aleatory components is elaborated on in Quote (NNSA-4). This is an important distinction that can have significant effects on the conceptual basis and computational design of an analysis and also on the interpretation of the results of an analysis.

When viewed at a high level, the application of QMU can be divided into two distinct cases: (i) comparison of experimental results against a requirement without the use of a mathematical model to transform the experimental results, and (ii) comparison of predictions from a mathematical model against a requirement. This presentation is restricted to the second case, and as a result, the presented concepts, computational procedures and discussions should be viewed in the context of comparing model (i.e., computer) predictions with a requirement. In particular, the strictly statistical issues associated with the direct comparison of experimental results with a requirement are not considered.

Although the descriptor “risk assessment” does not appear in Quotes (NNSA-1)–(NNSA-4), the QMU process being described in these quotes is clearly a form of risk assessment in that it involves the determination of consequences (i.e., analysis outcomes and associated margins), likelihoods (i.e., the effects of aleatory uncertainties), and state of knowledge uncertainties (i.e., epistemic uncertainties). Such determinations are the essence of a risk assessment. As a result, the NNSA’s mandate for QMU is a continuation of the extensive and ongoing use of risk assessment in many different areas. As indicated in the following three paragraphs, there is an extensive body of prior studies and techniques that are relevant to the NNSA’s mandated use of QMU.

Risk assessment for complex systems has a long history and many examples relevant to QMU exist, including (i) early studies of missile reliability (Ref. [8], Section 3.2), (ii) the U.S. Nuclear Regulatory Commission’s (NRC’s) assessment of the risk from commercial nuclear power plants, which is known as WASH-1400 after a report number [9], (iii) the NRC’s reassessment of the risk from commercial nuclear power plants, which is known as NUREG-1150 after a report number [10,11], (iv) the NRC’s study of margins in reactor safety [12–18], (v) the NRC’s analysis of the LaSalle Nuclear Power Station as part of its Risk Methods Investigation and Evaluation Program [19], (vi) the DOE’s performance assessment for the Waste Isolation Pilot Plant (WIPP) in support of a successful Compliance Certification Application to the U.S. Environmental Protection Agency (EPA) [20,21], and (vii) the DOE’s performance assessment for the proposed repository for high-level radioactive waste at Yucca Mountain, Nevada, carried out in support of a licensing application to the NRC [22].

The NRC’s WASH-1400 analysis is rightfully considered to be the seminal study in the analysis of complex systems. After its completion, the NRC commissioned a review of the WASH-1400 analysis known as the Lewis Committee Report after the chairman of the review committee [23]. This review was highly complimentary with respect to the overall WASH-1400 analysis but noted that the analysis had inadequately represented the (epistemic) uncertainty in its results. This led to an extensive interest in the appropriate incorporation of epistemic uncertainty into analyses for complex systems and significantly influenced the NRC’s program to develop a risk assessment methodology to assess the geologic disposal of high-level radioactive waste [24–26], the NRC’s development of the MELCOR code system for the analysis of nuclear reactor accidents [27–29], and the design and implementation of the analyses indicated in (iii)–(vii) above. Similarly to the analyses in (iii)–(vii), NNSA’s mandate for QMU is effectively one more descendent of the WASH-1400 analyses and the associated Lewis Committee Report.

Additional information on the development of risk assessment methods for complex systems is available in the excellent review by Rechar [8]. The recent review by Zio is also a valuable source of background and perspectives on risk and reliability analysis for complex systems [30]. Further, the book by Bernstein is highly recommended for a broader perspective on the evolution of the ideas underlying the assessment of risk [31].

The QMU process also quite naturally falls into a broad area of study known as uncertainty and sensitivity analysis, where uncertainty analysis refers to the determination of the uncertainty in analysis results that derives from uncertainty in analysis inputs and sensitivity analysis refers to the determination of the contributions of the uncertainty in individual analysis inputs to the uncertainty in analysis results. The uncertainty being referred to in the preceding sentence is usually of an epistemic nature. Clearly, uncertainty analysis is a fundamental component of QMU; indeed, when viewed broadly, QMU is simply a call for uncertainty analyses focused on margins (i.e., differences between required performance and obtainable performance) associated with the assessment of nuclear weapon reliability and performance. However, sensitivity analysis is also a fundamental part of QMU as indicated by reference to “identification and prioritization of actions” in Quote (NNSA-1) and “assessment of the relationship between margin and uncertainties” in Quote (NNSA-3). Specifically, the indicated actions require a sensitivity analysis to determine the effects of the uncertainty in individual analysis inputs on the uncertainty in analysis results of interest (e.g., margins).

As a result of its fundamental importance in analyses of complex systems, a number of approaches to uncertainty and sensitivity analysis have been developed, including differential analysis [32–37], response surface methodology [38–44], Monte Carlo analysis [29,45–56], and variance decomposition procedures [57–61]. Overviews of these approaches are available in several reviews [62–71]. Of the indicated approaches to uncertainty and sensitivity analysis, sampling-based (i.e., Monte Carlo) approaches are likely to be the most generally useful in QMU analyses. The review by Helton et al. [56] provides an introduction to analyses of this type and also background and additional references for many of the ideas introduced in this presentation.

A number of presentations discussing the QMU process are available [2,72–77]. Of particular importance is the recently published National Academy of Science/National Research Council (NAS/NRC) report, which provides an overview of, and a broad perspective on, QMU at the national security laboratories [77]. However, these presentations tend to be written at a high level and, as a result, lack detail on the conceptual basis and computational organization that must underlie a real QMU analysis if that

analysis is to be a manifestation of a “scientific methodology” as indicated in Quote (NNSA-3).

The purpose of this presentation is to describe the conceptual basis and computational organization of QMU analyses that use models to produce results that are then compared with requirements. The basic idea is that a QMU analysis must start with a clear understanding of the conceptual (i.e., mathematical) model used to represent uncertainty. In turn, this model leads to (i) the manner in which the uncertainty in individual analysis inputs is characterized, (ii) the procedures that are used to propagate uncertainty through the analysis, (iii) the procedures that are available for sensitivity analysis, and (iv) the interpretations and representations that are available for analysis results of interest (e.g., margins). It is important to recognize that in most real analyses there will probably be many results of interest in addition to a single margin that is the outcome of comparing a single calculated result with a single requirement.

The presentation is organized as follows. First, the important concepts of aleatory and epistemic uncertainty are discussed (Section 2). Next, the use of probability in the representation of uncertainty is described and two example problems are introduced that will be used to illustrate different potential QMU analyses (Section 3). Specifically, the first example problem involves only epistemic uncertainty and is used to illustrate QMU analyses that involve only epistemic uncertainty (Section 4). The second example problem involves both aleatory and epistemic uncertainty and is used to illustrate QMU analyses that involve both aleatory and epistemic uncertainty (Section 5). The presentation then ends with a summary discussion (Section 6). The content of this presentation is adapted from Sections 1–5 and 11 of Ref. [78].

For added perspective, additional information on the implementation and interpretation of analyses involving QMU is provided in two companion presentations [79,80]. Specifically, Ref. [79] describes the presence of QMU-type margin analyses in several real, complex and computationally demanding analyses that involve a separation of aleatory and epistemic uncertainty, and Ref. [80] describes alternative mathematical structures for the representation of uncertainty (i.e., interval analysis, possibility theory, evidence theory, and probability theory) and then illustrates the use of these structures with notional QMU analyses involving only epistemic uncertainty and both aleatory and epistemic uncertainty.

2. Types of uncertainty

In the design and implementation of analyses for complex systems, it is useful to distinguish between two types of uncertainty: aleatory uncertainty and epistemic uncertainty [81–93]. The importance of this distinction is recognized by the NNSA in Quote (NNSA-4) and also emphasized in the NAS/NRC report on QMU (Finding 1–3, pp. 22–23, Ref. [77]).

Aleatory uncertainty arises from an inherent randomness in the properties or behavior of the system under study. For example, the weather conditions at the time of a reactor accident are inherently random with respect to our ability to predict the future. Other examples include the variability in the properties of a population of weapon components and the variability in the possible future environmental conditions that a weapon component could be exposed to. Alternative designations for aleatory uncertainty include variability, stochastic, irreducible and type A.

Epistemic uncertainty derives from a lack of knowledge about the appropriate value to use for a quantity that is assumed to have a fixed value in the context of a particular analysis. For example, the pressure at which a given reactor containment would fail for a specified set of pressurization conditions is fixed but not amenable

to being unambiguously defined. Other examples include minimum voltage required for the operation of a system and the maximum temperature that a system can withstand before failing. Alternative designations for epistemic uncertainty include state of knowledge, subjective, reducible and type B.

The appropriate separation of aleatory and epistemic uncertainty is an important component of the design and computational implementation of an analysis of a complex system and also of the decisions that are made on the basis of this analysis. This point can be made with a simple notional example. Suppose an analysis concludes that the probability of a particular component failing to operate correctly is 0.01. Without the specification of additional information, there are two possible interpretations to the indicated probability. The first interpretation, which is inherently aleatoric, is that 1 in every 100 components of this type will fail to operate properly; or, put another way, there is a probability of 0.99 that a randomly selected component will operate properly and a probability of 0.01 that a randomly selected component will not operate properly. The second interpretation, which is inherently epistemic, is that there is a probability of 0.99 that all components of this type will operate properly and a probability of 0.01 that no components of this type will operate properly. Clearly, the implications of the two interpretations of the indicated probability are very different, and as a consequence, any resultant decisions about the system under study can also be expected to be very different.

The analysis of a complex system typically involves answering the following three questions about the system:

- What can happen? (Q1)
- How likely is it to happen? (Q2)
- What are the consequences if it happens? (Q3)

and one additional question about the analysis itself:

- How much confidence exists in the answers to the first three questions? (Q4)

The answers to Questions Q1 and Q2 involve the characterization of aleatory uncertainty, and the answer to Question Q4 involves the characterization of epistemic uncertainty. The answer to Question Q3 typically involves numerical modeling of the system conditional on specific realizations of aleatory and epistemic uncertainty. The posing and answering of Questions Q1 – Q3 gives rise to what is often referred to as the Kaplan–Garrick ordered triple representation for risk [92], which is discussed in more detail in Section 3.7.

The use of probability to characterize both aleatory uncertainty and epistemic uncertainty is described and illustrated in Sections 3–5 and can be traced back to at least the beginning of the formal development of probability theory in the late seventeenth century [31,94,95]. However, as discussed and illustrated in Ref. [80], several alternative mathematical structures for the representation of epistemic uncertainty have been developed in the last several decades. It is possible that some of these alternative structures may be more appropriate than probability in certain contexts for the representation of epistemic uncertainty.

3. Representation of uncertainty with probability

The following topics related to the representation of uncertainty with probability are now introduced: probability spaces, cumulative distribution functions, and complementary cumulative distribution functions (Section 3.1), the basic entities that underlie an analysis that involves a representation of uncertainty

(Section 3.2), analysis in the presence of only epistemic uncertainty (Section 3.3), an example analysis in the presence of only epistemic uncertainty (Section 3.4), analysis in the presence of aleatory and epistemic uncertainty (Section 3.5), an example analysis in the presence of aleatory and epistemic uncertainty (Section 3.6), the Kaplan–Garrick ordered triple representation for risk (Section 3.7), verification and validation (Section 3.8), and an admonition about the importance of a clear specification of concepts in the representation of uncertainty (Section 3.9).

The NAS/NRC report on QMU emphasizes the importance of formal uncertainty quantification (Finding 1–2, p. 20, Ref. [77]). The concepts and mathematical structures introduced in this section are fundamental to such quantification.

3.1. Probability spaces, cumulative distribution functions and complementary cumulative distribution functions

Probability provides the mathematical structure traditionally used to represent both aleatory uncertainty and epistemic uncertainty [81,83,86,89,90]. Formally, a probabilistic characterization of the uncertainty associated with a quantity \mathbf{x} is provided by a probability space $(\mathcal{X}, \mathbb{X}, p_X)$, where (i) \mathcal{X} is the set of all possible values for \mathbf{x} , (ii) \mathbb{X} is a suitably restricted set of subsets of \mathcal{X} for which probability is defined, and (iii) p_X is a function that defines probability for individual elements of \mathbb{X} (i.e., if $\mathcal{U} \in \mathbb{X}$, then $p_X(\mathcal{U})$ is the probability of \mathcal{U}) (Section 4.4, Ref. [96]). Additional discussion of probability spaces is provided in Section 2.4 of Ref. [80].

In practice, a probability space $(\mathcal{X}, \mathbb{X}, p_X)$ is often represented by a density function $d_X(\mathbf{x})$, where

$$p_X(\mathcal{U}) = \int_{\mathcal{U}} d_X(\mathbf{x}) d\mathbf{U} \quad (3.1)$$

for $\mathcal{U} \in \mathbb{X}$. Integrals of the form appearing in Eq. (3.1) are usually taken to be Lebesgue integrals in formal developments of probability theory (e.g., [96,97]). However, for the purposes of this presentation, all presented integrals can be intuitively thought of as corresponding to the Riemann integral of elementary calculus. In computational practice, high-dimensional integrals involving probability spaces are usually evaluated with sampling-based (i.e., Monte Carlo) procedures.

When \mathbf{x} corresponds to a scalar x rather than a vector, a probability space $(\mathcal{X}, \mathbb{X}, p_X)$ can be summarized with a cumulative distribution function (CDF) or a complementary cumulative distribution function (CCDF). Specifically, the CDF and CCDF for x are defined by plots of the points

$$[x, p_X(\mathcal{U}_x)] \text{ and } [x, p_X(\mathcal{U}_x^c)], \quad (3.2)$$

respectively, for $x \in \mathcal{X}$, where

$$\mathcal{U}_x = \{\tilde{x} : \tilde{x} \in \mathcal{X} \text{ and } \tilde{x} \leq x\},$$

$p_X(\mathcal{U}_x)$ = probability of \mathcal{U}_x (i.e., of a value $\tilde{x} \leq x$)

$$= \int_{\mathcal{U}_x} d_X(\tilde{x}) d\tilde{x} = \int_{\mathcal{X}} \delta_X(\tilde{x}) d_X(\tilde{x}) d\tilde{x},$$

$p_X(\mathcal{U}_x^c)$ = probability of \mathcal{U}_x^c (i.e., of a value $\tilde{x} > x$)

$$= \int_{\mathcal{U}_x^c} d_X(\tilde{x}) d\tilde{x} = \int_{\mathcal{X}} \bar{\delta}_X(\tilde{x}) d_X(\tilde{x}) d\tilde{x},$$

$$\delta_X(\tilde{x}) = \begin{cases} 1 & \text{if } \tilde{x} \leq x \\ 0 & \text{otherwise} \end{cases}$$

and

$$\bar{\delta}_X(\tilde{x}) = 1 - \delta_X(\tilde{x}) = \begin{cases} 1 & \text{if } \tilde{x} > x \\ 0 & \text{otherwise} \end{cases}.$$

Further, it is usually assumed for plotting purposes that (i) $p_X(\mathcal{U}_x) = 1$ and $p_X(\mathcal{U}_x^c) = 0$ for $x > \sup(\mathcal{X})$ and (ii) $p_X(\mathcal{U}_x) = 0$ and $p_X(\mathcal{U}_x^c) = 1$ for $x < \inf(\mathcal{X})$.

The results of risk assessments are often summarized with CCDFs because CCDFs provide an answer to the question “How likely is it to be this large or larger?”, which is typically the type of question that risk assessments are intended to answer. In contrast, CDFs answer the question “How likely is it to be this small or smaller?”, which is likely to be the question of primary interest in a margin analysis.

As an example, the CDF and CCDF for x with a loguniform distribution on [2,10] is presented in Fig. 3.1. For this example,

$$d_X(x) = 1/[x \ln(10/2)] = 1/[x \ln(5)], \quad 2 \leq x \leq 10, \quad (3.3)$$

is the corresponding density function, and the probabilities $p_X(\mathcal{U}_x)$ and $p_X(\mathcal{U}_x^c)$ that define the CDF and CCDF are given by

$$p_X(\mathcal{U}_x) = \int_2^x \{1/[\tilde{x} \ln(5)]\} d\tilde{x} = \ln(x/2)/\ln(5) \quad (3.4)$$

and

$$p_X(\mathcal{U}_x^c) = \int_x^{10} \{1/[\tilde{x} \ln(5)]\} d\tilde{x} = \ln(10/x)/\ln(5), \quad (3.5)$$

respectively, for $2 \leq x \leq 10$. In practice, most probability spaces and their associated density functions are too complex to permit simple closed-form representations as shown in Eqs. (3.4) and (3.5); rather, CDFs and CCDFs must be determined through the use of various numerical procedures.

Other summary measures for the distribution of x (i.e., for the probability space $(\mathcal{X}, \mathbb{X}, p_X)$) include the expected value $E_X(x)$ for x , the variance $V_X(x)$ for x , and the q quantile $Q_{Xq}(x)$ for x , where

$$E_X(x) = \int_{\mathcal{X}} \tilde{x} d_X(\tilde{x}) d\tilde{x}, \quad (3.6)$$

$$V_X(x) = \int_{\mathcal{X}} [\tilde{x} - E_X(x)]^2 d_X(\tilde{x}) d\tilde{x}, \quad (3.7)$$

and $Q_{Xq}(x)$ corresponds to the value of x for which

$$q = p_X(\mathcal{U}_x) = \int_{\mathcal{X}} \delta_X(\tilde{x}) d_X(\tilde{x}) d\tilde{x}. \quad (3.8)$$

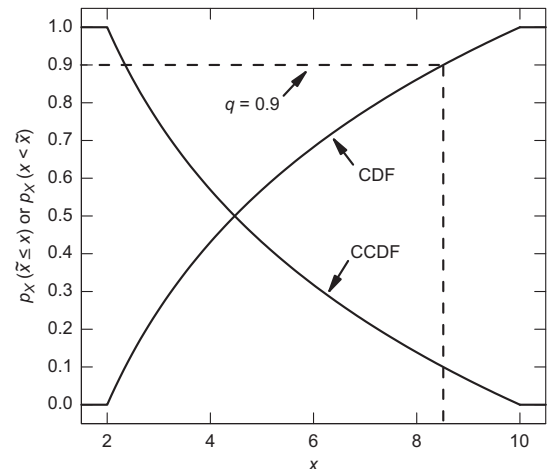


Fig. 3.1. Example CDF and CCDF for variable x with (i) a loguniform distribution on [2,10] and (ii) $p_X(\tilde{x} \leq x)$ and $p_X(\tilde{x} > x)$ used as mnemonics for the probabilities $p_X(\mathcal{U}_x)$ and $p_X(\mathcal{U}_x^c)$ defined in conjunction with Eq. (3.2).

Conceptually, the q quantile $Q_{xq}(x)$ corresponds to the value of x obtained by (i) starting at q on the ordinate of the CDF for x , (ii) drawing a horizontal line to the CDF, and (iii) then drawing a vertical line down to the abscissa. The value for x at the point where the indicated vertical line intersects the abscissa corresponds to the q quantile $Q_{xq}(x)$ for x (Fig. 3.1).

In most analyses, the result of interest is a function

$$\mathbf{y} = f(\mathbf{x}) \quad (3.9)$$

of uncertain analysis inputs. If \mathbf{x} is uncertain as quantified by a probability space $(\mathcal{X}, \mathbb{X}, p_X)$, then \mathbf{y} is also uncertain, with this uncertainty quantified by a probability space $(\mathcal{Y}, \mathbb{Y}, p_Y)$ that derives from the function $f(\mathbf{x})$ and the probability space $(\mathcal{X}, \mathbb{X}, p_X)$ for \mathbf{x} . In concept, it is possible to derive the probability space $(\mathcal{Y}, \mathbb{Y}, p_Y)$. In practice, $(\mathcal{Y}, \mathbb{Y}, p_Y)$ is usually approximated with sampling-based procedures [55,56].

If \mathbf{y} corresponds to a scalar y or y is a component of the vector \mathbf{y} , then the uncertainty in y that derives from the uncertainty in \mathbf{x} is usually represented by a CDF or a CCDF that summarizes the corresponding probability space $(\mathcal{Y}, \mathbb{Y}, p_Y)$ for y . Specifically, the CDF and CCDF for y are defined by plots of the points

$$[y, p_Y(\mathcal{U}_y)] \quad \text{and} \quad [y, p_Y(\mathcal{U}_y^c)], \quad (3.10)$$

respectively, for $y \in \mathcal{Y}$, where

$$\mathcal{U}_y = \{\tilde{y} : \tilde{y} \in \mathcal{Y} \quad \text{and} \quad \tilde{y} \leq y\},$$

$p_Y(\mathcal{U}_y)$ = probability of \mathcal{U}_y (i.e., of a value $\tilde{y} \leq y$)

$$= \int_{\mathcal{X}} \delta_y[f(\mathbf{x})] d_X(\mathbf{x}) d\mathbf{x} \cong \sum_{i=1}^{nSX} \delta_y[f(\mathbf{x}_i)] / nSX = \hat{p}_Y(\mathcal{U}_y),$$

$p_Y(\mathcal{U}_y^c)$ = probability of \mathcal{U}_y^c (i.e., of a value $\tilde{y} > y$)

$$= \int_{\mathcal{X}} \bar{\delta}_y[f(\mathbf{x})] d_X(\mathbf{x}) d\mathbf{x} \cong \sum_{i=1}^{nSX} \bar{\delta}_y[f(\mathbf{x}_i)] / nSX = \hat{p}_Y(\mathcal{U}_y^c),$$

δ_y and $\bar{\delta}_y$ are defined analogously to δ_x and $\bar{\delta}_x$ in conjunction with Eq. (3.2), and $\mathbf{x}_i, i=1, 2, \dots, nSX$, is a sample from \mathcal{X} generated in a manner consistent with the probability space $(\mathcal{X}, \mathbb{X}, p_X)$. The sampling-based (i.e., Monte Carlo) approximations to $p_Y(\mathcal{U}_y)$ and $p_Y(\mathcal{U}_y^c)$ are introduced because, in general, the defining integrals for $p_Y(\mathcal{U}_y)$ and $p_Y(\mathcal{U}_y^c)$ will be high-dimensional and thus too complex for a closed-form or quadrature-based evaluation.

As an example, approximations to the CDF and CCDF for

$$y = f(\mathbf{x}) = x_1^2 + 2x_1x_2 + x_2^2 \quad (3.11)$$

generated with a random sample

$$\mathbf{x}_i = [x_{i1}, x_{i2}], \quad i = 1, 2, \dots, nSX = 100, \quad (3.12)$$

from uniform distributions on [0,2] for x_1 and x_2 are shown in Fig. 3.2.

Similarly to the summary measures for x in Eqs. (3.6)–(3.8), additional summary measures for the distribution of $y = f(\mathbf{x})$ (i.e., for the probability space $(\mathcal{Y}, \mathbb{Y}, p_Y)$) include the expected value $E_Y(y)$ for y , the variance $V_Y(y)$ for y , and the q quantile $Q_{Yq}(y)$ for y , where

$$E_Y(y) = E_X[f(\mathbf{x})] = \int_{\mathcal{X}} f(\tilde{\mathbf{x}}) d_X(\tilde{\mathbf{x}}) d\mathbf{x}, \quad (3.13)$$

$$V_Y(y) = V_X[f(\mathbf{x})] = \int_{\mathcal{X}} [f(\tilde{\mathbf{x}}) - E_X[f(\mathbf{x})]]^2 d_X(\tilde{\mathbf{x}}) d\mathbf{x}, \quad (3.14)$$

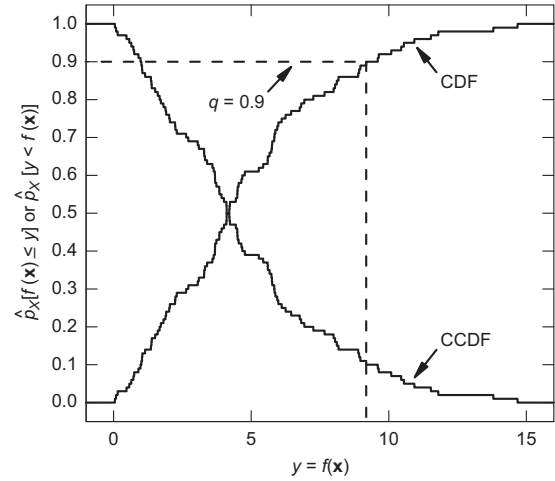


Fig. 3.2. Example CDF and CCDF for $y = f(\mathbf{x}) = x_1^2 + 2x_1x_2 + x_2^2$ generated with (i) a random sample $\mathbf{x}_i = [x_{i1}, x_{i2}]$, $i = 1, 2, \dots, 100$, from uniform distributions on [0,2] for x_1 and x_2 and (ii) $\hat{p}_X[f(\mathbf{x}) \leq y]$ and $\hat{p}_X[y < f(\mathbf{x})]$ used as mnemonics for the estimated probabilities $\hat{p}_Y(\mathcal{U}_y)$ and $\hat{p}_Y(\mathcal{U}_y^c)$ defined in conjunction with Eq. (3.10) to emphasize the dependence of $p_Y(\mathcal{U}_y)$ and $p_Y(\mathcal{U}_y^c)$ on the probability space $(\mathcal{X}, \mathbb{X}, p_X)$.

and $Q_{Yq}(y) = Q_{Xq}(f(\mathbf{x}))$ corresponds to the value of y for which

$$q = p_Y(\mathcal{U}_y) = \int_{\mathcal{X}} \delta_y[f(\tilde{\mathbf{x}})] d_X(\tilde{\mathbf{x}}) d\mathbf{x}. \quad (3.15)$$

In practice, $Q_{Yq}(y)$ is usually approximated by the value y such that

$$q = p_Y(\mathcal{U}_y) \cong \sum_{i=1}^{nSX} \delta_y[f(\mathbf{x}_i)] / nSX, \quad (3.16)$$

where $\mathbf{x}_i, i=1, 2, \dots, nSX$, is a sample from \mathcal{X} generated in a manner consistent with the probability space $(\mathcal{X}, \mathbb{X}, p_X)$ as illustrated in Fig. 3.2. Further, $E_Y(y)$ and $V_Y(y)$ can be approximated in a similar manner with the indicated sample.

3.2. Basic entities underlying an analysis

The posing and answering of Questions (Q1)–(Q4) introduced in Section 2 gives rise to an analysis predicated on three basic entities [98,99]:

A probabilistic characterization of aleatory uncertainty, (EN1)

A model that predicts system behavior, (EN2)

and

A probabilistic characterization of epistemic uncertainty. (EN3)

Formally, EN1 corresponds to a probability space $(\mathcal{A}, \mathbb{A}, p_A)$ for aleatory uncertainty and provides the answers to Questions Q1 and Q2: “What can happen?” and “How likely is it to happen?”; EN2 corresponds to a function f (e.g., the solution of a system of differential or partial differential equations) that determines analysis outcomes of interest and provides the answer to Question Q3: “What are the consequences if it does happen?”; and EN3 corresponds to a probability space $(\mathcal{E}, \mathbb{E}, p_E)$ for epistemic uncertainty and provides the basis for answering Question Q4: “How much confidence exists in the answers to the first three questions?”

The sample space \mathcal{A} for the probability space $(\mathcal{A}, \mathbb{A}, p_A)$ for aleatory uncertainty is a set of the form

$$\mathcal{A} = \{\mathbf{a} : \mathbf{a} = [a_1, a_2, \dots, a_{nA}]\}, \quad (3.17)$$

where each vector \mathbf{a} contains the defining properties (e.g., time, size, location,...) for a single random occurrence associated with the system under study. In practice, $(\mathcal{A}, \mathbb{A}, p_A)$ is usually defined

by specifying probability distributions that characterize the occurrence of the individual components of \mathbf{a} and hence the occurrence of the individual elements of \mathcal{A} . Further, the value of nA (i.e., the dimension of \mathbf{a}) may change for different elements of \mathcal{A} . For example, the elements of \mathcal{A} might be of the form

$$\mathbf{a} = [n, t_1, \mathbf{p}_1, t_2, \mathbf{p}_2, \dots, t_n, \mathbf{p}_n], \quad (3.18)$$

where n is the number of occurrences of a Poisson process over a specified period of time, t_i is the time of the i th occurrence, and \mathbf{p}_i is a vector of properties associated with the i th occurrence. When needed, the density function associated with the probability space $(\mathcal{A}, \mathbb{A}, p_A)$ is represented by $d_A(\mathbf{a})$.

Similarly, the sample space \mathcal{E} for the probability space $(\mathcal{E}, \mathbb{E}, p_E)$ for epistemic uncertainty is a set of the form

$$\mathcal{E} = \{\mathbf{e} : \mathbf{e} = [e_1, e_2, \dots, e_{nE}]\}, \quad (3.19)$$

where each vector \mathbf{e} contains possible values for the nE epistemically uncertain variables under consideration. When needed, the density function associated with the probability space $(\mathcal{E}, \mathbb{E}, p_E)$ is represented by $d_E(\mathbf{e})$.

In practice, $(\mathcal{E}, \mathbb{E}, p_E)$ is usually defined by specifying probability distributions that characterize the epistemic uncertainty associated with the individual components of \mathbf{e} . Specifically, the distributions for the elements of \mathbf{e} are providing a quantitative characterization of degrees of belief based on all available information with respect to where appropriate values of these elements are located for use in the analysis under consideration. The development of these distributions often involves an extensive expert review process [100–106]. The importance of expert review and judgment in the characterization of epistemic uncertainty is specifically recognized in the NAS/NRC report on QMU (Finding 1–5, p. 30, Ref. [77]).

In many analyses, \mathbf{e} has the form

$$\mathbf{e} = [\mathbf{e}_A, \mathbf{e}_M], \quad (3.20)$$

where

$$\mathbf{e}_A = [\mathbf{e}_{A1}, \mathbf{e}_{A2}, \dots, \mathbf{e}_{A,nEA}]$$

is a vector of nEA epistemically uncertain quantities used in the characterization of aleatory uncertainty (e.g., an imprecisely known rate λ that defines a Poisson process) and

$$\mathbf{e}_M = [\mathbf{e}_{M1}, \mathbf{e}_{M2}, \dots, \mathbf{e}_{M,nEM}]$$

is a vector of nEM epistemically uncertain quantities used in the modeling of one or more physical processes (e.g., an imprecisely known thermal conductivity).

In some situations involving margin analyses, it may be appropriate to further decompose \mathbf{e}_M into

$$\mathbf{e}_M = [\mathbf{e}_R, \mathbf{e}_P], \quad (3.21)$$

where \mathbf{e}_R is a vector of epistemically uncertain quantities used in the definition of the requirements that underlie the margins under consideration and \mathbf{e}_P is a vector of epistemically uncertain quantities that correspond to model parameters. The possible presence of epistemic uncertainty in the definition of requirements is specifically recognized by the NNSA in Quote (NNSA-3). Also, the NAS/NRC report on QMU recognizes the possibility of epistemic uncertainty in a requirement in a notional example involving the determination of a margin (pp. 25–26, Ref. [77]).

When \mathbf{e} has the form $\mathbf{e} = [\mathbf{e}_A, \mathbf{e}_M]$ indicated in Eq. (3.20), the analysis in effect has two probability spaces for epistemic uncertainty: a probability space $(\mathcal{E}_A, \mathbb{E}_A, p_{EA})$ that characterizes the uncertainty in \mathbf{e}_A , and a probability space $(\mathcal{E}_M, \mathbb{E}_M, p_{EM})$ that characterizes the uncertainty in \mathbf{e}_M . In turn,

$$\mathcal{E} = \mathcal{E}_A \times \mathcal{E}_M \quad (3.22)$$

is the sample space for the probability space $(\mathcal{E}, \mathbb{E}, p_E)$. In practice, the probability spaces $(\mathcal{E}_A, \mathbb{E}_A, p_{EA})$ and $(\mathcal{E}_M, \mathbb{E}_M, p_{EM})$ are defined by assigning distributions to the components of \mathbf{e}_A and \mathbf{e}_M , respectively, which in effect also defines the probability space $(\mathcal{E}, \mathbb{E}, p_E)$. Although the probability spaces $(\mathcal{E}_A, \mathbb{E}_A, p_{EA})$ and $(\mathcal{E}_M, \mathbb{E}_M, p_{EM})$ are incorporated into the probability space $(\mathcal{E}, \mathbb{E}, p_E)$, it is often convenient to maintain their separate identities for conceptual and notational purposes. When needed, the density functions associated with $(\mathcal{E}_A, \mathbb{E}_A, p_{EA})$ and $(\mathcal{E}_M, \mathbb{E}_M, p_{EM})$ are represented by $d_{EA}(\mathbf{e}_A)$ and $d_{EM}(\mathbf{e}_M)$, respectively. As a reminder, a different probability space $(\mathcal{A}, \mathbb{A}, p_A)$ for aleatory uncertainty with corresponding density function $d_A(\mathbf{a}|\mathbf{e}_A)$ results for each element \mathbf{e}_A of \mathcal{E}_A .

As previously indicated, the probability spaces $(\mathcal{A}, \mathbb{A}, p_A)$ and $(\mathcal{E}, \mathbb{E}, p_E)$ correspond to the Entities EN1 and EN3. In turn, Entity EN2 corresponds to a function of the form

$$\mathbf{y}(t|\mathbf{a}, \mathbf{e}_M) = [y_1(t|\mathbf{a}, \mathbf{e}_M), y_2(t|\mathbf{a}, \mathbf{e}_M), \dots, y_{nY}(t|\mathbf{a}, \mathbf{e}_M)] = \mathbf{f}(t|\mathbf{a}, \mathbf{e}_M), \quad (3.23)$$

where $\mathbf{a} \in \mathcal{A}$, $\mathcal{E} = \mathcal{E}_A \times \mathcal{E}_M$ as indicated in Eq. (3.22), $\mathbf{e}_M \in \mathcal{E}_M$, t corresponds to time with the assumption that time-dependent results are under consideration, and the vertical line in $\mathbf{y}(t|\mathbf{a}, \mathbf{e}_M)$ is used to indicate the concept of “conditional on”. Further, in a QMU analysis, one or more elements of $\mathbf{y}(t|\mathbf{a}, \mathbf{e}_M)$ will either be margins or analysis results used in the definition of margins. In most real analyses, the number of results under consideration (i.e., nY) is likely to be very large. However, for notational simplicity, a real-valued result

$$y(t|\mathbf{a}, \mathbf{e}_M) = f(t|\mathbf{a}, \mathbf{e}_M) \quad (3.24)$$

is assumed to be under consideration.

The uncertainty associated with $y(t|\mathbf{a}, \mathbf{e}_M)$ is often studied in one of two contexts. In the first context, \mathbf{a} is assumed to be fixed, and the uncertainty in $y(t|\mathbf{a}, \mathbf{e}_M)$ that derives from the epistemic uncertainty associated with \mathbf{e}_M is analyzed. In essence, this context involves only the Entity EN2 corresponding to the function $y(t|\mathbf{a}, \mathbf{e}_M)$ and the Entity EN3 corresponding to the probability space $(\mathcal{E}_M, \mathbb{E}_M, p_{EM})$ that characterizes the epistemic uncertainty associated with \mathbf{e}_M . The Entity EN1 corresponding to the probability space $(\mathcal{A}, \mathbb{A}, p_A)$ that characterizes the aleatory uncertainty associated with \mathbf{a} does not enter into the analysis as a result of fixing \mathbf{a} at a specific value.

In the second context, \mathbf{a} is not assumed to be fixed, and the distributions of $y(t|\mathbf{a}, \mathbf{e}_M)$ that derive from the aleatory uncertainty associated with \mathbf{a} characterized by probability spaces $(\mathcal{A}, \mathbb{A}, p_A)$ conditional on specific values for $\mathbf{e} = [\mathbf{e}_A, \mathbf{e}_M]$ are central to the analysis. In this context, all three entities are present, with the analysis involving distributions that derive from epistemic uncertainty for (i) CDFs and CCDFs that derive from aleatory uncertainty or (ii) summary quantities (e.g., expected values, quantiles) for CDFs and CCDFs that derive from aleatory uncertainty. Specifically, each CDF and each CCDF indicated in the preceding sentence derives from aleatory uncertainty conditional on a specific value for $\mathbf{e} = [\mathbf{e}_A, \mathbf{e}_M]$; in turn, the epistemic uncertainty associated with \mathbf{e} and characterized by the probability space $(\mathcal{E}, \mathbb{E}, p_E)$ results in distributions of these CDFs and CCDFs and also in distributions of quantities such as means and variances that summarize these CDFs and CCDFs. The preceding distributions that derive from epistemic uncertainty are the focus of study in this second analysis context.

The two indicated analysis contexts are discussed in the next four sections (Sections 3.3–3.6). However, most large analyses that involve both aleatory uncertainty and epistemic uncertainty will have various subanalyses that involve each of these analysis contexts. Specifically, some subanalyses will be carried out conditional on specific realizations of aleatory uncertainty

(i.e., analyses in the sense of the first context as discussed in Sections 3.3 and 3.4) and some subanalyses will be carried out that address the epistemic uncertainty associated with results that derive from aleatory uncertainty (i.e., analyses in the sense of the second context as discussed in Sections 3.5 and 3.6).

3.3. Analysis in the presence of only epistemic uncertainty

This section presents a formal description of the representation of uncertainty in an analysis that involves only epistemic uncertainty. The following section (Section 3.4) then presents a simple example illustrating the formal concepts presented in the present section. If desired, Section 3.4 can be read before Section 3.3, with Section 3.3 being referred to only when a more technical description of the results in Section 3.4 is desired. The importance of the quantification of the epistemic uncertainty in analysis results that derives from epistemic uncertainty in analysis inputs is emphasized in the NAS/NRC report on QMU (Recommendation 1–2, p. 22, Ref. [77]).

The CDF and CCDF introduced in the first analysis context at the end of the preceding section and conditional on specific values for t and \mathbf{a} are defined as indicated in Eq. (3.10). Specifically, the CDF and CCDF for $y(t|\mathbf{a}, \mathbf{e}_M)$ that derive from the different possible values for \mathbf{e}_M are defined by plots of the points

$$\{y, p_{EM}[\mathcal{U}_y(t|\mathbf{a})]\} \quad \text{and} \quad \{y, p_{EM}[\mathcal{U}_y^c(t|\mathbf{a})]\}, \quad (3.25)$$

respectively, for $y \in \mathcal{Y}(t|\mathbf{a})$, where

$$\mathcal{Y}(t|\mathbf{a}) = \{y : y = y(t|\mathbf{a}, \mathbf{e}_M) \text{ for } \mathbf{e}_M \in \mathcal{EM}\},$$

$$\mathcal{U}_y(t|\mathbf{a}) = \{\tilde{y} : \tilde{y} \in \mathcal{Y}(t|\mathbf{a}) \text{ and } \tilde{y} \leq y\},$$

$p_{EM}[\mathcal{U}_y(t|\mathbf{a})]$ = probability of $\mathcal{U}_y(t|\mathbf{a})$ (i.e., of a value $\tilde{y} \leq y$)

$$\begin{aligned} &= \int_{\mathcal{EM}} \delta_y[y(t|\mathbf{a}, \mathbf{e}_M)] d_{EM}(\mathbf{e}_M) dEM \\ &\cong \sum_{i=1}^{nSE} \delta_y[y(t|\mathbf{a}, \mathbf{e}_{Mi})] / nSE \\ &= \hat{p}_{EM}[\mathcal{U}_y(t|\mathbf{a})], \end{aligned}$$

$p_{EM}[\mathcal{U}_y^c(t|\mathbf{a})]$ = probability of $\mathcal{U}_y^c(t|\mathbf{a})$ (i.e., of a value $\tilde{y} > y$)

$$\begin{aligned} &= \int_{\mathcal{EM}} \bar{\delta}_y[y(t|\mathbf{a}, \mathbf{e}_M)] d_{EM}(\mathbf{e}_M) dEM \\ &\cong \sum_{i=1}^{nSE} \bar{\delta}_y[y(t|\mathbf{a}, \mathbf{e}_{Mi})] / nSE \\ &= \hat{p}_{EM}[\mathcal{U}_y^c(t|\mathbf{a})], \end{aligned}$$

δ_y and $\bar{\delta}_y$ are defined analogously to δ_x and $\bar{\delta}_x$ in conjunction with Eq. (3.2), and \mathbf{e}_{Mi} , $i=1, 2, \dots, nSE$, is a sample from \mathcal{EM} generated in a manner consistent with the probability space $(\mathcal{EM}, \mathbb{EM}, p_{EM})$ and its associated density function $d_{EM}(\mathbf{e}_M)$. The result is a CDF and CCDF of the form shown in Fig. 3.2 that summarize the epistemic uncertainty in $y(t|\mathbf{a}, \mathbf{e}_M)$ that derives from the epistemic uncertainty in \mathbf{e}_M characterized by the probability space $(\mathcal{EM}, \mathbb{EM}, p_{EM})$.

The CDF and CCDF defined in Eq. (3.25) can also be summarized with various real-valued quantities, including an expected value $E_{EM}[y(t|\mathbf{a}, \mathbf{e}_M)]$, a variance $V_{EM}[y(t|\mathbf{a}, \mathbf{e}_M)]$, and selected quantiles $Q_{EMq}[y(t|\mathbf{a}, \mathbf{e}_M)]$. As described in Eqs. (3.13)–(3.16),

$$\begin{aligned} E_{EM}[y(t|\mathbf{a}, \mathbf{e}_M)] &= \int_{\mathcal{EM}} y(t|\mathbf{a}, \mathbf{e}_M) d_{EM}(\mathbf{e}_M) dEM \\ &\cong \sum_{i=1}^{nSE} y(t|\mathbf{a}, \mathbf{e}_{Mi}) / nSE \\ &= \hat{E}_{EM}[y(t|\mathbf{a}, \mathbf{e}_M)], \end{aligned} \quad (3.26)$$

$$\begin{aligned} V_{EM}[y(t|\mathbf{a}, \mathbf{e}_M)] &= \int_{\mathcal{EM}} \{y(t|\mathbf{a}, \mathbf{e}_M) - E_{EM}[y(t|\mathbf{a}, \mathbf{e}_M)]\}^2 d_{EM}(\mathbf{e}_M) dEM \\ &\cong \sum_{i=1}^{nSE} \{y(t|\mathbf{a}, \mathbf{e}_{Mi}) - \hat{E}_{EM}[y(t|\mathbf{a}, \mathbf{e}_M)]\}^2 / nSE \\ &= \hat{V}_{EM}[y(t|\mathbf{a}, \mathbf{e}_M)], \end{aligned} \quad (3.27)$$

and $Q_{EMq}[y(t|\mathbf{a}, \mathbf{e}_M)]$ corresponds to the value y such that

$$\begin{aligned} q = p_{EM}[\mathcal{U}_y(t|\mathbf{a})] &= \int_{\mathcal{EM}} \delta_y[y(t|\mathbf{a}, \mathbf{e}_M)] d_{EM}(\mathbf{e}_M) dEM \\ &\cong \sum_{i=1}^{nSE} \delta_y[y(t|\mathbf{a}, \mathbf{e}_{Mi})] / nSE, \end{aligned} \quad (3.28)$$

where \mathbf{e}_{Mi} , $i=1, 2, \dots, nSE$, is the sample indicated in conjunction with Eq. (3.25).

As discussed in Ref. [56], the sample \mathbf{e}_{Mi} , $i=1, 2, \dots, nSE$, also provides the basis for the implementation of a variety of sensitivity analysis procedures. The use of such procedures is a natural and important part of any sampling-based uncertainty analysis. The importance and usefulness of appropriate sensitivity analyses is emphasized in the NAS/NRC report on QMU (pp. 14–15, Ref. [77]).

3.4. Example analysis in the presence of only epistemic uncertainty

A simple example is now presented to illustrate the concepts introduced in Section 3.3. This example will also be used in Section 4 of this presentation and in Section 3 of Ref. [80] to illustrate potential QMU analyses involving only epistemic uncertainty.

The example is based on a closed electrical circuit that is under consideration for some unstated realization \mathbf{a} of aleatory uncertainty. For example, \mathbf{a} might simply correspond to nominal (i.e., unperturbed) conditions for the system under study. Specifically, the behavior of this circuit is described by a differential equation

$$\begin{aligned} L d^2 Q / dt^2 + R dQ / dt + Q / C &= E_0 \exp(-\lambda t), \\ Q(0) &= 0, \quad dQ(0) / dt = 0, \end{aligned} \quad (3.29)$$

where (i) $Q(t)$ is the electrical charge (coulombs) at time t (s), (ii) L is the inductance (henrys), (iii) R is the resistance (ohms), (iv) C is the capacitance (farads), (v) $E_0 \exp(-\lambda t)$ is the electromotive force (volts), and (vi) dQ/dt is the current (amperes). For this example, it is also assumed that R , L and C have values such that the inequality

$$R^2 - 4L/C < 0 \quad (3.30)$$

holds.

The significance of the preceding inequality is that it results in $Q(t)$ displaying a damped, oscillatory behavior. In particular, the closed-form solution to Eq. (3.29) when the inequality in Eq. (3.30) holds is

$$\begin{aligned} Q(t) &= \exp[(-R/2L)t] \left\{ c_1 \cos \left[\left(\sqrt{|R^2 - 4L/C|} / 2L \right) t \right] \right. \\ &\quad \left. + c_2 \sin \left[\left(\sqrt{|R^2 - 4L/C|} / 2L \right) t \right] \right\} - c_1 \exp(-\lambda t) \end{aligned} \quad (3.31)$$

with

$$\begin{aligned} c_1 &= -CE_0 / (CL\lambda^2 - CR\lambda + 1) \\ c_2 &= \frac{2L}{\sqrt{|R^2 - 4L/C|}} \times \left[\frac{\lambda CE_0}{CL\lambda^2 - CR\lambda + 1} - \frac{RCE_0}{2L(CL\lambda^2 - CR\lambda + 1)} \right]. \end{aligned}$$

As an example, $Q(t)$ is illustrated in Fig. 3.3 with $L=1$ henry, $R=100$ ohms, $C=10^{-4}$ farads, $E_0=1000$ volts and $\lambda=0.1 \text{ s}^{-1}$.

For the examples of this section, the vector \mathbf{e}_M of epistemically uncertain analysis inputs for the model defined in Eqs. (3.29)–(3.31) is

$$\mathbf{e}_M = [e_{M1}, e_{M2}, e_{M3}, e_{M4}, e_{M5}] = [L, R, C, E_0, \lambda], \quad (3.32)$$

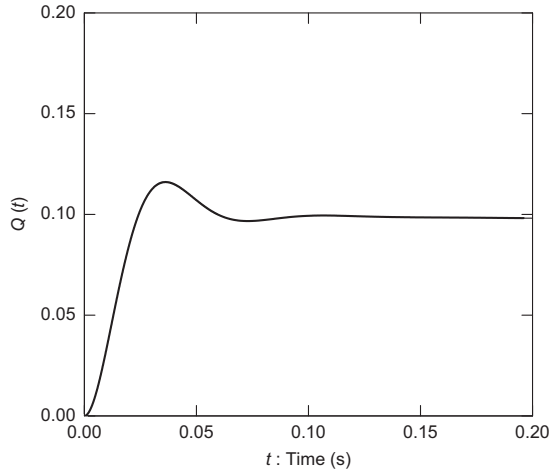


Fig. 3.3. Solution $Q(t)$ shown in Eq. (3.31) to differential equation in Eq. (3.29) obtained with $L=1$ henry, $R=100$ ohms, $C=10^{-4}$ farads, $E_0=1000$ volts, and $\lambda=0.1 \text{ s}^{-1}$.

with $e_{M1}, e_{M2}, \dots, e_{M5}$ used in place of L, R, \dots, λ to represent the elements of \mathbf{e}_M when notationally convenient. Incorporation of \mathbf{a} and \mathbf{e}_M into the notation for $Q(t)$ results in the representation $Q(t|\mathbf{a}, \mathbf{e}_M)$, with $Q(t|\mathbf{a}, \mathbf{e}_M)$ corresponding to the generic representation $y(t|\mathbf{a}, \mathbf{e}_M)$ in Eq. (3.24).

The appropriate values for L, R, C, E_0 and λ are assumed to be contained in the intervals

$$\mathcal{EM}_1 = \{L : L_{mn} \leq L \leq L_{mx}\} = \{L : 0.8 \leq L \leq 1.2 \text{ henrys}\}, \quad (3.33)$$

$$\mathcal{EM}_2 = \{R : R_{mn} \leq R \leq R_{mx}\} = \{R : 50 \leq R \leq 100 \text{ ohms}\}, \quad (3.34)$$

$$\mathcal{EM}_3 = \{C : C_{mn} \leq C \leq C_{mx}\} = \{C : 0.9 \times 10^{-4} \leq C \leq 1.1 \times 10^{-4} \text{ farads}\}, \quad (3.35)$$

$$\mathcal{EM}_4 = \{E_0 : E_{mn} \leq E_0 \leq E_{mx}\} = \{E_0 : 900 \leq E_0 \leq 1100 \text{ volts}\}, \quad (3.36)$$

and

$$\mathcal{EM}_5 = \{\lambda : \lambda_{mn} \leq \lambda \leq \lambda_{mx}\} = \{\lambda : 0.4 \leq \lambda \leq 0.8 \text{ s}^{-1}\}, \quad (3.37)$$

respectively.

A probabilistic characterization of the epistemic uncertainty associated with L, R, \dots, λ is provided by a probability distribution defined on each of the preceding intervals. Specifically, four subintervals are considered for each of the intervals \mathcal{EM}_i , $i=1, 2, \dots, 5$, defined in Eqs. (3.33)–(3.37):

$$\mathcal{E}_{i1} = [a, b - (b-a)/4], \quad (3.38)$$

$$\mathcal{E}_{i2} = [a + (b-a)/4, b], \quad (3.39)$$

$$\mathcal{E}_{i3} = [a + (b-a)/8, b - 3(b-a)/8], \quad (3.40)$$

$$\mathcal{E}_{i4} = [a + 3(b-a)/8, b - (b-a)/8], \quad (3.41)$$

where $[a, b]$ corresponds to $[L_{mn}, L_{mx}]$, $[R_{mn}, R_{mx}]$, $[C_{mn}, C_{mx}]$, $[E_{mn}, E_{mx}]$ and $[\lambda_{mn}, \lambda_{mx}]$ for $i=1, 2, 3, 4$ and 5 , respectively (Fig. 3.4). For example and for a given element e_{Mi} of \mathbf{e}_M , each of the preceding intervals could have been indicated by a different source as containing the correct value to use for e_{Mi} in the analysis under consideration.

In turn, the corresponding density function $d_i(e_{Mi})$ for the set \mathcal{EM}_i is given by

$$d_i(e_{Mi}) = \sum_{j=1}^4 \delta_{ij}(e_{Mi}) / 4[\max(\mathcal{E}_{ij}) - \min(\mathcal{E}_{ij})] \quad (3.42)$$

under the assumption that the four sources that provided the intervals in Eqs. (3.38)–(3.41) for an element e_{Mi} of \mathbf{e}_M are equally

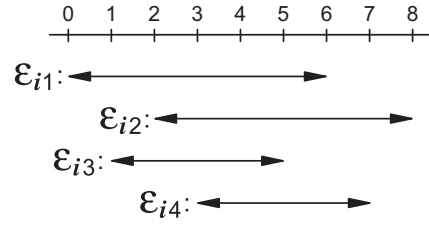


Fig. 3.4. Illustration of sets \mathcal{E}_{i1} , \mathcal{E}_{i2} , \mathcal{E}_{i3} and \mathcal{E}_{i4} defined in Eqs. (3.38)–(3.41) with the interval $[a, b]$ normalized to the interval $[0, 8]$ for representational simplicity.

credible, where

$$\delta_{ij}(e_{Mi}) = \begin{cases} 1 & \text{if } e_{Mi} \in \mathcal{E}_{ij} \\ 0 & \text{otherwise.} \end{cases}$$

The preceding specification for $d_i(e_{Mi})$ corresponds to defining a uniform distribution on each interval \mathcal{E}_{ij} and then weighting each distribution equally. The equal weighting derives from an assumption of equal credibility for the four sources of the intervals in Eqs. (3.38)–(3.41). The definition of the density functions $d_i(e_{Mi})$ in Eq. (3.42) results in the assignment of more probability where the intervals supplied by the four sources overlap and less probability where the intervals do not overlap. The density functions $d_i(e_{Mi})$ in essence define probability spaces $(\mathcal{EM}_i, \mathbb{EM}_i, p_{EM,i})$ for the variables e_{Mi} , $i=1, 2, \dots, 5$.

The set \mathcal{EM} of possible values for \mathbf{e}_M is given by

$$\mathcal{EM} = \mathcal{EM}_1 \times \mathcal{EM}_2 \times \mathcal{EM}_3 \times \mathcal{EM}_4 \times \mathcal{EM}_5, \quad (3.43)$$

where $\mathcal{EM}_1, \mathcal{EM}_2, \dots, \mathcal{EM}_5$ are defined in Eqs. (3.33)–(3.37). In turn, \mathcal{EM} has a probabilistic structure that derives from the distributions characterizing the uncertainty in $e_{M1}, e_{M2}, \dots, e_{M5}$. Formally, this structure corresponds to a probability space $(\mathcal{EM}, \mathbb{EM}, p_{EM})$ that, in effect, is defined by the density functions introduced in Eq. (3.42).

The epistemic uncertainty associated with $Q(t|\mathbf{a}, \mathbf{e}_M)$ that derives from the probability space $(\mathcal{EM}, \mathbb{EM}, p_{EM})$ is now considered. As indicated in Eqs. (3.25)–(3.28), this uncertainty can be characterized by various quantities defined by integrals over \mathcal{EM} . However, such integrals are difficult to determine in closed form (i.e., by use of antiderivatives in conjunction with the Fundamental Theorem of Calculus) because of the high dimensionality of \mathbf{e}_M and the complexity of the function being integrated. Instead, sampling-based methods are used in most analyses to determine these quantities.

Consistent with this approach, the present example uses a Latin hypercube sample (LHS)

$$\mathbf{e}_{Mi} = [e_{M1,i}, e_{M2,i}, \dots, e_{M5,i}], \quad i = 1, 2, \dots, nSE, \quad (3.44)$$

of size $nSE=200$ generated from \mathcal{EM} in consistency with the probability space $(\mathcal{EM}, \mathbb{EM}, p_{EM})$ (i.e., in consistency with the distributions associated with the density functions defined in Eq. (3.42)). As discussed in Refs. [45,55,56], Latin hypercube sampling is widely used in sampling-based uncertainty and sensitivity analyses involving computationally demanding models because of its efficient stratification properties. In addition, this sampling-based approach also provides the basis for the application of a variety of sensitivity analysis procedures [56].

The sample in Eq. (3.44) results in $nSE=200$ time-dependent results: $Q(t|\mathbf{a}, \mathbf{e}_{Mi})$, $i=1, 2, \dots, 200$ (Fig. 3.5). The spread of the curves in Fig. 3.5 provides a nonquantitative indication of the epistemic uncertainty associated with $Q(t|\mathbf{a}, \mathbf{e}_M)$ that derives from the uncertainty in \mathbf{e}_M as quantified by the probability space $(\mathcal{EM}, \mathbb{EM}, p_{EM})$. Only 50 of the 200 time-dependent results for $Q(t|\mathbf{a}, \mathbf{e}_{Mi})$ are presented in Fig. 3.5 as presentation of all 200

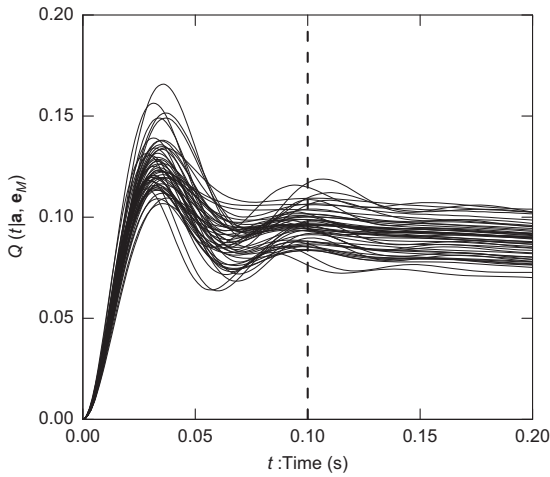


Fig. 3.5. Solutions $Q(t|\mathbf{a}, \mathbf{e}_M)$ to differential equation in Eq. (3.29) obtained with the first 50 elements of the LHS in Eq. (3.44) (i.e., with \mathbf{e}_{Mi} for $i=1,2, \dots, 50$).

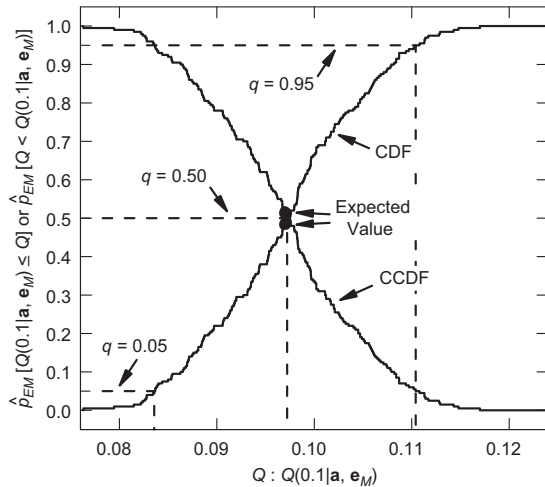


Fig. 3.6. Estimated CDF and CCDF for $Q(0.1|\mathbf{a}, \mathbf{e}_M)$ (i) obtained with the LHS of size 200 in Eq. (3.44) generated from \mathcal{EM} in consistency with the defining density functions for the probability space $(\mathcal{EM}, \mathbf{EM}, p_{EM})$ and (ii) presented with $\hat{p}_{EM}[Q(0.1|\mathbf{a}, \mathbf{e}_M) \leq Q]$ and $\hat{p}_{EM}[Q < Q(0.1|\mathbf{a}, \mathbf{e}_M)]$ used as mnemonics for estimated probabilities of the form $\hat{p}_{EM}[\mathcal{U}_Y(0.1|\mathbf{a})]$ and $\hat{p}_{EM}[\mathcal{U}_Y^c(0.1|\mathbf{a})]$ defined in conjunction with Eq. (3.25).

curves results in an almost solid band of overlapping curves that obscures the shape of the individual curves.

A quantitative summary of the epistemic uncertainty in $Q(t|\mathbf{a}, \mathbf{e}_M)$ that derives from the epistemic uncertainty in \mathbf{e}_M is provided by the CDFs and CCDFs for $Q(t|\mathbf{a}, \mathbf{e}_M)$ at selected points in time. As an example, approximations to the CDF and CCDF at $t=0.1$ s obtained with use of the sample in Eq. (3.44) are shown in Fig. 3.6. Specifically, the CDF and CCDF in Fig. 3.6 are constructed from the values for $Q(0.1|\mathbf{a}, \mathbf{e}_{Mi})$ associated with the vertical line in Fig. 3.5 as described in conjunction with Eq. (3.25). With respect to notation, the expressions $\hat{p}_{EM}[Q(0.1|\mathbf{a}, \mathbf{e}_M) \leq Q]$ and $\hat{p}_{EM}[Q < Q(0.1|\mathbf{a}, \mathbf{e}_M)]$ on the ordinate of Fig. 3.6 correspond to the defining probabilities for the CDF and CCDF, respectively, for $Q(0.1|\mathbf{a}, \mathbf{e}_M)$. Specifically, $\hat{p}_{EM}[Q(0.1|\mathbf{a}, \mathbf{e}_M) \leq Q]$ is the estimated probability that $Q(0.1|\mathbf{a}, \mathbf{e}_M)$ is less than or equal to a value Q on the abscissa, and $\hat{p}_{EM}[Q < Q(0.1|\mathbf{a}, \mathbf{e}_M)]$ is the estimated probability that $Q(0.1|\mathbf{a}, \mathbf{e}_M)$ is greater than a value Q on the abscissa. The indicated probabilities are characterizing epistemic uncertainty and thus are indicating degrees of belief with respect to where the correct value for $Q(0.1|\mathbf{a}, \mathbf{e}_M)$ is located. Thus, for example, there is a “degree of

belief” probability of 0.9 that $Q(0.1|\mathbf{a}, \mathbf{e}_M)$ is located between the 0.05 and 0.95 quantiles in Fig. 3.6. Further, the expected value and quantile values indicated in Fig. 3.6 are obtained as described in Eqs. (3.26) and (3.28), respectively. In this example, the expected value and median value are very close together; this is often not the case in analyses that involve substantial epistemic uncertainties.

The presentation of CDFs and CCDFs of the form shown in Fig. 3.6 for multiple values of t is cumbersome. An effective alternative is to plot expected values and quantiles as functions of time (Fig. 3.7). With this presentation format, expected values and quantiles as indicated in Fig. 3.6 are determined for a sequence of values for t and then plotted above these values to obtain the expected value and quantile curves in Fig. 3.7. Specifically, the expected value curve in Fig. 3.7 is a plot of the points

$$(t, \hat{E}_{EM}[y(t|\mathbf{a}, \mathbf{e}_M)]), \quad 0 \leq t \leq 0.20, \quad (3.45)$$

with $\hat{E}_{EM}[y(t|\mathbf{a}, \mathbf{e}_M)]$ defined as indicated in Eq. (3.26), and the quantile curves in Fig. 3.7 are plots of points

$$(t, \hat{Q}_{EMq}[y(t|\mathbf{a}, \mathbf{e}_M)]), \quad 0 \leq t \leq 0.20, \quad (3.46)$$

for $q=0.05, 0.5$ and 0.95 with $\hat{Q}_{EMq}[y(t|\mathbf{a}, \mathbf{e}_M)]$ defined as indicated in Eq. (3.28). In this example, the expected value and median value (i.e., 0.5 quantile) curves almost exactly overlap.

3.5. Analysis in the presence of aleatory and epistemic uncertainty

This section presents a formal description of the representation of uncertainty in an analysis that involves both aleatory and epistemic uncertainty. The following section (Section 3.6) then presents a simple example illustrating the formal concepts presented in the present section. If desired, Section 3.6 can be read before Section 3.5, with Section 3.5 being referred to only when a more technical description of the results in Section 3.6 is desired.

The analyses described in Sections 3.5 and 3.6 involve what the NAS/NRC report on QMU refers to as the “probability of frequency approach” and recommends for use in QMU analyses (Recommendation 1–7, p. 33, and App. A, Ref. [77]). Specifically, the descriptor “probability of frequency approach” designates an analysis in which a careful distinction and separation is maintained between the effects and implications of aleatory uncertainty and the effects and implications of epistemic uncertainty.

The CDF and CCDF introduced in the second analysis context described in Section 3.2 and conditional on specific values for t and $\mathbf{e}=[\mathbf{e}_A, \mathbf{e}_M]$ are also defined as indicated in Eq. (3.10).

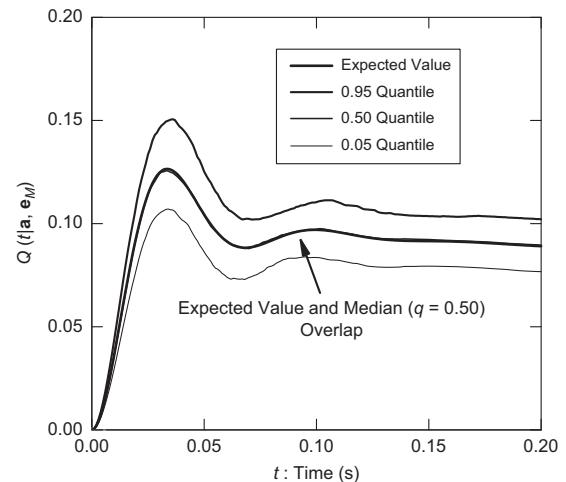


Fig. 3.7. Estimated time-dependent expected value and quantile curves for $Q(t|\mathbf{a}, \mathbf{e}_M)$ obtained with the LHS of size 200 in Eq. (3.44) generated from \mathcal{EM} in consistency with the defining density functions for the probability space $(\mathcal{EM}, \mathbf{EM}, p_{EM})$.

Specifically, the CDF and CCDF for $y(t|\mathbf{a}, \mathbf{e}_M)$ that derive from the different possible values for \mathbf{a} are defined by the plots of the points

$$\{y, p_A[\mathcal{U}_y(t|\mathbf{e})|\mathbf{e}_A]\} \text{ and } \{y, p_A[\mathcal{U}_y^c(t|\mathbf{e})|\mathbf{e}_A]\}, \quad (3.47)$$

respectively, for $y \in \mathcal{Y}(t|\mathbf{e})$, where

$$\mathcal{Y}(t|\mathbf{e}) = \{y : y = y(t|\mathbf{a}, \mathbf{e}_M) \text{ for } \mathbf{a} \in \mathcal{A}\},$$

$$\mathcal{U}_y(t|\mathbf{e}) = \{\tilde{y} : \tilde{y} \in \mathcal{Y}(t|\mathbf{e}) \text{ and } \tilde{y} \leq y\},$$

$p_A[\mathcal{U}_y(t|\mathbf{e})|\mathbf{e}_A]$ = probability of $\mathcal{U}_y(t|\mathbf{e})$ (i.e., of a value $\tilde{y} \leq y$)

$$\begin{aligned} &= \int_{\mathcal{A}} \delta_y[y(t|\mathbf{a}, \mathbf{e}_M)] d_A(\mathbf{a}|\mathbf{e}_A) d\mathbf{A} \\ &\cong \sum_{j=1}^{nSA} \delta_y[y(t|\mathbf{a}_j, \mathbf{e}_M)] / nSA \\ &= \hat{p}_A[\mathcal{U}_y(t|\mathbf{e})|\mathbf{e}_A], \end{aligned}$$

$p_A[\mathcal{U}_y^c(t|\mathbf{e})|\mathbf{e}_A]$ = probability of $\mathcal{U}_y^c(t|\mathbf{e})$ (i.e., of a value $\tilde{y} > y$)

$$\begin{aligned} &= \int_{\mathcal{A}} \bar{\delta}_y[y(t|\mathbf{a}, \mathbf{e}_M)] d_A(\mathbf{a}|\mathbf{e}_A) d\mathbf{A} \\ &\cong \sum_{j=1}^{nSA} \bar{\delta}_y[y(t|\mathbf{a}_j, \mathbf{e}_M)] / nSA \\ &= \hat{p}_A[\mathcal{U}_y^c(t|\mathbf{e})|\mathbf{e}_A], \end{aligned}$$

δ_y and $\bar{\delta}_y$ are defined analogously to δ_x and $\bar{\delta}_x$ in conjunction with Eq. (3.2) and $\mathbf{a}_j, j=1, 2, \dots, nSA$, is a sample from \mathcal{A} generated in a manner consistent with the probability space $(\mathcal{A}, \mathbb{A}, p_A)$ and its associated density function $d_A(\mathbf{a}|\mathbf{e}_A)$. The result is a CDF and CCDF of the form shown in Fig. 3.2 that summarize the aleatory uncertainty in $y(t|\mathbf{a}, \mathbf{e}_M)$ that derives from the aleatory uncertainty in \mathbf{a} characterized by the probability space $(\mathcal{A}, \mathbb{A}, p_A)$.

In general, the set \mathcal{A} could be, and often is, a function of elements of \mathbf{e}_A . In this case, the sets \mathcal{A} and \mathbb{A} would appropriately be represented by $\mathcal{A}(\mathbf{e}_A)$ and $\mathbb{A}(\mathbf{e}_A)$. Then, the representation for the probability space $(\mathcal{A}, \mathbb{A}, p_A)$ conditional on an element $\mathbf{e}=[\mathbf{e}_A, \mathbf{e}_M]$ of \mathcal{E} would be $[\mathcal{A}(\mathbf{e}_A), \mathbb{A}(\mathbf{e}_A), p_A(\mathcal{U}|\mathbf{e}_A)]$. To reduce notational clutter, this fully general representation for $(\mathcal{A}, \mathbb{A}, p_A)$ is not used. Instead, the possible dependence of $(\mathcal{A}, \mathbb{A}, p_A)$ on the elements of \mathbf{e}_A is indicated through the use of the notations $p_A(\mathcal{U}|\mathbf{e}_A)$ and $d_A(\mathbf{a}|\mathbf{e}_A)$.

Similarly to the CDF and CCDF defined in Eq. (3.10), the CDF and CCDF defined in Eq. (3.47) can also be summarized with various real-valued quantities, including an expected value $E_A[y(t|\mathbf{a}, \mathbf{e}_M)|\mathbf{e}_A]$, a variance $V_A[y(t|\mathbf{a}, \mathbf{e}_M)|\mathbf{e}_A]$ and selected quantiles $Q_{Aq}[y(t|\mathbf{a}, \mathbf{e}_M)|\mathbf{e}_A]$. The definitions of $E_A[y(t|\mathbf{a}, \mathbf{e}_M)|\mathbf{e}_A]$, $V_A[y(t|\mathbf{a}, \mathbf{e}_M)|\mathbf{e}_A]$ and $Q_{Aq}[y(t|\mathbf{a}, \mathbf{e}_M)|\mathbf{e}_A]$ are effectively the same as the definitions for $E_{EM}[y(t|\mathbf{a}, \mathbf{e}_M)]$, $V_{EM}[y(t|\mathbf{a}, \mathbf{e}_M)]$ and $Q_{EMq}[y(t|\mathbf{a}, \mathbf{e}_M)]$ in Eqs. (3.26)–(3.28) with the only difference being that integrations are performed with respect to the probability space $(\mathcal{A}, \mathbb{A}, p_A)$ and its associated density function $d_A(\mathbf{a}|\mathbf{e}_A)$ rather than with respect to the probability space $(\mathcal{EM}, \mathbb{EM}, p_{EM})$ and its associated density function $d_{EM}(\mathbf{e}_M)$. Specifically,

$$\begin{aligned} E_A[y(t|\mathbf{a}, \mathbf{e}_M)|\mathbf{e}_A] &= \int_{\mathcal{A}} y(t|\mathbf{a}, \mathbf{e}_M) d_A(\mathbf{a}|\mathbf{e}_A) d\mathbf{A} \\ &\cong \sum_{j=1}^{nSA} y(t|\mathbf{a}_j, \mathbf{e}_M) / nSA \\ &= \hat{E}_A[y(t|\mathbf{a}, \mathbf{e}_M)|\mathbf{e}_A], \end{aligned} \quad (3.48)$$

$$\begin{aligned} V_A[y(t|\mathbf{a}, \mathbf{e}_M)|\mathbf{e}_A] &= \int_{\mathcal{A}} \{y(t|\mathbf{a}, \mathbf{e}_M) - E_A[y(t|\mathbf{a}, \mathbf{e}_M)|\mathbf{e}_A]\}^2 d_A(\mathbf{a}|\mathbf{e}_A) d\mathbf{A} \\ &\cong \sum_{j=1}^{nSA} \{y(t|\mathbf{a}_j, \mathbf{e}_M) - \hat{E}_A[y(t|\mathbf{a}, \mathbf{e}_M)|\mathbf{e}_A]\}^2 / nSA \\ &= \hat{V}_A[y(t|\mathbf{a}, \mathbf{e}_M)|\mathbf{e}_A], \end{aligned} \quad (3.49)$$

and $Q_{Aq}[y(t|\mathbf{a}, \mathbf{e}_M)|\mathbf{e}_A]$ and its approximation $\hat{Q}_{Aq}[y(t|\mathbf{a}, \mathbf{e}_M)|\mathbf{e}_A]$ correspond to the value y such that

$$\begin{aligned} q &= p_A[\mathcal{U}_y(t|\mathbf{e})|\mathbf{e}_A] = \int_{\mathcal{A}} \delta_y[y(t|\mathbf{a}, \mathbf{e}_M)] d_A(\mathbf{a}|\mathbf{e}_A) d\mathbf{A} \\ &\cong \sum_{j=1}^{nSA} \delta_y[y(t|\mathbf{a}_j, \mathbf{e}_M)] / nSA, \end{aligned} \quad (3.50)$$

where $\mathbf{a}_j, j=1, 2, \dots, nSA$, is the sample indicated in conjunction with Eq. (3.47).

Distributions of CDFs and CCDFs result from the different possible values for $\mathbf{e}=[\mathbf{e}_A, \mathbf{e}_M]$. As indicated in conjunction with Eq. (3.47), each value for \mathbf{e} results in a different CDF and associated CCDF that summarize the effects of aleatory uncertainty. In turn, these CDFs, CCDFs and their associated summary measures have distributions that characterize epistemic uncertainty and derive from the epistemic uncertainty in \mathbf{e} characterized by the probability space $(\mathcal{E}, \mathbb{E}, p_E)$.

In general, the probability space $(\mathcal{E}, \mathbb{E}, p_E)$ will result in infinitely many CDFs and CCDFs of the form defined in conjunction with Eq. (3.47). Thus, some way of summarizing these CDFs and CCDFs is necessary. As illustrated in Section 3.6, this summary is provided by expected value curves and quantile curves (e.g., $q=0.05, 0.5, 0.95$) defined by

$$(y, E_E\{p_A[\mathcal{U}_y(t|\mathbf{e})|\mathbf{e}_A]\}) \text{ and } (y, Q_{Eq}\{p_A[\mathcal{U}_y(t|\mathbf{e})|\mathbf{e}_A]\}) \quad (3.51)$$

and

$$(y, E_E\{p_A[\mathcal{U}_y^c(t|\mathbf{e})|\mathbf{e}_A]\}) \text{ and } (y, Q_{Eq}\{p_A[\mathcal{U}_y^c(t|\mathbf{e})|\mathbf{e}_A]\}) \quad (3.52)$$

for distributions of CDFs and CCDFs, respectively, where (i)

$$\begin{aligned} E_E\{p_A[\mathcal{U}_y(t|\mathbf{e})|\mathbf{e}_A]\} &= \int_{\mathcal{E}} p_A[\mathcal{U}_y(t|\mathbf{e})|\mathbf{e}_A] d_E(\mathbf{e}) d\mathbf{E} \\ &= \int_{\mathcal{E}} \left\{ \int_{\mathcal{A}} \delta_y[y(t|\mathbf{a}, \mathbf{e}_M)] d_A(\mathbf{a}|\mathbf{e}_A) d\mathbf{A} \right\} d_E(\mathbf{e}) d\mathbf{E} \\ &\cong \sum_{i=1}^{nSE} \left\{ \sum_{j=1}^{nSA} \delta_y[y(t|\mathbf{a}_{ij}, \mathbf{e}_{Mi})] / nSA \right\} / nSE \\ &= \hat{E}_E\{p_A[\mathcal{U}_y(t|\mathbf{e})|\mathbf{e}_A]\} \end{aligned}$$

and

$$\begin{aligned} E_E\{p_A[\mathcal{U}_y^c(t|\mathbf{e})|\mathbf{e}_A]\} &= \int_{\mathcal{E}} p_A[\mathcal{U}_y^c(t|\mathbf{e})|\mathbf{e}_A] d_E(\mathbf{e}) d\mathbf{E} \\ &= \int_{\mathcal{E}} \left\{ \int_{\mathcal{A}} \bar{\delta}_y[y(t|\mathbf{a}, \mathbf{e}_M)] d_A(\mathbf{a}|\mathbf{e}_A) d\mathbf{A} \right\} d_E(\mathbf{e}) d\mathbf{E} \\ &\cong \sum_{i=1}^{nSE} \left\{ \sum_{j=1}^{nSA} \bar{\delta}_y[y(t|\mathbf{a}_{ij}, \mathbf{e}_{Mi})] / nSA \right\} / nSE \\ &= \hat{E}_E\{p_A[\mathcal{U}_y^c(t|\mathbf{e})|\mathbf{e}_A]\}, \end{aligned}$$

(ii) $Q_{Eq}\{p_A[\mathcal{U}_y(t|\mathbf{e})|\mathbf{e}_A]\}$ and the associated approximation $\hat{Q}_{Eq}\{p_A[\mathcal{U}_y(t|\mathbf{e})|\mathbf{e}_A]\}$ correspond to the probability p such that

$$\begin{aligned} q &= \int_{\mathcal{E}-p} \{p_A[\mathcal{U}_y(t|\mathbf{e})|\mathbf{e}_A]\} d_E(\mathbf{e}) d\mathbf{E} \\ &= \int_{\mathcal{E}-p} \left\{ \int_{\mathcal{A}} \delta_y[y(t|\mathbf{a}, \mathbf{e}_M)] d_A(\mathbf{a}|\mathbf{e}_A) d\mathbf{A} \right\} d_E(\mathbf{e}) d\mathbf{E} \\ &\cong \sum_{i=1}^{nSE} \left\{ \sum_{j=1}^{nSA} \delta_y[y(t|\mathbf{a}_{ij}, \mathbf{e}_{Mi})] / nSA \right\} / nSE, \end{aligned}$$

(iii) $Q_{Eq}\{p_A[\mathcal{U}_y^c(t|\mathbf{e})|\mathbf{e}_A]\}$ and the associated approximation $\hat{Q}_{Eq}\{p_A[\mathcal{U}_y^c(t|\mathbf{e})|\mathbf{e}_A]\}$ correspond to the probability p such that

$$\begin{aligned} q &= \int_{\mathcal{E}-p} \{p_A[\mathcal{U}_y^c(t|\mathbf{e})|\mathbf{e}_A]\} d_E(\mathbf{e}) d\mathbf{E} \\ &= \int_{\mathcal{E}-p} \left\{ \int_{\mathcal{A}} \bar{\delta}_y[y(t|\mathbf{a}, \mathbf{e}_M)] d_A(\mathbf{a}|\mathbf{e}_A) d\mathbf{A} \right\} d_E(\mathbf{e}) d\mathbf{E} \end{aligned}$$

$$\cong \sum_{i=1}^{nSE} \delta_p \left\{ \sum_{j=1}^{nSA} \bar{\delta}_y [y(t|\mathbf{a}_{ij}, \mathbf{e}_{Mi})/nSA] \right\} / nSE,$$

- (iv) $\mathbf{e}_i = [\mathbf{e}_{Ai}, \mathbf{e}_{Mi}]$, $i = 1, 2, \dots, nSE$, is a sample from \mathcal{E} generated in a manner consistent with the probability space $(\mathcal{E}, \mathbb{E}, p_E)$ and its associated density function, and (v) \mathbf{a}_{ij} , $j = 1, 2, \dots, nSA$, is a sample from \mathcal{A} generated in a manner consistent with the probability space $(\mathcal{A}, \mathbb{A}, p_A)$ and its associated density function $d_A(\mathbf{a}|\mathbf{e}_{Ai})$ for each \mathbf{e}_i . Although not incorporated into the notation in use, the sample size nSA could change for each \mathbf{e}_i .

An alternative summary is provided by reducing each CDF to its corresponding expected value $E_A[y(t|\mathbf{a}, \mathbf{e}_M)|\mathbf{e}_A]$ as indicated in Eq. (3.48) and then presenting the CDF and CCDF for $E_A[y(t|\mathbf{a}, \mathbf{e}_M)|\mathbf{e}_A]$ that result from the epistemic uncertainty associated with $\mathbf{e} = [\mathbf{e}_A, \mathbf{e}_M]$. Similarly to the results presented in conjunction with Eq. (3.10), the CDF and CCDF for $E_A[y(t|\mathbf{a}, \mathbf{e}_M)|\mathbf{e}_A]$ are defined by plots of the points

$$\{\bar{y}, p_E[\mathcal{U}_{\bar{y}}(t)]\} \quad \text{and} \quad \{\bar{y}, p_E[\mathcal{U}_{\bar{y}}^c(t)]\}, \quad (3.53)$$

respectively, for $\bar{y} \in \bar{\mathcal{Y}}(t)$, where

$$\bar{\mathcal{Y}}(t) = \{\bar{y} : \bar{y} = E_A[y(t|\mathbf{a}, \mathbf{e}_M)|\mathbf{e}_A] \text{ for } \mathbf{e} = [\mathbf{e}_A, \mathbf{e}_M] \in \mathcal{E},$$

$$\mathcal{U}_{\bar{y}}(t) = \{\tilde{y} : \tilde{y} \in \bar{\mathcal{Y}}(t) \text{ and } \tilde{y} \leq \bar{y}\},$$

$p_E[\mathcal{U}_{\bar{y}}(t)]$ = probability of $\mathcal{U}_{\bar{y}}(t)$ (i.e., of a value $\tilde{y} \leq \bar{y}$)

$$\begin{aligned} &= \int_{\mathcal{E}} \bar{\delta}_{\bar{y}} \{E_A[y(t|\mathbf{a}, \mathbf{e}_M)|\mathbf{e}_A]\} d_E(\mathbf{e}) d\mathbf{E} \\ &\cong \sum_{i=1}^{nSE} \delta_{\bar{y}} \left\{ \sum_{j=1}^{nSA} y(t|\mathbf{a}_{ij}, \mathbf{e}_{Mi})/nSA \right\} / nSE \\ &= \hat{p}_E[\mathcal{U}_{\bar{y}}(t)], \end{aligned}$$

$p_E[\mathcal{U}_{\bar{y}}^c(t)]$ = probability of $\mathcal{U}_{\bar{y}}^c(t)$ (i.e., of a value $\tilde{y} > \bar{y}$)

$$\begin{aligned} &= \int_{\mathcal{E}} \bar{\delta}_{\bar{y}} \{E_A[y(t|\mathbf{a}, \mathbf{e}_M)|\mathbf{e}_A]\} d_E(\mathbf{e}) d\mathbf{E} \\ &\cong \sum_{i=1}^{nSE} \bar{\delta}_{\bar{y}} \left\{ \sum_{j=1}^{nSA} y(t|\mathbf{a}_{ij}, \mathbf{e}_{Mi})/nSA \right\} / nSE \\ &= \hat{p}_E[\mathcal{U}_{\bar{y}}^c(t)], \end{aligned}$$

and the samples $\mathbf{e}_i = [\mathbf{e}_{Ai}, \mathbf{e}_{Mi}]$, $i = 1, 2, \dots, nSE$, and \mathbf{a}_{ij} , $j = 1, 2, \dots, nSA$, are defined the same as indicated in conjunction with Eqs. (3.51) and (3.52).

If desired, the reduction indicated in the preceding paragraph can be carried further by reducing the expected value $E_A[y(t|\mathbf{a}, \mathbf{e}_M)|\mathbf{e}_A]$ over aleatory uncertainty defined in Eq. (3.48) to an expected value $E_E\{E_A[y(t|\mathbf{a}, \mathbf{e}_M)|\mathbf{e}_A]\}$ over aleatory and epistemic uncertainty defined by

$$\begin{aligned} &E_E\{E_A[y(t|\mathbf{a}, \mathbf{e}_M)|\mathbf{e}_A]\} \\ &= \int_{\mathcal{E}} E_A[y(t|\mathbf{a}, \mathbf{e}_M)|\mathbf{e}_A] d_E(\mathbf{e}) d\mathbf{E} \\ &= \int_{\mathcal{E}} \left[\int_{\mathcal{A}} y(t|\mathbf{a}, \mathbf{e}_M) d_A(\mathbf{a}|\mathbf{e}_A) d\mathbf{A} \right] d_E(\mathbf{e}) d\mathbf{E} \\ &\cong \sum_{i=1}^{nSE} \left[\sum_{j=1}^{nSA} y(t|\mathbf{a}_{ij}, \mathbf{e}_{Mi})/nSA \right] / nSE \\ &= \hat{E}_E\{E_A[y(t|\mathbf{a}, \mathbf{e}_M)|\mathbf{e}_A]\}, \end{aligned} \quad (3.54)$$

where the samples $\mathbf{e}_i = [\mathbf{e}_{Ai}, \mathbf{e}_{Mi}]$, $i = 1, 2, \dots, nSE$, and \mathbf{a}_{ij} , $j = 1, 2, \dots, nSA$, are again defined the same as in conjunction with Eqs. (3.51) and (3.52). The expected value $E_E\{E_A[y(t|\mathbf{a}, \mathbf{e}_M)|\mathbf{e}_A]\}$ is the result of reducing all the information associated with the probability space $(\mathcal{E}, \mathbb{E}, p_E)$ for epistemic uncertainty, the probability space $(\mathcal{A}, \mathbb{A}, p_A)$

for aleatory uncertainty and the function $y(t|\mathbf{a}, \mathbf{e}_M)$ to a single number.

3.6. Example analysis in the presence of aleatory and epistemic uncertainty

A simple, randomly perturbed system is now presented to illustrate the concepts introduced in Section 3.5. This example will also be used in Section 5 of this presentation and in Section 4 of Ref. [80] to illustrate potential QMU analyses involving aleatory and epistemic uncertainty. Further, the results from real analyses presented in Ref. [79] are of the form described in the present section.

The system is assumed to receive random perturbations in time whose occurrence is characterized as a stationary Poisson process with a rate λ (s^{-1}). The amplitudes (i.e., magnitudes) for the individual perturbations are assumed to vary randomly and to undergo exponential decay in a manner characterized by a rate constant r (s^{-1}). In concept, any of a large variety of systems could be under consideration, with the result that the perturbation might involve a mechanical force, an electrical impulse, a radiation impulse, a heat impulse, the injection of a material, or some additional possibility. For notational convenience, the initial perturbations will be represented by A_0 and assumed to have units of force (kg m/s^2). As a result of the indicated exponential decay,

$$A(t) = A_0 \exp[-r(t-t_0)] \quad (3.55)$$

is the amplitude at time t of a perturbation of size A_0 that occurs at time t_0 . Further, the amplitudes of the individual perturbations are assumed to be characterized by a triangular distribution defined on an interval $[a, b]$ with a mode of m .

This example involves both aleatory and epistemic uncertainty. For a given time interval (e.g., $[0, 10 \text{ s}]$), the different possible realizations of aleatory uncertainty correspond to vectors of the form

$$\mathbf{a} = [n, t_1, A_{01}, t_2, A_{02}, \dots, t_n, A_{0n}], \quad (3.56)$$

where (i) n is the number of perturbations that occur in the time interval, (ii) $t_1 < t_2 < \dots < t_n$ are the times at which the individual perturbations occur, and (iii) $A_{01}, A_{02}, \dots, A_{0n}$ are the initial amplitudes for the individual perturbations. In turn,

$$\mathcal{A} = \{\mathbf{a} : \mathbf{a} = [n, t_1, A_{01}, t_2, A_{02}, \dots, t_n, A_{0n}]\} \quad (3.57)$$

is the sample space for aleatory uncertainty, and the probabilistic structure required to formally complete the definition of the corresponding probability space $(\mathcal{A}, \mathbb{A}, p_A)$ derives from λ and the probability distribution for A_0 .

For a given element \mathbf{a} of \mathcal{A} and a given value for r , the resultant amplitude $A(t|\mathbf{a})$ at time t is given by

$$A(t|\mathbf{a}, r) = \begin{cases} 0 & \text{if } t < t_1 \\ \sum_{k=1}^{\tilde{n}} A_{0k} \exp[-r(t-t_k)] & \text{if } t \geq t_1, \end{cases} \quad (3.58)$$

where $\tilde{n} = \max\{k : t_k \leq t\}$.

For this example, λ , a , m , b and r are assumed to be uncertain in an epistemic sense. As a result,

$$\mathbf{e} = [\mathbf{e}_A, \mathbf{e}_M] = [e_1, e_2, e_3, e_4, e_5] = [\lambda, a, m, b, r] \quad (3.59)$$

is the vector of epistemically uncertain variables under consideration, with $\mathbf{e}_A = [\lambda, a, m, b]$ and $\mathbf{e}_M = [r]$. Specifically, λ , a , m and b are involved in the definition of probability distributions that characterize aleatory uncertainty, and r relates to the physical processes involved in the decay of an initial perturbation A_0 .

The appropriate values for λ , a , m , b and r are assumed to be contained in the intervals

$$\mathcal{EA}_1 = \{\lambda : \lambda_{mn} \leq \lambda \leq \lambda_{mx}\} = \{\lambda : 0.5 \leq \lambda \leq 1.5 \text{ s}^{-1}\} \quad (3.60)$$

$$\mathcal{EA}_2 = \{a : a_{mn} \leq a \leq a_{mx}\} = \{a : 1.0 \leq a \leq 2.0 \text{ kg m/s}^2\} \quad (3.61)$$

$$\mathcal{EA}_3 = \{m : m_{mn} \leq m \leq m_{mx}\} = \{m : 2.0 \leq m \leq 4.0 \text{ kg m/s}^2\} \quad (3.62)$$

$$\mathcal{EA}_4 = \{b : b_{mn} \leq b \leq b_{mx}\} = \{b : 4.0 \leq b \leq 5.0 \text{ kg m/s}^2\} \quad (3.63)$$

and

$$\mathcal{EM}_1 = \{r : r_{mn} \leq r \leq r_{mx}\} = \{r : 0.2 \leq r \leq 1.2 \text{ s}^{-1}\}, \quad (3.64)$$

respectively.

The resultant sample space for the vector \mathbf{e} of epistemically uncertain variables is

$$\mathcal{E} = \mathcal{EA}_1 \times \mathcal{EA}_2 \times \mathcal{EA}_3 \times \mathcal{EA}_4 \times \mathcal{EM}_1 \quad (3.65)$$

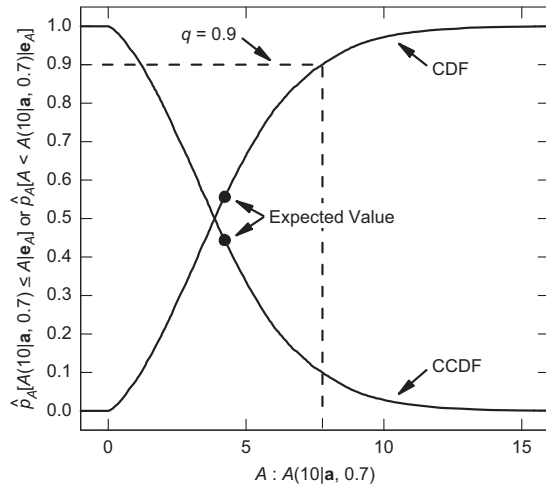


Fig. 3.8. Estimated CDF and CCDF for amplitude $A(10|\mathbf{a}, 0.7)$ with $\mathbf{e}_A = [1.0, 1.5, 3.0, 4.5]$ and $\mathbf{e}_M = [0.7]$ (i) determined with a sample of size $nSA = 10,000$ from the set \mathcal{A} of possible values for \mathbf{a} conditional on $\mathbf{e} = [\mathbf{e}_A, \mathbf{e}_M] = [1.0, 1.5, 3.0, 4.5, 0.7]$ and (ii) presented with $\hat{P}_A[A(10|\mathbf{a}, 0.7) \leq A|\mathbf{e}_A]$ and $\hat{P}_A[A < A(10|\mathbf{a}, 0.7)|\mathbf{e}_A]$ used as mnemonics for estimated probabilities of the form $\hat{P}_A[\mathcal{U}_y(10|\mathbf{e})|\mathbf{e}_A]$ and $\hat{P}_A[\mathcal{U}_y(10|\mathbf{e})|\mathbf{e}_A]$ defined in conjunction with Eq. (3.47).

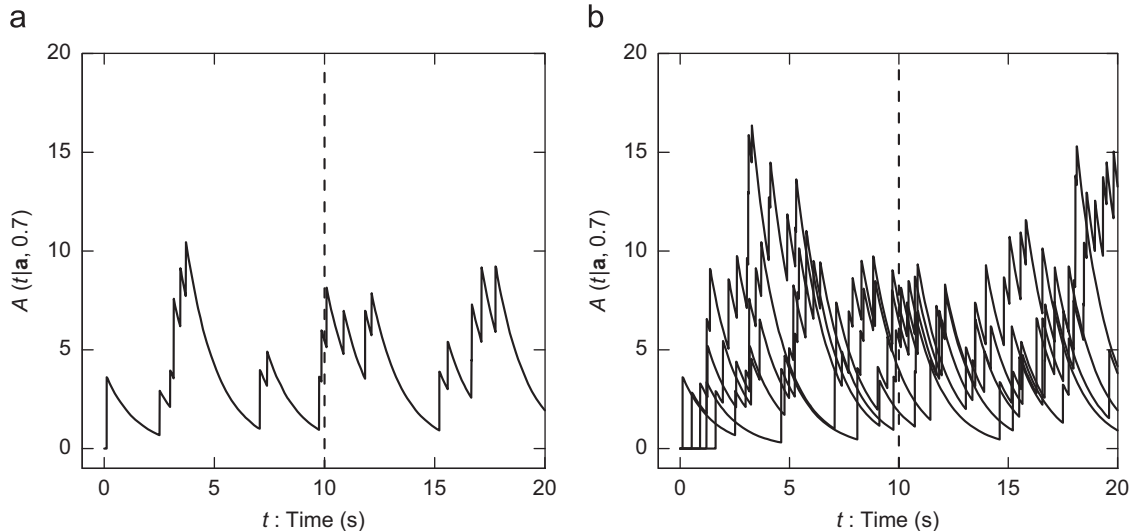


Fig. 3.9. Illustration of time-dependent amplitudes $A(t|\mathbf{a}_j, 0.7)$ used in generation of CDF and CCDF in Fig. 3.8 for aleatory uncertainty in amplitude at $t = 10$ s conditional on $\mathbf{e} = [1.0, 1.5, 3.0, 4.5, 0.7]$: (a) $A(t|\mathbf{a}_j, 0.7)$ for $j=1$, and (b) $A(t|\mathbf{a}_j, 0.7)$ for $j=1, 2, \dots, 5$.

with $\mathcal{EA}_1, \mathcal{EA}_2, \dots, \mathcal{EM}_1$ defined in Eqs. (3.60)–(3.64). Further, associated probability spaces $(\mathcal{EA}_i, \mathbb{E}\mathbb{A}_i, p_{\mathcal{EA}_i})$, $i=1, 2, 3, 4$, and $(\mathcal{EM}_1, \mathbb{E}\mathbb{M}_1, p_{\mathcal{EM}_1})$ for the individual elements of \mathbf{e} (i.e., λ , a , m , b and r) and also the probability space $(\mathcal{E}, \mathbb{E}, p_{\mathcal{E}})$ for \mathbf{e} are defined in the same manner as for the elements of $\mathbf{e} = [L, R, C, E_0, \lambda]$ in Eqs. (3.38)–(3.42).

For a given value for $\mathbf{e} = [\lambda, a, m, b, r]$, a distribution for $A(t|\mathbf{a}, \mathbf{e}_M) = A(t|\mathbf{a}, r)$ over the possible values for \mathbf{a} results for each time t as indicated in conjunction with Eq. (3.47). As an example, the CDF and CCDF for $A(t|\mathbf{a}, r)$ at $t = 10$ s conditional on $\mathbf{e} = [1.0, 1.5, 3.0, 4.5, 0.7]$ (i.e., for $A(10|\mathbf{a}, 0.7)$) is illustrated in Fig. 3.8. The results in Fig. 3.8 were generated with a random sample

$$\mathbf{a}_j, j = 1, 2, \dots, nSA, \quad (3.66)$$

of size $nSA = 10,000$ from \mathcal{A} obtained in consistency with the distributions for perturbation time t and perturbation magnitude A_0 that derive from $\lambda = 1.0 \text{ s}^{-1}$, $a = 1.5 \text{ kg m/s}^2$, $m = 3.0 \text{ kg m/s}^2$, and $b = 4.5 \text{ kg m/s}^2$ (i.e., from $\mathbf{e}_A = [1.0, 1.5, 3.0, 4.5]$). In addition, estimates for the expected value $E_A[A(10|\mathbf{a}, 0.7)|\mathbf{e}_A]$ and the $q = 0.9$ quantile $Q_{A,0.9}[A(10|\mathbf{a}, 0.7)|\mathbf{e}_A]$ for $A(10|\mathbf{a}, 0.7)$ obtained with the preceding sample as indicated in Eqs. (3.48) and (3.50) are also shown in Fig. 3.8.

A subset of the results used in the generation of Fig. 3.8 is shown in Fig. 3.9. Each of the curves in Fig. 3.9 is a plot of $A(t|\mathbf{a}_j, 0.7)$ for $0 \leq t \leq 20$ s and a specific element \mathbf{a}_j of the sample indicated in Eq. (3.66). Specifically, a plot of $A(t|\mathbf{a}_1, 0.7)$ is shown in Fig. 3.9a, and plots of $A(t|\mathbf{a}_j, 0.7)$ for $j=1, 2, \dots, 5$ are shown in Fig. 3.9b. The CDF and CCDF in Fig. 3.8 summarize the aleatory uncertainty (i.e., intrinsic variability) in the values for $A(10|\mathbf{a}, 0.7)$ associated with the vertical line originating at $t = 10$ s in Fig. 3.9 for all elements of the sample in Eq. (3.66).

The CCDF in Fig. 3.8 summarizes the aleatory uncertainty in $A(t|\mathbf{a}, 0.7)$ at $t = 10$ s as indicated by the vertical line in Fig. 3.9. Corresponding summaries are possible for each value of t in the interval under consideration. However, presentation of such summaries for a large number of values for t is cumbersome. A more compact summary is to present the expected value for $A(t|\mathbf{a}, 0.7)$ and selected quantiles for $A(t|\mathbf{a}, 0.7)$ (e.g., 0.05, 0.25, 0.5, 0.75, 0.95) as functions of time (Fig. 3.10). This format presents the primary uncertainty information for $A(t|\mathbf{a}, 0.7)$ as a function of time in a single plot. The expected values and quantiles in Fig. 3.10 are obtained from the sample in Eq. (3.66) as described in Eqs. (3.51) and (3.52) and illustrated in Fig. 3.8.

If $\mathbf{e} = [\lambda, a, m, b, r]$ was precisely known, then results of the form shown in Figs. 3.8 and 3.10 would be the unique outcomes of the analysis. However, \mathbf{e} is not precisely known and has many possible values. As a result, there are many possible values for the results in Figs. 3.8 and 3.10. For example, there are many possible values for the CDF and CCDF in Fig. 3.8 (Fig. 3.11), with each possible CDF and CCDF deriving from a different element $\mathbf{e} = [\lambda, a, m, b, r]$ of the set \mathcal{E} defined in Eq. (3.65).

Specifically, the results in Fig. 3.11 were generated with an LHS

$$\mathbf{e}_i = [\mathbf{e}_{Ai}, \mathbf{e}_{Mi}] = [\lambda_i, a_i, m_i, b_i, r_i], \quad i = 1, 2, \dots, nSE, \quad (3.67)$$

of size $nSE = 200$ from the set \mathcal{E} in consistency with the distributions that define the probability space $(\mathcal{E}, \mathbb{E}, p_E)$ for epistemic uncertainty. In turn, a different CDF and associated CCDF results for each sample element \mathbf{e}_i . Further, the individual CDFs and CCDFs were estimated with random samples

$$\mathbf{a}_j = [n_j, t_{1j}, A_{01j}, t_{2j}, A_{02j}, \dots, t_{n_j}, A_{0n_j}], \quad j = 1, 2, \dots, nSA, \quad (3.68)$$

of size $nSA = 10,000$ from \mathcal{A} generated in consistency with $\mathbf{e}_{Ai} = [\lambda_i, a_i, m_i, b_i]$ and the corresponding probability space $(\mathcal{A}, \mathbb{A}, p_A)$ for aleatory uncertainty and its associated density function $d_A(\mathbf{a}|\mathbf{e}_{Ai})$. Although not explicitly incorporated into the notation in use, the set \mathcal{A} changes for

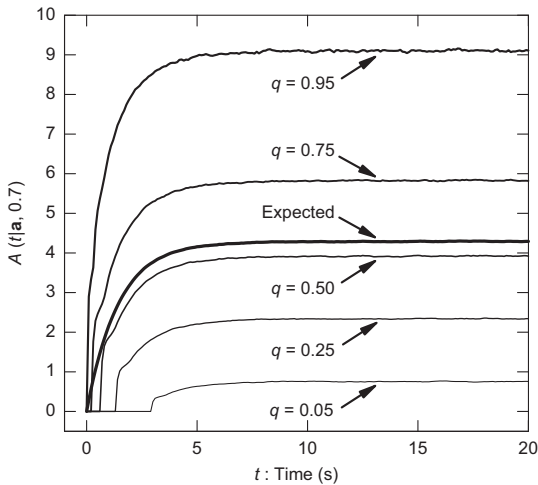


Fig. 3.10. Estimated expected value and quantile curves for aleatory uncertainty in amplitude $A(t|\mathbf{a}, 0.7)$ as a function of time conditional on $\mathbf{e} = [1.0, 1.5, 3.0, 4.5, 0.7]$.

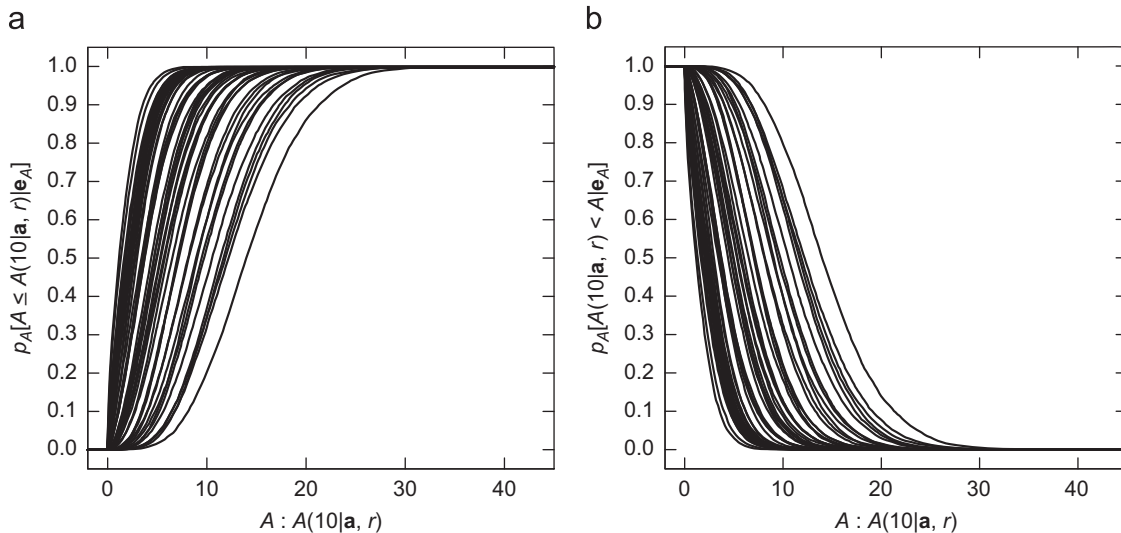


Fig. 3.11. Estimated CDFs and CCDFs for amplitude $A(10|\mathbf{a}, r)$ obtained for the first 50 elements of the LHS in Eq. (3.67) and estimated with the random samples of size $nSA = 10,000$ in Eq. (3.68) from the corresponding sets \mathcal{A} of possible values for \mathbf{a} : (a) CDFs, and (b) CCDFs.

each \mathbf{e}_{Ai} as a result of the effect of the interval $[a_i, b_i]$ on the set of possible values for the size of the perturbation associated with each occurrence of the Poisson process under consideration.

When small exceedance probabilities arising from aleatory uncertainty are the analysis outcomes of interest, CCDFs are usually plotted with log-transformed values on the ordinate (Fig. 3.12a). Use of log-transformed values allows small exceedance probabilities to be displayed; in contrast, small exceedance probabilities are difficult, and sometimes impossible, to determine from plotted results when a linear scale is used on the ordinate (e.g., compare the CCDFs in Figs. 3.11b and 3.12a). In many QMU analyses, it is likely that small exceedance probabilities will be the analysis outcomes of greatest interest.

Distributions of CDFs and CCDFs can be summarized with expected value and quantile curves as indicated in conjunction with Eqs. (3.51) and (3.52). As an example, a summary of this form is presented in Fig. 3.12b for CCDFs with log-transformed exceedance probabilities.

As indicated in conjunction with Eq. (3.53), distributions of CDFs and CCDFs can also be summarized by reducing each CDF and corresponding CCDF to an expected value and then presenting the CDF and CCDF for the resultant expected values (Fig. 3.13). Specifically, Fig. 3.13 shows the CDF and CCDF for the expected values associated with the individual CDFs and CCDFs in Figs. 3.11 and 3.12. Each expected value $\hat{E}_A[A(10|\mathbf{a}, r)|\mathbf{e}_{Ai}]$ is calculated as indicated in Eq. (3.48), and the resultant CDF and CCDF are calculated as indicated in conjunction with Eq. (3.53). In consistency with the results in Figs. 3.11 and 3.12, the preceding calculations use the samples indicated in Eqs. (3.67) and (3.68).

The estimated expected value $\hat{E}_E\{E_A[A(10|\mathbf{a}, r)|\mathbf{e}_A]\}$ over aleatory and epistemic uncertainty is also shown in Fig. 3.13 and corresponds to the estimated expected value $\hat{E}_E\{E_A[y(t|\mathbf{a}, \mathbf{e}_M)|\mathbf{e}_A]\}$ defined in Eq. (3.54). The quantity $\hat{E}_E\{E_A[A(10|\mathbf{a}, r)|\mathbf{e}_A]\}$ is the outcome of reducing all the information in Figs. 3.11 and 3.12 to a single number.

3.7. Kaplan–Garrick ordered triple representation for risk

The Kaplan–Garrick ordered triple representation for risk is introduced in conjunction with Questions Q1, Q2 and Q3 in Section 2 as a way of intuitively describing risk. More formally, this representation characterizes risk as an ordered triple of the form

$$(S_j, pS_j, \mathbf{c}S_j), \quad j = 1, 2, \dots, nS, \quad (3.69)$$

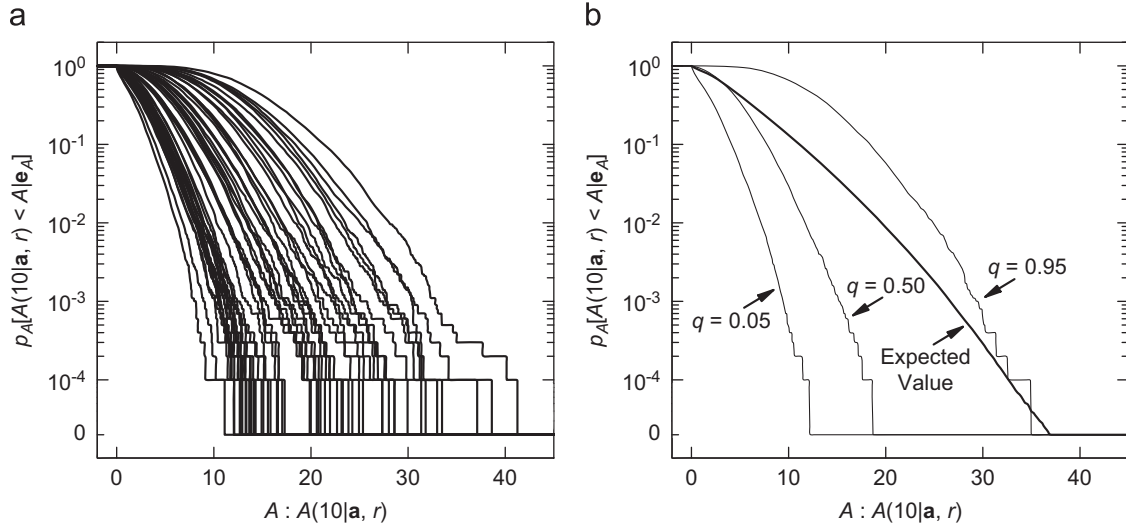


Fig. 3.12. Estimated CCDFs plotted with log-transformed exceedance probabilities for amplitude $A(10|\mathbf{a}, r)$ obtained for individual elements of the LHS in Eq. (3.67) and estimated with the random samples of size $nSA = 10,000$ in Eq. (3.68) from the corresponding sets \mathcal{A} of possible values for \mathbf{a} : (a) individual CCDFs for 50 elements in the LHS, and (b) summary statistics for the distribution of CCDFs.

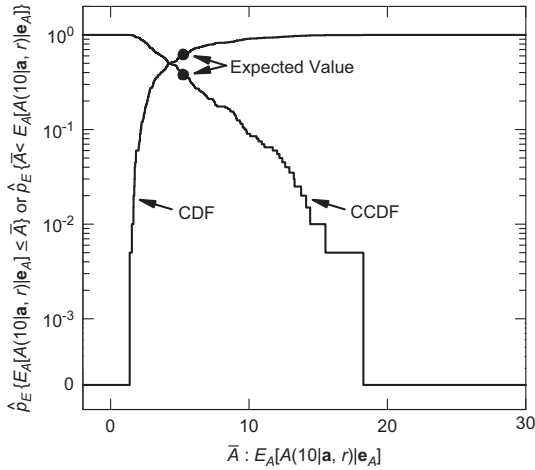


Fig. 3.13. Estimated CDF and CCDF (i) for expected values $E_A[A(10|\mathbf{a}, r_i)|\mathbf{e}_A]$, $i = 1, 2, \dots, nSE = 200$, associated with CDFs and CCDFs in Figs. 3.11 and 3.12 and (ii) with $\hat{p}_E\{E_A[A(10|\mathbf{a}, r)|\mathbf{e}_A] \leq \bar{A}\}$ and $\hat{p}_E\{\bar{A} < E_A[A(10|\mathbf{a}, r)|\mathbf{e}_A]\}$ used as mnemonics for estimated probabilities of the form $\hat{p}_E[\mathcal{U}_Y(10)]$ and $\hat{p}_E[\mathcal{U}_Y^c(10)]$ defined in conjunction with Eq. (3.53).

where S_j is a set of similar occurrences, pS_j is the probability of the set S_j , \mathbf{cS}_j is a vector of consequences associated with S_j , the sets S_j are disjoint (i.e., $S_i \cap S_j = \emptyset$ for $i \neq j$), and the set $\cup S_j$ contains all risk significant occurrences in the particular universe under consideration.

The representation in Eq. (3.69) is simply a way to describe the components of approximations to integrals of the form appearing in Eq. (3.48) obtained with stratified sampling from the sample space \mathcal{A} for aleatory uncertainty. With stratified sampling, the expected value $E_A[y(t|\mathbf{a}, \mathbf{e}_M)|\mathbf{e}_A]$ and its defining integral in Eq. (3.48) are approximated by

$$E_A[y(t|\mathbf{a}, \mathbf{e}_M)|\mathbf{e}_A] = \int_{\mathcal{A}} y(t|\mathbf{a}, \mathbf{e}_M) d\mathbf{a}(\mathbf{a}|\mathbf{e}_A) \cong \sum_{j=1}^{nSA} y(t|\mathbf{a}_j, \mathbf{e}_M) p_A(\mathcal{A}_j|\mathbf{e}_A), \quad (3.70)$$

where the \mathcal{A}_j are disjoint subsets of \mathcal{A} with $\cup \mathcal{A}_j = \mathcal{A}$, $p_A(\mathcal{A}_j|\mathbf{e}_A)$ is the probability of \mathcal{A}_j , and \mathbf{a}_j is a representative element of \mathcal{A}_j . With respect to the representation in Eq. (3.69), \mathcal{A}_j corresponds to

S_j , $p_A(\mathcal{A}_j|\mathbf{e}_A)$ corresponds to pS_j , $y(t|\mathbf{a}_j, \mathbf{e}_M)$ corresponds to an element of \mathbf{cS}_j , and nSA corresponds to nS .

In turn, the defining probabilities for CDFs and CCDFs are given by

$$p_A[y(t|\mathbf{a}, \mathbf{e}_M) \leq y|\mathbf{e}_A] \cong \sum_{j=1}^{nSA} \delta_y[y(t|\mathbf{a}_j, \mathbf{e}_M)] p_A(\mathcal{A}_j|\mathbf{e}_A) \quad (3.71)$$

and

$$p_A[y < y(t|\mathbf{a}, \mathbf{e}_M)|\mathbf{e}_A] \cong \sum_{j=1}^{nSA} \bar{\delta}_y[y(t|\mathbf{a}_j, \mathbf{e}_M)] p_A(\mathcal{A}_j|\mathbf{e}_A), \quad (3.72)$$

respectively.

In summary, the Kaplan–Garrick ordered triple representation for risk provides a simple and intuitive description of the basic components of a risk assessment. Specifically, this representation provides a display of the answers to the first three basic questions that underlie a risk assessment: (i) “What can happen?”, (ii) “How likely is it to happen?”, and (iii) “What are the consequences if it does happen?”. However, it is important to recognize that this representation is simply a way of decomposing approximations to integrals involving aleatory uncertainty into their basic components as indicated in Eqs. (3.70)–(3.72). Use of the Kaplan–Garrick ordered triple representation for risk is suggested in App. A of the NAS/NRC report on QMU [77].

3.8. Verification and validation

Verification and validation are two very important components of a QMU analysis that are intimately connected with the assessment and representation of uncertainty, where (i) verification is the process of determining that a model implementation accurately represents the developers’ conceptual description of the model and the solution to the model, and (ii) validation is the process of determining the degree to which a model is an accurate representation of the real world from the perspective of the intended uses of the model (p. 3, [107]; [108–113]).

Sampling-based sensitivity analysis as described in Ref. [56] and illustrated in Sections 4 and 5 is a powerful tool for checking for analysis errors and thus is an important component of analysis verification. Further, model validation is an important contributor

to the insights that ultimately lead to the definition of the probability space that characterizes epistemic uncertainty.

Techniques for verification and validation are not the focus of this presentation but are necessary components of a credible QMU analysis. The importance of verification and validation is emphasized in the NAS/NRC report on QMU (p. 22, Ref. [77]).

3.9. An Admonition

As the reader has undoubtedly observed, this section essentially presents the same calculation over again and over again as different expected values and probabilities are calculated. As a reminder, the probabilities that define CDFs and CCDFs are actually themselves expected values; specifically, these probabilities are expected values for indicator functions (i.e., functions of the form $\delta_x(\tilde{x})$ and $\bar{\delta}_x(\tilde{x})$ as defined in conjunction with Eq. (3.2)). What is changing in the calculations is the sample space under consideration (e.g., $\mathcal{EA}, \mathcal{EM}, \mathcal{E} = \mathcal{EA} \times \mathcal{EM}, \mathcal{A}, \dots$), the probability space associated with the sample space (e.g., $(\mathcal{EA}, \mathbb{EA}, p_{EA}), (\mathcal{EM}, \mathbb{EM}, p_{EM}), (\mathcal{E}, \mathbb{E}, p_E), (\mathcal{A}, \mathbb{A}, p_A), \dots$), and the function being integrated (e.g., $y(t|\mathbf{a}, \mathbf{e}_M), \delta_y[y(t|\mathbf{a}, \mathbf{e}_M)], \bar{\delta}_y[y(t|\mathbf{a}, \mathbf{e}_M)], E_A[y(t|\mathbf{a}, \mathbf{e}_M)|\mathcal{A}], \dots$). However, at a conceptual level, the basic calculation remains the same. The calculations are repeated to be explicit about the sample space, probability space and function involved rather than because of inherent conceptual differences in the probabilistic basis of the calculation.

Now for the admonition. When confronted with a probability or a calculation involving probability, the first two questions to ask are “What is the sample space?” and “What subset of the sample space is under consideration?”. If you do not know the answers to these two questions, then you do not know enough to meaningfully assess the probability or calculated result under consideration. Further, if the source of the probability or calculated result cannot supply precise answers to these two questions, then there is reason to be cautious with respect to the meaning and correctness of such results. Basically, having a probability without knowing the associated sample space and the subset of that sample space for which the probability is defined is analogous to knowing the answer to a question without knowing what the question is.

For the preceding reason, this section has been very explicit in stating the sample space and the relevant subsets of that sample as different quantities have been introduced and defined. This results in some repetition at a conceptual level but has the positive effect of unambiguously defining the individual quantities under consideration.

4. QMU with epistemic uncertainty: characterization with probability

The use of probability to represent the epistemic uncertainty associated with results of the form

$$y(t|\mathbf{a}, \mathbf{e}_M) = f(t|\mathbf{a}, \mathbf{e}_M) \quad (4.1)$$

is extensively discussed in Section 3.3, where $y(t|\mathbf{a}, \mathbf{e}_M)$ is a generic real-valued quantity conditional on a specific realization \mathbf{a} of aleatory uncertainty and \mathbf{e}_M is a vector of epistemically uncertain analysis inputs. The result $y(t|\mathbf{a}, \mathbf{e}_M)$ is epistemically uncertain as a consequence of the epistemic uncertainty associated with the elements of \mathbf{e}_M . Given that the realization \mathbf{a} of aleatory uncertainty is fixed, analyses related to $y(t|\mathbf{a}, \mathbf{e}_M)$ involve two of the three basic analysis components discussed in Section 3.2: (i) EN2, a model that predicts system behavior (i.e., a function $f(t|\mathbf{a}, \mathbf{e}_M)$), and (ii) EN3, a probabilistic characterization of epistemic uncertainty (i.e., a probability space $(\mathcal{EM}, \mathbb{EM}, p_{EM})$ that characterizes the epistemic uncertainty associated with the elements of \mathbf{e}_M).

Margins can be defined for $y(t|\mathbf{a}, \mathbf{e}_M)$ in a variety of ways, and in turn, the epistemic uncertainty associated with \mathbf{e}_M results in uncertainty in $y(t|\mathbf{a}, \mathbf{e}_M)$ and the margins that derive from $y(t|\mathbf{a}, \mathbf{e}_M)$. At an intuitive level, a margin corresponds to a difference between a required level of performance and an estimated level of performance, with a positive margin indicating that the required level of performance is met and a negative margin indicating that the required level of performance is not met. Multiple examples of how margins could be defined are introduced in this section, in Section 5 and also in Ref. [80].

This section uses the function $Q(t|\mathbf{a}, \mathbf{e}_M)$ introduced in Section 3.4 to illustrate a variety of ways in which QMU analyses could arise and be carried out in the context of analyses that involve a generic result $y(t|\mathbf{a}, \mathbf{e}_M)$ of the form indicated in Eqs. (3.24) and (4.1). Further,

$$\mathbf{e}_M = [e_{M1}, e_{M2}, e_{M3}, e_{M4}, e_{M5}] = [L, R, C, E_0, \lambda] \quad (4.2)$$

has the properties defined in conjunction with Eq. (3.32), and the corresponding probability space $(\mathcal{EM}, \mathbb{EM}, p_{EM})$ that characterizes the epistemic uncertainty associated with \mathbf{e}_M is defined in conjunction with Eqs. (3.33)–(3.43). The time-dependent behavior of $Q(t|\mathbf{a}, \mathbf{e}_M)$ is illustrated in Fig. 3.5.

The examples presented in this section use an LHS

$$\mathbf{e}_{Mi} = [e_{M1,i}, e_{M2,i}, \dots, e_{M5,i}] = [L_i, R_i, C_i, E_{0i}, \lambda_i], \quad i = 1, 2, \dots, nSE = 200, \quad (4.3)$$

from \mathcal{EM} generated in consistency with the distributions that define the probability space $(\mathcal{EM}, \mathbb{EM}, p_{EM})$. In turn, evaluation of $Q(t|\mathbf{a}, \mathbf{e}_{Mi})$ for elements of the preceding sample produces a mapping

$$[\mathbf{e}_{Mi}, Q(t|\mathbf{a}, \mathbf{e}_{Mi})], \quad i = 1, 2, \dots, nSE = 200, \quad (4.4)$$

from uncertain analysis inputs to analysis results that is used in the generation of the example results presented in this section.

The following topics related to QMU in the presence of only epistemic uncertainty are considered in this section: epistemic uncertainty with a specified bound (Section 4.1), epistemic uncertainty with a specified bounding interval (Section 4.2), epistemic uncertainty with a specified bounding interval over time (Section 4.3), epistemic uncertainty with an uncertain bound (Section 4.4), and information loss associated with a “margin/uncertainty” ratio (Section 4.5). The bounds considered in Sections 4.1–4.4 correspond to the requirements that give rise to margins (i.e., the differences between required system performance and predicted system performance).

As indicated at the beginning of Section 3.3, the NAS/NRC report on QMU emphasizes the importance of the quantification of the epistemic uncertainty in analysis results that derives from epistemic uncertainty in analysis inputs (Recommendation 1–2, p. 22, Ref. [77]). The results presented in Sections 4.1–4.4 illustrate analyses of this type.

4.1. Epistemic uncertainty with a specified bound

For this example, a fixed bound is assumed to exist with respect to the value for $Q(0.1|\mathbf{a}, \mathbf{e}_M)$. Possibilities include lower bounds on $Q(0.1|\mathbf{a}, \mathbf{e}_M)$ (e.g., $Q_{b1} = 0.075$ and $Q_{b2} = 0.09$ in Fig. 4.1a) and upper bounds on $Q(0.1|\mathbf{a}, \mathbf{e}_M)$ (e.g., $Q_{b3} = 0.105$ and $Q_{b4} = 0.125$ in Fig. 4.1b). Consistent with the nature of the bounds being illustrated, the distribution of possible values for $Q(0.1|\mathbf{a}, \mathbf{e}_M)$ is summarized with a CDF in Fig. 4.1a, and the distribution of possible values for $Q(0.1|\mathbf{a}, \mathbf{e}_M)$ is summarized with a CCDF in Fig. 4.1b. Specifically, the CDF in Fig. 4.1a displays the probability of being less than a specific bound, which is the probability of interest for the lower bounds Q_{b1} and Q_{b2} , and the CCDF in Fig. 4.1b displays the probability of being greater than a specified bound, which is the probability of interest for the upper bounds

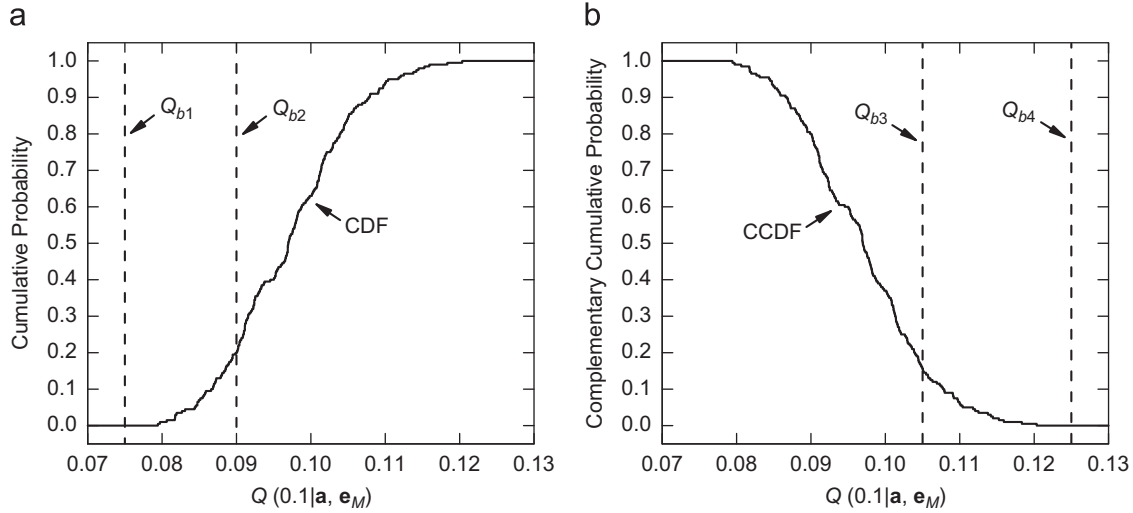


Fig. 4.1. Example bounds on $Q(0.1|\mathbf{a}, \mathbf{e}_M)$: (a) lower bounds $Q_{b1}=0.075$ and $Q_{b2}=0.09$ and estimated CDF for $Q(0.1|\mathbf{a}, \mathbf{e}_M)$, and (b) upper bounds $Q_{b3}=0.105$ and $Q_{b4}=0.125$ and estimated CCDF for $Q(0.1|\mathbf{a}, \mathbf{e}_M)$.

Q_{b3} and Q_{b4} . The CDF and CCDF in Fig. 4.1 were generated with the sample and associated mapping in Eqs. (4.3) and (4.4) as described in conjunction with Eq. (3.25).

For notational simplicity, the ordinates in Fig. 4.1a and b are assigned the labels “Cumulative Probability” and “Complementary Cumulative Probability” rather than the more explicit but also more complex labeling used with CDFs and CCDFs in Section 3. This labeling convention is also used with other similar Figures.

All sampled values for $Q(0.1|\mathbf{a}, \mathbf{e}_{Mi})$ are above the bound Q_{b1} . However, this is not the case for Q_{b2} , with the CDF in Fig. 4.1a indicating that the probability of $Q(0.1|\mathbf{a}, \mathbf{e}_M)$ being below $Q_{b2}=0.09$ is approximately 0.200.

All sampled values for $Q(0.1|\mathbf{a}, \mathbf{e}_{Mi})$ are below the bound Q_{b4} . However, this is not the case for Q_{b3} , with the CCDF in Fig. 4.1b indicating that the probability of $Q(0.1|\mathbf{a}, \mathbf{e}_M)$ being above $Q_{b3}=0.105$ is approximately 0.155.

The margins between $Q(0.1|\mathbf{a}, \mathbf{e}_M)$ and the bounds Q_{bk} , $k=1, 2, 3, 4$, indicated in Fig. 4.1 are defined by

$$Q_{mk}(0.1|\mathbf{a}, \mathbf{e}_M) = \begin{cases} Q(0.1|\mathbf{a}, \mathbf{e}_M) - Q_{bk} & \text{for } k=1, 2 \\ Q_{bk} - Q(0.1|\mathbf{a}, \mathbf{e}_M) & \text{for } k=3, 4, \end{cases} \quad (4.5)$$

with $Q_{mk}(0.1|\mathbf{a}, \mathbf{e}_M) > 0$ indicating that a specified bound is satisfied and $Q_{mk}(0.1|\mathbf{a}, \mathbf{e}_M) < 0$ indicating that a specified bound is not satisfied (i.e., a positive margin is good and a negative margin is bad). As a result of $Q(0.1|\mathbf{a}, \mathbf{e}_M)$ being epistemically uncertain, the corresponding margins $Q_{mk}(0.1|\mathbf{a}, \mathbf{e}_M)$, $k=1, 2, 3, 4$, are also epistemically uncertain and have an uncertainty structure that derives from the uncertainty structure assumed for \mathbf{e}_M (Fig. 4.2). Representations of the form shown in Fig. 4.2 provide a complete display of the uncertainty associated with the margins $Q_{mk}(0.1|\mathbf{a}, \mathbf{e}_M)$, $k=1, 2, 3, 4$, and thus a complete QMU representation of margin uncertainty.

An alternative format involves the use of normalized margins defined by

$$Q_{nk}(0.1|\mathbf{a}, \mathbf{e}_M) = Q_{mk}(0.1|\mathbf{a}, \mathbf{e}_M) / Q_{bk} = \begin{cases} [Q(0.1|\mathbf{a}, \mathbf{e}_M) - Q_{bk}] / Q_{bk} & \text{for } k=1, 2 \\ [Q_{bk} - Q(0.1|\mathbf{a}, \mathbf{e}_M)] / Q_{bk} & \text{for } k=3, 4, \end{cases} \quad (4.6)$$

which expresses margin as a fraction of the corresponding bounding value (Fig. 4.3). This format has the advantage in that it presents margin as a multiple of the bounding value, which is a presentation format that some individuals prefer. However, it has the disadvantage that it does not present the actual size of the margin.

It is sometimes stated that QMU corresponds to the determination of the ratio “margin/uncertainty.” Unfortunately, it is not always apparent how this imagined concept translates into quantities that are mathematically defined and conceptually useful. In contrast, margin results of the form illustrated in Fig. 4.2 are mathematically well-defined, computationally practicable, and meaningful in a decision context as all available information about margins and their associated uncertainty is presented.

Two possible definitions of “margin/uncertainty” for an arbitrary margin $Q_m(t|\mathbf{a}, \mathbf{e}_M)$ (e.g., $Q_{mk}(0.1|\mathbf{a}, \mathbf{e}_M)$ for $k=1, 2, 3$ or 4) are

$$Q_{m/u}(t|\mathbf{a}, \mathbf{e}_M) = \frac{Q_{m,0.5}(t|\mathbf{a}, \mathbf{e}_M)}{Q_{m,0.5}(t|\mathbf{a}, \mathbf{e}_M) - Q_{m,0.05}(t|\mathbf{a}, \mathbf{e}_M)} \quad (4.7)$$

and

$$\bar{Q}_{m/u}(t|\mathbf{a}, \mathbf{e}_M) = \frac{\bar{Q}_m(t|\mathbf{a}, \mathbf{e}_M)}{\bar{Q}_m(t|\mathbf{a}, \mathbf{e}_M) - Q_{m,0.05}(t|\mathbf{a}, \mathbf{e}_M)}, \quad (4.8)$$

where (i) $Q_{m,0.5}(t|\mathbf{a}, \mathbf{e}_M)$ is the median (i.e., $q=0.5$ quantile) for $Q_m(t|\mathbf{a}, \mathbf{e}_M)$, (ii) $Q_{m,0.05}(t|\mathbf{a}, \mathbf{e}_M)$ is the 0.05 quantile for $Q_m(t|\mathbf{a}, \mathbf{e}_M)$, and (iii) $\bar{Q}_m(t|\mathbf{a}, \mathbf{e}_M)$ is the expected value for $Q_m(t|\mathbf{a}, \mathbf{e}_M)$.

As illustrated in Fig. 4.2, quantities such as $Q_{m,0.5}(t|\mathbf{a}, \mathbf{e}_M)$, $Q_{m,0.05}(t|\mathbf{a}, \mathbf{e}_M)$ and $\bar{Q}_m(t|\mathbf{a}, \mathbf{e}_M)$ are typically estimated with sampling-based procedures. With respect to the more detailed notation used in Sections 3.3 and 3.4, $Q_{m,0.5}(t|\mathbf{a}, \mathbf{e}_M)$ and $Q_{m,0.05}(t|\mathbf{a}, \mathbf{e}_M)$ correspond to $Q_{EMq}[Q_m(t|\mathbf{a}, \mathbf{e}_M)]$ for $q=0.5$ and 0.05, respectively, and $\bar{Q}_m(t|\mathbf{a}, \mathbf{e}_M)$ corresponds to $E_{EM}[Q_m(t|\mathbf{a}, \mathbf{e}_M)]$.

The quantities $Q_{m/u}(t|\mathbf{a}, \mathbf{e}_M)$ and $\bar{Q}_{m/u}(t|\mathbf{a}, \mathbf{e}_M)$ defined in Eqs. (4.7) and (4.8) are based on using the median and mean margins $Q_{m,0.5}(t|\mathbf{a}, \mathbf{e}_M)$ and $\bar{Q}_m(t|\mathbf{a}, \mathbf{e}_M)$ as best estimates for an uncertain margin and then defining uncertainty as the difference between this best estimate and a low quantile (e.g., $q=0.05$) of the uncertainty distribution for margin. In general, large positive margins are good and small or negative margins are bad; in turn, margins associated with small quantiles correspond to small differences between required bounds and predicted system behavior and thus are less desirable than margins associated with larger quantiles. As a result, the differences in the denominators in Eqs. (4.7) and (4.8) provides a measure of the epistemic uncertainty present in the determination of the margin under consideration.

At least notionally, values for $Q_{m/u}(t|\mathbf{a}, \mathbf{e}_M)$ and $\bar{Q}_{m/u}(t|\mathbf{a}, \mathbf{e}_M)$ significantly larger than 1 are good because this situation results when $Q_{m,0.5}(t|\mathbf{a}, \mathbf{e}_M)$ and $\bar{Q}_m(t|\mathbf{a}, \mathbf{e}_M)$ are close to $Q_{m,0.05}(t|\mathbf{a}, \mathbf{e}_M)$ in value, which in turn implies that there is little epistemic

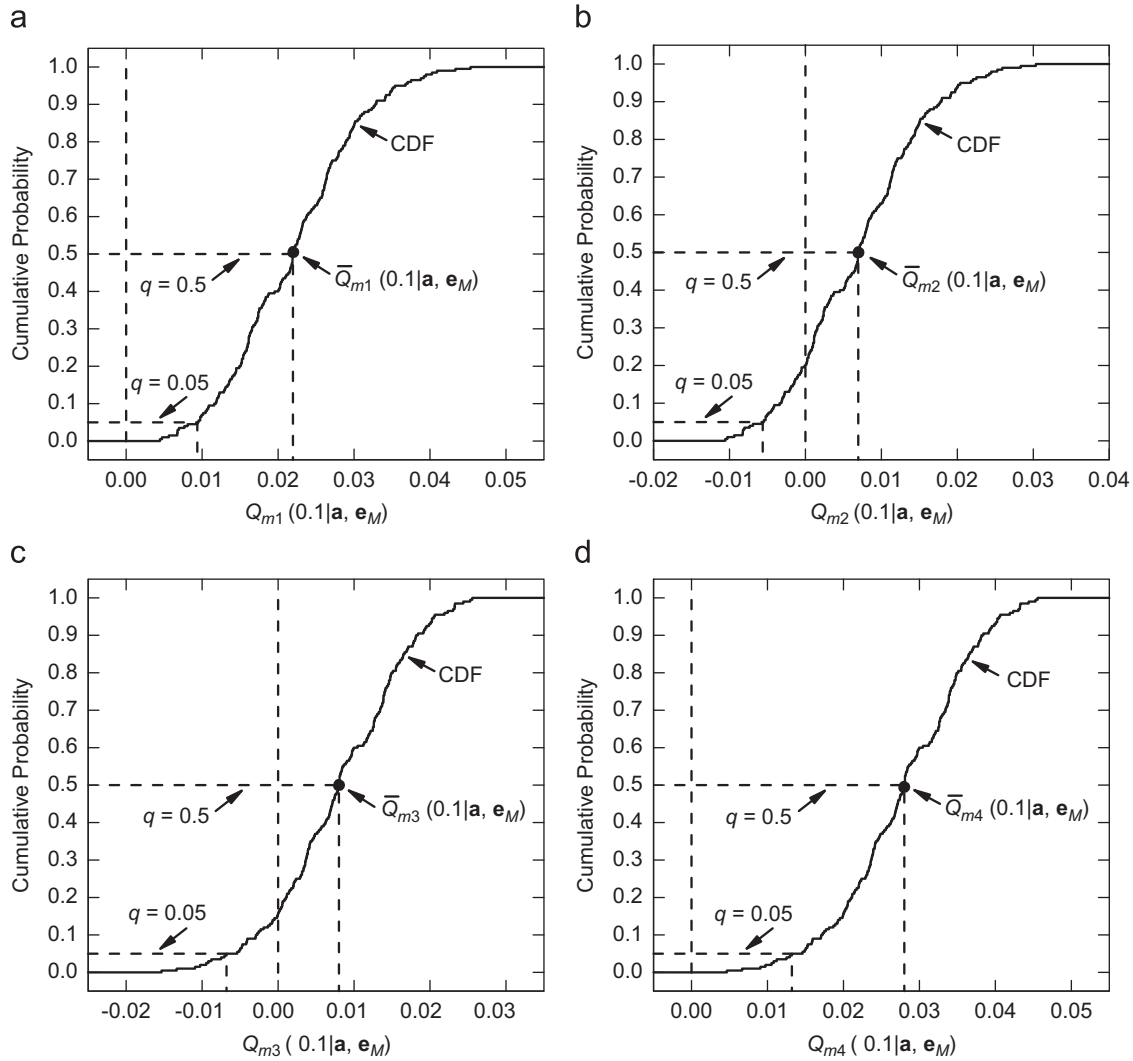


Fig. 4.2. Estimated CDFs for margins $Q_{mk}(0.1|\mathbf{a}, \mathbf{e}_M)$ associated with bounds Q_{bk} for $k=1, 2, 3, 4$: (a) $Q_{m1}(0.1|\mathbf{a}, \mathbf{e}_M)$ for $Q_{b1}=0.075$, (b) $Q_{m2}(0.1|\mathbf{a}, \mathbf{e}_M)$ for $Q_{b2}=0.09$, (c) $Q_{m3}(0.1|\mathbf{a}, \mathbf{e}_M)$ for $Q_{b3}=0.105$, and (d) $Q_{m4}(0.1|\mathbf{a}, \mathbf{e}_M)$ for $Q_{b4}=0.125$.

uncertainty present in the estimation of the margin under consideration. However, values for $Q_{m/u}(t|\mathbf{a}, \mathbf{e}_M)$ and $\bar{Q}_{m/u}(t|\mathbf{a}, \mathbf{e}_M)$ significantly greater than 1 do not exclude the undesirable situation in which the estimated margins are very close to 0. Values for $Q_{m/u}(t|\mathbf{a}, \mathbf{e}_M)$ and $\bar{Q}_{m/u}(t|\mathbf{a}, \mathbf{e}_M)$ equal to or only slightly larger than 1 are undesirable because this situation results when $Q_{m,0.05}(t|\mathbf{a}, \mathbf{e}_M)$ is equal to or only slightly larger than 0, and values for $Q_{m/u}(t|\mathbf{a}, \mathbf{e}_M)$ and $\bar{Q}_{m/u}(t|\mathbf{a}, \mathbf{e}_M)$ less than 1 are bad because this situation results when $Q_{m,0.05}(t|\mathbf{a}, \mathbf{e}_M)$ is negative. It is important to recognize that very different distributions for $Q_m(t|\mathbf{a}, \mathbf{e}_M)$ can result in similar values for $Q_{m/u}(t|\mathbf{a}, \mathbf{e}_M)$ and also for $\bar{Q}_{m/u}(t|\mathbf{a}, \mathbf{e}_M)$. As a result, consideration of only summary values such as $Q_{m/u}(t|\mathbf{a}, \mathbf{e}_M)$ and $\bar{Q}_{m/u}(t|\mathbf{a}, \mathbf{e}_M)$ can result in an incomplete and potentially misleading assessment of the implications of the uncertainty associated with the margin $Q_m(t|\mathbf{a}, \mathbf{e}_M)$. Additional discussion of the nature of “margin/uncertainty” results is provided in Section 4.5.

For the example margins under consideration in this section (Fig. 4.2) and the normalization defined in Eq. (4.7), the values for $Q_{m/u}(0.1|\mathbf{a}, \mathbf{e}_M)$ are

$$Q_{m/u,1}(0.1|\mathbf{a}, \mathbf{e}_M) = 0.022 / (0.022 - 0.009) = 1.7, \quad (4.9)$$

$$Q_{m/u,2}(0.1|\mathbf{a}, \mathbf{e}_M) = 0.0070 / [0.0070 - (-0.0056)] = 0.56, \quad (4.10)$$

$$Q_{m/u,3}(0.1|\mathbf{a}, \mathbf{e}_M) = 0.0080 / [0.0080 - (-0.0068)] = 0.54, \quad (4.11)$$

and

$$Q_{m/u,4}(0.1|\mathbf{a}, \mathbf{e}_M) = 0.028 / (0.028 - 0.013) = 1.9. \quad (4.12)$$

The values for $\bar{Q}_{m/u,k}(0.1|\mathbf{a}, \mathbf{e}_M)$ are essentially the same as the values for $Q_{m/u,k}(0.1|\mathbf{a}, \mathbf{e}_M)$ in Eqs. (4.9)–(4.12) because of the similarity of the mean and median values for $Q_{mk}(0.1|\mathbf{a}, \mathbf{e}_M)$ (see Fig. 4.2). However, such similarity will not exist in many analyses.

As discussed in Section 4.5, “margin/uncertainty” ratios of the form defined in Eqs. (4.7) and (4.8) and illustrated in Eqs. (4.9)–(4.12) are in (i) the interval $[1, +\infty)$ if the best margin estimate (e.g., the mean or median) is positive and the lower margin estimate (e.g., the 0.05 quantile) is nonnegative, (ii) the interval $[0, 1)$ if the best margin estimate is nonnegative and the lower margin estimate is negative, and (iii) the interval $(-\infty, 0)$ if the best margin estimate and the lower margin estimate are both negative. With respect to the preceding statements, it is tacitly assumed that the best margin estimate is greater than the lower margin estimate. Further, the indicated ratio (i) equals 1 only when the best estimate is positive and the lower estimate is 0, (ii) equals 0 only when the best estimate is 0 and the lower estimate is negative, and (iii) is undefined when the best estimate

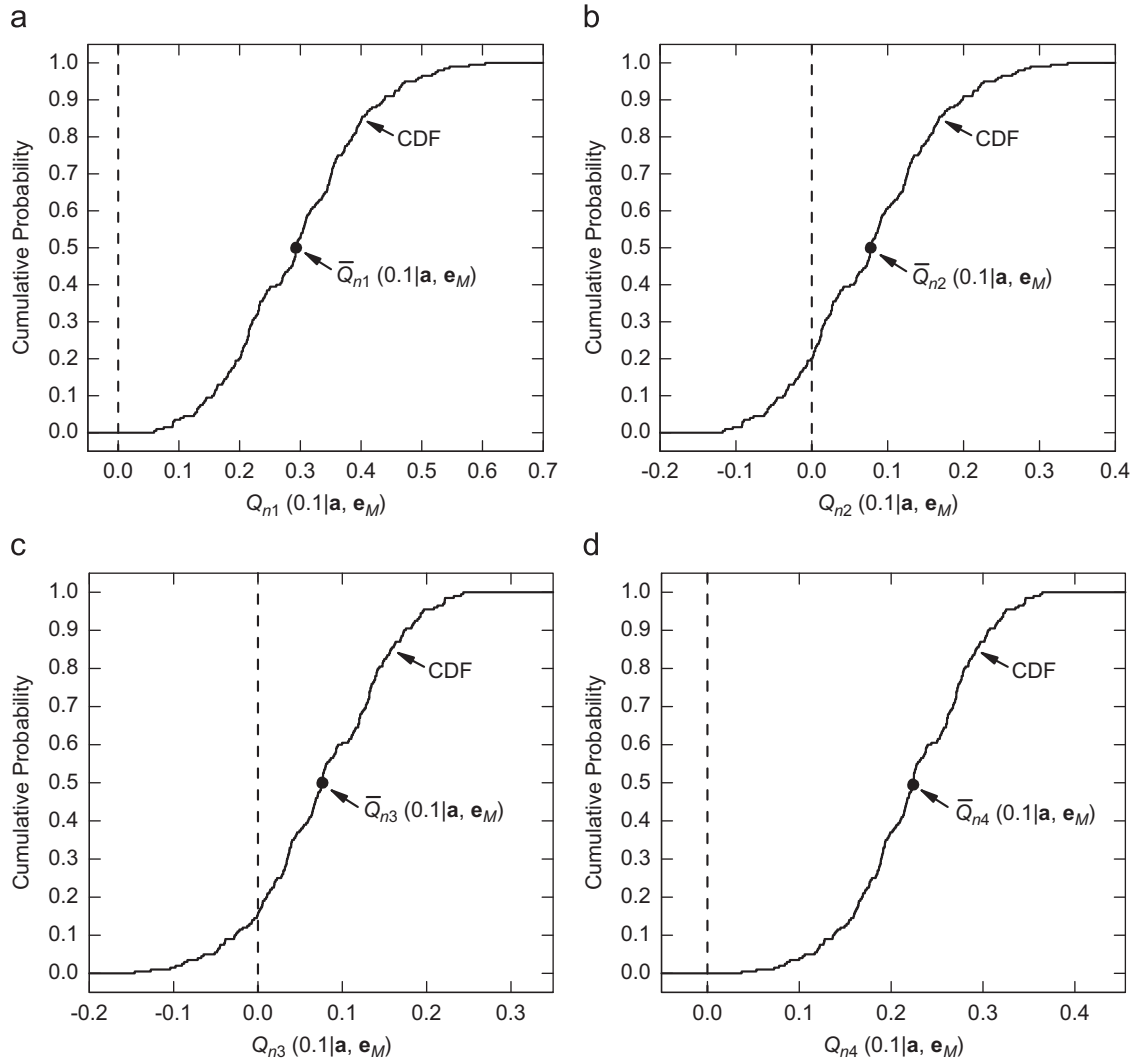


Fig. 4.3. Estimated CDFs for normalized margins $Q_{nk}(0.1|\mathbf{a}, \mathbf{e}_M)$ associated with bounds Q_{bk} for $k=1, 2, 3, 4$: (a) $Q_{n1}(0.1|\mathbf{a}, \mathbf{e}_M)$ for $Q_{b1}=0.075$, (b) $Q_{n2}(0.1|\mathbf{a}, \mathbf{e}_M)$ for $Q_{b2}=0.09$, (c) $Q_{n3}(0.1|\mathbf{a}, \mathbf{e}_M)$ for $Q_{b3}=0.105$, and (d) $Q_{n4}(0.1|\mathbf{a}, \mathbf{e}_M)$ for $Q_{b4}=0.125$.

and the lower estimate are equal. Consistent with the indicated relationships, the “margin/uncertainty” ratios $Q_{m/u,1}(0.1|\mathbf{a}, \mathbf{e}_M)=1.7$ and $Q_{m/u,4}(0.1|\mathbf{a}, \mathbf{e}_M)=1.9$ in Eqs. (4.9)–(4.12) are greater than 1 because both the best and lower margin estimates are nonnegative, and the “margin/uncertainty” ratios $Q_{m/u,2}(0.1|\mathbf{a}, \mathbf{e}_M)=0.56$ and $Q_{m/u,3}(0.1|\mathbf{a}, \mathbf{e}_M)=0.54$ in Eqs. (4.10) and (4.11) are in the interval $(0, 1)$ because the best and lower margin estimates are positive and negative, respectively.

The “margin/uncertainty” results defined in Eqs. (4.7) and (4.8) and illustrated in Eqs. (4.9)–(4.12) reduce the individual CDFs in Fig. 4.2 to single numbers. As a result, a large amount of information is lost in this reduction. Further, as discussed and illustrated in Section 4.5, a “margin/uncertainty” ratio provides no information on the actual values for the best and lower margin values used in the determination of this ratio. Thus, for example, there is no way to use the results in Eqs. (4.9)–(4.12) to retrieve the margin values used in the determination of these results. Simply put, all the information in Figs. 4.1 and 4.2 has been lost.

At their most extreme, $Q_{m/u}(t|\mathbf{a}, \mathbf{e}_M)$ and $\bar{Q}_{m/u}(t|\mathbf{a}, \mathbf{e}_M)$ have the forms

$$Q_{m/u}(t|\mathbf{a}, \mathbf{e}_M) = \frac{Q_{m,0.5}(t|\mathbf{a}, \mathbf{e}_M)}{Q_{m,0.5}(t|\mathbf{a}, \mathbf{e}_M) - Q_{m,0.00}(t|\mathbf{a}, \mathbf{e}_M)} \quad (4.13)$$

and

$$\bar{Q}_{m/u}(t|\mathbf{a}, \mathbf{e}_M) = \frac{\bar{Q}_m(t|\mathbf{a}, \mathbf{e}_M)}{\bar{Q}_m(t|\mathbf{a}, \mathbf{e}_M) - Q_{m,0.00}(t|\mathbf{a}, \mathbf{e}_M)}, \quad (4.14)$$

where

$$Q_{m,0.00}(t|\mathbf{a}, \mathbf{e}_M) = 0.00 \text{ quantile for } Q_m(t|\mathbf{a}, \mathbf{e}_M) \\ = \inf\{Q_m(t|\mathbf{a}, \mathbf{e}_M) : \mathbf{e}_M \in \mathcal{E}\}.$$

In words, $Q_{m,0.00}(t|\mathbf{a}, \mathbf{e}_M)$ is the smallest possible value for the margin $Q_m(t|\mathbf{a}, \mathbf{e}_M)$. As a result of the inequality

$$Q_{m,0.00}(t|\mathbf{a}, \mathbf{e}_M) \leq Q_{m,0.05}(t|\mathbf{a}, \mathbf{e}_M), \quad (4.15)$$

use of $Q_{m,0.00}(t|\mathbf{a}, \mathbf{e}_M)$ in the definition of $Q_{m/u}(t|\mathbf{a}, \mathbf{e}_M)$ and $\bar{Q}_{m/u}(t|\mathbf{a}, \mathbf{e}_M)$ results in smaller values for these quantities than the use of $Q_{m,0.05}(t|\mathbf{a}, \mathbf{e}_M)$.

For the example margins under consideration in this section, the values for $Q_{m/u}(0.1|\mathbf{a}, \mathbf{e}_M)$ obtained with $Q_{m,0.00}(0.1|\mathbf{a}, \mathbf{e}_M)$ as indicated in Eq. (4.13) are

$$Q_{m/u,1}(0.1|\mathbf{a}, \mathbf{e}_M) = 0.022/(0.022 - 0.004) = 1.2, \quad (4.16)$$

$$Q_{m/u,2}(0.1|\mathbf{a}, \mathbf{e}_M) = 0.0070/[0.0070 - (-0.0106)] = 0.40, \quad (4.17)$$

$$Q_{m/u,3}(0.1|\mathbf{a}, \mathbf{e}_M) = 0.0080/[0.0080 - (-0.0153)] = 0.34, \quad (4.18)$$

and

$$Q_{m/u,4}(0.1|\mathbf{a}, \mathbf{e}_M) = 0.028/(0.028-0.005) = 1.2. \quad (4.19)$$

Again, the values for $\bar{Q}_{m/u,k}(0.1|\mathbf{a}, \mathbf{e}_M)$ defined in Eq. (4.14) are very similar to the values for $Q_{m/u,k}(0.1|\mathbf{a}, \mathbf{e}_M)$ defined in Eq. (4.13) because of the similarity of the mean and median values for $Q_{mk}(0.1|\mathbf{a}, \mathbf{e}_M)$. As noted in conjunction with the inequality in Eq. (4.15), “margin/uncertainty” ratios obtained with $Q_{m,0.00}(0.1|\mathbf{a}, \mathbf{e}_M)$ are smaller than the ratios obtained with $Q_{m,0.05}(0.1|\mathbf{a}, \mathbf{e}_M)$ (i.e., compare results in Eqs. (4.9)–(4.12) with results in Eqs. (4.16)–(4.19)).

The importance of sensitivity analysis is recognized in the NAS/NRC report on QMU (pp. 14–15, Ref. [77]). Indeed, sensitivity analysis should be an integral part of any QMU analysis. As an example, a sensitivity analysis for $Q(0.1|\mathbf{a}, \mathbf{e}_M)$ based on stepwise regression analysis is presented in Table 4.1. Specifically, stepwise regression analysis is used to explore the mapping

$$[\mathbf{e}_{Mi}, Q(0.1|\mathbf{a}, \mathbf{e}_{Mi})], \quad i = 1, 2, \dots, nSE = 200, \quad (4.20)$$

used to generate the uncertainty results in Figs. 4.1–4.3. With this procedure, variable importance is indicated by the order in which variables are selected in the stepwise process, the incremental changes in R^2 values with the entry of individual variables into the regression model, and the sizes and signs of the standardized regression coefficients (SRCs) in the final regression model (see Ref. [56] for additional discussion of regression-based sensitivity analysis).

As examination of Table 4.1 shows, the dominant variables affecting the uncertainty in $Q(0.1|\mathbf{a}, \mathbf{e}_M)$ are E_0 and C . Specifically, the positive SRCs associated with E_0 and C indicate that $Q(0.1|\mathbf{a}, \mathbf{e}_M)$ tends to increase in value as each of these variables increases.

Table 4.1
Stepwise regression analysis to identify uncertain variables affecting $Q(0.1|\mathbf{a}, \mathbf{e}_M)$.

Step ^a	Variable ^b	SRC ^c	R^{2d}
1	E_0	0.70	0.51
2	C	0.63	0.91
3	R	−0.22	0.96
4	λ	−0.12	0.98
5	L	0.06	0.98

^a Steps in stepwise regression analysis with an α -value of 0.01 or less required for a variable to enter a regression model.

^b Variables listed in the order of selection in regression analysis.

^c SRCs for variables in final regression model.

^d Cumulative R^2 value with entry of each variable into regression model.

In addition, small negative effects are indicated for R and λ , and a small positive effect is indicated for L .

The examination of scatterplots is also an informative part of sampling-based sensitivity analysis. For example, the scatterplots in Fig. 4.4 clearly reveal the positive effects of E_0 and C on $Q(0.1|\mathbf{a}, \mathbf{e}_M)$ and the resultant outcomes that negative or small positive margins associated with requirements Q_{b1} and Q_{b2} occur for small values of E_0 and C and (ii) negative or small positive margins associated with requirements Q_{b3} and Q_{b4} occur for large values of E_0 and C .

Regression-based sensitivity analysis could also be carried out for the margins $Q_{mk}(0.1|\mathbf{a}, \mathbf{e}_M)$, $k=1, 2, 3, 4$, defined in Eq. (4.5) and illustrated in Fig. 4.2. However, given that the margins are simply affine transformations (i.e., linear scalings plus constant shifts) of $Q(0.1|\mathbf{a}, \mathbf{e}_M)$ defined by the bounds Q_{bk} , $k=1, 2, 3, 4$, the resultant regression analyses for $Q_{mk}(0.1|\mathbf{a}, \mathbf{e}_M)$, $k=1, 2$, would be the same as presented in Table 4.1 as a result of the defining transformation

$$Q_{mk}(0.1|\mathbf{a}, \mathbf{e}_M) = Q(0.1|\mathbf{a}, \mathbf{e}_M) - Q_{bk} \quad (4.21)$$

for $k=1, 2$, and the resultant regression analyses for $Q_{mk}(0.1|\mathbf{a}, \mathbf{e}_M)$, $k=3, 4$, would also be the same as presented in Table 4.1 except for a reversal in the signs of the SRCs as a result of the defining transformation

$$Q_{mk}(0.1|\mathbf{a}, \mathbf{e}_M) = Q_{bk} - Q(0.1|\mathbf{a}, \mathbf{e}_M) \quad (4.22)$$

for $k=3, 4$. Similarly, the scatterplots for the margins $Q_{mk}(0.1|\mathbf{a}, \mathbf{e}_M)$, $k=1, 2, 3, 4$, would effectively convey the same information as the scatterplots for $Q(0.1|\mathbf{a}, \mathbf{e}_M)$ in Fig. 4.4.

4.2. Epistemic uncertainty with a specified bounding interval

A QMU problem involving a bounding interval rather than simply an upper or lower bound is now considered. Specifically, the problem involves a specified interval within which the quantity of interest is required to be located. For the quantity $Q(0.1|\mathbf{a}, \mathbf{e}_M)$, this involves the specification of an interval $[Q_b, \bar{Q}_b]$ such that the inequalities

$$Q_b \leq Q(0.1|\mathbf{a}, \mathbf{e}_M) \leq \bar{Q}_b \quad (4.23)$$

hold (Fig. 4.5). For illustration, $[Q_b, \bar{Q}_b]$ is assumed to equal $[0.08, 0.12]$ as indicated in Fig. 4.5. This example corresponds to consideration of what is called a “gate” in some discussions of QMU [1,4].

There are several ways in which the epistemic uncertainty associated with compliance with the specified bounds can be

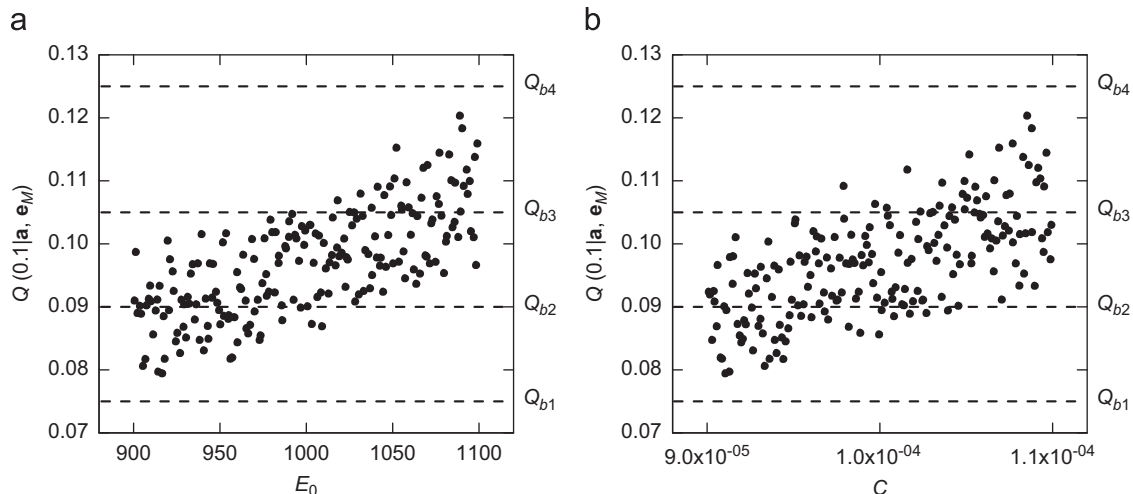


Fig. 4.4. Scatterplots for $Q(0.1|\mathbf{a}, \mathbf{e}_M)$: (a) $[E_{0i}, Q(0.1|\mathbf{a}, \mathbf{e}_{0i})]$, $i=1, 2, \dots, nSE=200$, and (b) $[C_i, Q(0.1|\mathbf{a}, \mathbf{e}_{Ci})]$, $i=1, 2, \dots, nSE=200$.

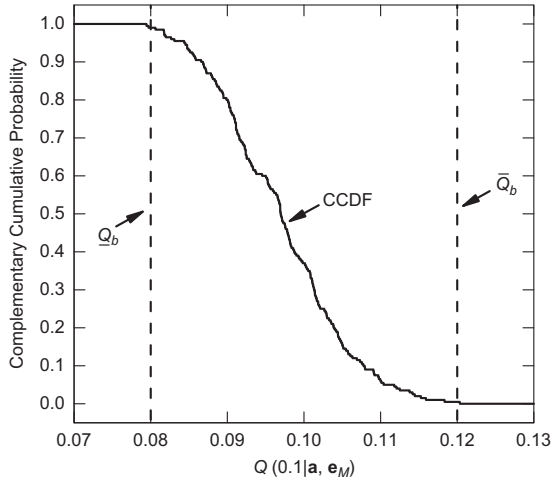


Fig. 4.5. Example bounding interval $[Q_b, \bar{Q}_b] = [0.08, 0.12]$ for $Q(0.1|\mathbf{a}, \mathbf{e}_M)$.

represented. The easiest is simply to consider whether or not $Q(0.1|\mathbf{a}, \mathbf{e}_M)$ falls within the specified bounds. This involves consideration of the indicator function

$$\delta[Q(0.1|\mathbf{a}, \mathbf{e}_M)] = \begin{cases} 1 & \text{if } Q_b \leq Q(0.1|\mathbf{a}, \mathbf{e}_M) \leq \bar{Q}_b \\ 0 & \text{otherwise} \end{cases} \quad (4.24)$$

and the associated sets

$$\mathcal{X}^+ = \{\mathbf{e}_M : \mathbf{e}_M \in \mathcal{EM} \text{ and } \delta[Q(0.1|\mathbf{a}, \mathbf{e}_M)] = 1\} \quad (4.25)$$

and

$$\mathcal{X}^- = \{\mathbf{e}_M : \mathbf{e}_M \in \mathcal{EM} \text{ and } \delta[Q(0.1|\mathbf{a}, \mathbf{e}_M)] = 0\}. \quad (4.26)$$

Then, the probabilities of compliance and noncompliance are given by

$$p_{EM}(\mathcal{X}^+) \cong \sum_{i=1}^{nSE} \delta[Q(0.1|\mathbf{a}, \mathbf{e}_{Mi})/nSE] = 0.985 \quad (4.27)$$

and

$$p_{EM}(\mathcal{X}^-) = 1 - p_{EM}(\mathcal{X}^+) \cong 1 - 0.985 = 0.015, \quad (4.28)$$

respectively.

The representation in the preceding paragraph summarizes the uncertainty in whether or not the specified interval bound will be satisfied. However, the uncertainty in the location of $Q(0.1|\mathbf{a}, \mathbf{e}_M)$ relative to the ends of the bounding interval $[Q_b, \bar{Q}_b]$ is not indicated. The consideration of this uncertainty requires the determination of margins and the uncertainty associated with these margins. Specifically, a margin associated with the containment of $Q(0.1|\mathbf{a}, \mathbf{e}_M)$ in the interval $[Q_b, \bar{Q}_b]$ can be defined by

$$Q_m(0.1|\mathbf{a}, \mathbf{e}_M) = \min \left\{ \begin{array}{l} Q(0.1|\mathbf{a}, \mathbf{e}_M) - Q_b \\ \bar{Q}_b - Q(0.1|\mathbf{a}, \mathbf{e}_M) \end{array} \right. \quad (4.29)$$

with the result that (i) $Q_m(0.1|\mathbf{a}, \mathbf{e}_M)$ is nonnegative if $Q(0.1|\mathbf{a}, \mathbf{e}_M)$ falls within the interval $[Q_b, \bar{Q}_b]$, and (ii) $Q_m(0.1|\mathbf{a}, \mathbf{e}_M)$ is negative if $Q(0.1|\mathbf{a}, \mathbf{e}_M)$ falls outside the interval $[Q_b, \bar{Q}_b]$. In turn, $Q_m(0.1|\mathbf{a}, \mathbf{e}_M)$ has an uncertainty structure that derives from the uncertainty structure imposed on \mathbf{e}_M (Fig. 4.6). The probability $p_{EM}(\mathcal{X}^-) = 0.015$ in Eq. (4.28) corresponds to the cumulative probability associated with $Q_m(0.1|\mathbf{a}, \mathbf{e}_M) = 0$ in Fig. 4.6.

An alternate representation is to use normalized margins. Specifically, the margin $Q_n(0.1|\mathbf{a}, \mathbf{e}_M)$ defined in Eq. (4.29) can

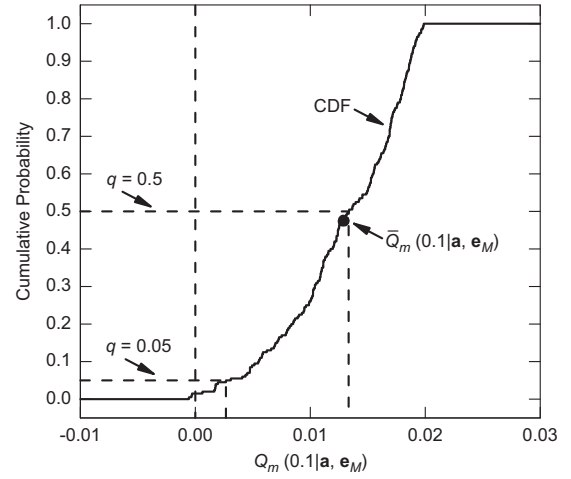


Fig. 4.6. Estimated CDF summarizing uncertainty in margin $Q_m(0.1|\mathbf{a}, \mathbf{e}_M)$ defined in Eq. (4.29) for bounding interval $[Q_b, \bar{Q}_b] = [0.08, 0.12]$.

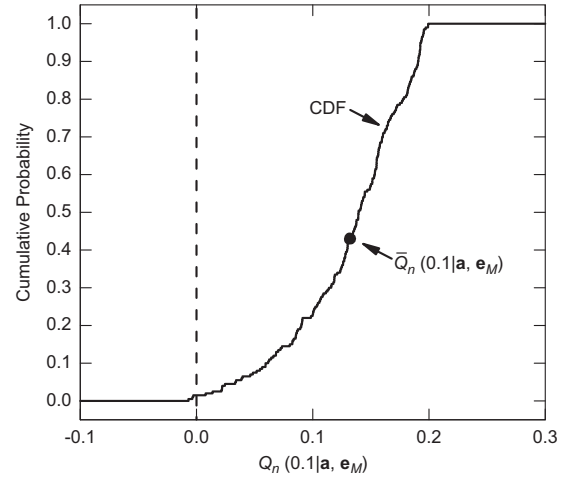


Fig. 4.7. Estimated CDF summarizing uncertainty in normalized margin $Q_n(0.1|\mathbf{a}, \mathbf{e}_M)$ defined in Eq. (4.30) for bounding interval $[Q_b, \bar{Q}_b] = [0.08, 0.12]$.

be replaced by a normalized margin $Q_n(0.1|\mathbf{a}, \mathbf{e}_M)$ defined by

$$Q_n(0.1|\mathbf{a}, \mathbf{e}_M) = \min \left\{ \begin{array}{l} [Q(0.1|\mathbf{a}, \mathbf{e}_M) - Q_b] / Q_b \\ [\bar{Q}_b - Q(0.1|\mathbf{a}, \mathbf{e}_M)] / \bar{Q}_b \end{array} \right. \quad (4.30)$$

which expresses margin as a fraction of the bounding value from which $Q(0.1|\mathbf{a}, \mathbf{e}_M)$ has the smallest fractional deviation (Fig. 4.7).

If desired, “margin/uncertainty” summary measures of the form defined in Eqs. (4.7), (4.8), (4.13) and (4.14) can be defined for the distribution of $Q_m(0.1|\mathbf{a}, \mathbf{e}_M)$ in Fig. 4.6. Specifically,

$$\begin{aligned} Q_{m/u}(t|\mathbf{a}, \mathbf{e}_M) &= \frac{Q_{m,0.5}(t|\mathbf{a}, \mathbf{e}_M)}{Q_{m,0.5}(t|\mathbf{a}, \mathbf{e}_M) - Q_{m,q}(t|\mathbf{a}, \mathbf{e}_M)} \\ &= \begin{cases} 0.013 / (0.013 - 0.003) = 1.30 & \text{for } q = 0.05 \\ 0.013 / [0.013 - (-0.001)] = 0.93 & \text{for } q = 0.00 \end{cases} \end{aligned} \quad (4.31)$$

for $t = 0.1$ s, and

$$\bar{Q}_{m/u}(t|\mathbf{a}, \mathbf{e}_M) = \frac{\bar{Q}_m(t|\mathbf{a}, \mathbf{e}_M)}{\bar{Q}_m(t|\mathbf{a}, \mathbf{e}_M) - Q_{m,q}(t|\mathbf{a}, \mathbf{e}_M)} \quad (4.32)$$

effectively has the same values as $Q_{m/u}(t|\mathbf{a}, \mathbf{e}_M)$ for $t = 0.1$ s because of the similarity of the mean and median values for $Q_m(0.1|\mathbf{a}, \mathbf{e}_M)$ (see Fig. 4.6). However, as previously discussed in

Section 4.1, a significant amount of information is lost when the results in Figs. 4.5 and 4.6 are reduced to a single number (see Section 4.5 for additional discussion).

The results of a sensitivity analysis for $Q(0.1|\mathbf{a}, \mathbf{e}_M)$ are presented in Table 4.1 and Fig. 4.4. Because $Q_m(0.1|\mathbf{a}, \mathbf{e}_M)$ as defined in Eq. (4.29) for bounding interval $\mathbf{e}=[\mathbf{e}_A, \mathbf{e}_M]$, is not an affine transformation of $Q(0.1|\mathbf{a}, \mathbf{e}_M)$, these analyses do not reveal the full effects of the elements of \mathbf{e}_M on $Q_m(0.1|\mathbf{a}, \mathbf{e}_M)$. To determine these effects, a stepwise regression analysis (Table 4.2) is initially performed for the mapping

$$[\mathbf{e}_{Mi}, Q_m(0.1|\mathbf{a}, \mathbf{e}_{Mi})], \quad i = 1, 2, \dots, nSE = 200, \quad (4.33)$$

and then followed by an examination of scatterplots.

The regression analysis in Table 4.2 for $Q_m(0.1|\mathbf{a}, \mathbf{e}_M)$ is very poor, with the final regression model containing E_0 and C having an R^2 value of only 0.16. As a reminder, E_0 and C are the dominant variables affecting the uncertainty in $Q(0.1|\mathbf{a}, \mathbf{e}_M)$ (see Table 4.1 and Fig. 4.4). Given the effects of E_0 and C on $Q(0.1|\mathbf{a}, \mathbf{e}_M)$, a natural next step is to examine the scatterplots for E_0 , C and $Q_m(0.1|\mathbf{a}, \mathbf{e}_M)$ (Fig. 4.8). Specifically, the scatterplots in Fig. 4.8 show that small values for $Q_m(0.1|\mathbf{a}, \mathbf{e}_M)$ are associated with both small and large values for E_0 and C . This is consistent with the monotonic effects of E_0 and C on $Q(0.1|\mathbf{a}, \mathbf{e}_M)$ shown in the scatterplots in Fig. 4.4 and the dependence of the margin $Q_m(0.1|\mathbf{a}, \mathbf{e}_M)$ on both small and large values for $Q(0.1|\mathbf{a}, \mathbf{e}_M)$ (see definition of $Q_m(0.1|\mathbf{a}, \mathbf{e}_M)$ in Eq. (4.29)). Given the monotonic effects of E_0 and C on $Q(0.1|\mathbf{a}, \mathbf{e}_M)$ and the definition of $Q_m(0.1|\mathbf{a}, \mathbf{e}_M)$, small values for $Q_m(0.1|\mathbf{a}, \mathbf{e}_M)$ will tend to occur when either (i) both E_0 and C are at the lower ends of their ranges or (ii) both E_0 and C are at the upper ends of their ranges.

The regression analysis for $Q_m(0.1|\mathbf{a}, \mathbf{e}_M)$ in Table 4.2 fails because of the nonmonotonic relationships involving E_0 , C and $Q_m(0.1|\mathbf{a}, \mathbf{e}_M)$ shown in Fig. 4.8. Given the complexity of the relationships involving E_0 , C and $Q_m(0.1|\mathbf{a}, \mathbf{e}_M)$, a successful

regression-based sensitivity analysis for $Q_m(0.1|\mathbf{a}, \mathbf{e}_M)$ would require the use of nonparametric regression procedures [114,115].

As indicated by this example, sensitivity analyses associated with margins defined for bounding intervals (i.e., gates) can be challenging. This can happen for at least two reasons. First, different subranges of a variable can affect compliance with upper and lower bounds. Second, different variables can affect compliance with upper and lower bounds. The outcome of these two effects can be complex relational patterns between margins and uncertain analysis inputs whose identification requires sophisticated sensitivity analysis procedures (e.g., [114–116]).

4.3. Epistemic uncertainty with a specified bounding interval over time

A QMU problem involving a bounding interval at a fixed point in time is considered in Section 4.2. This problem is now increased in complexity by considering a situation in which a bounding interval $[Q_b, \bar{Q}_b]$ is specified for a quantity such as $Q(t|\mathbf{a}, \mathbf{e}_M)$ that takes on values over a time interval $[t_{mn}, t_{mx}]$ (Fig. 4.9). Specifically, the requirement is that the values for $Q(t|\mathbf{a}, \mathbf{e}_M)$ stay within the bounding interval $[Q_b, \bar{Q}_b]$ for $t_{mn} \leq t \leq t_{mx}$ (e.g., $[Q_b, \bar{Q}_b] = [0.07, 0.14]$, $t_{mn} = 0.02$ s and $t_{mx} = 0.18$ s in Fig. 4.9).

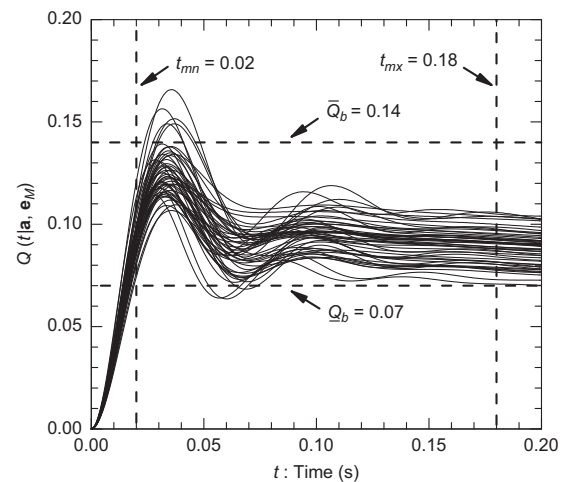


Fig. 4.9. Example bounding interval $[Q_b, \bar{Q}_b] = [0.07, 0.14]$ over the time interval $[t_{mn}, t_{mx}] = [0.02, 0.18]$ s for $Q(t|\mathbf{a}, \mathbf{e}_M)$.

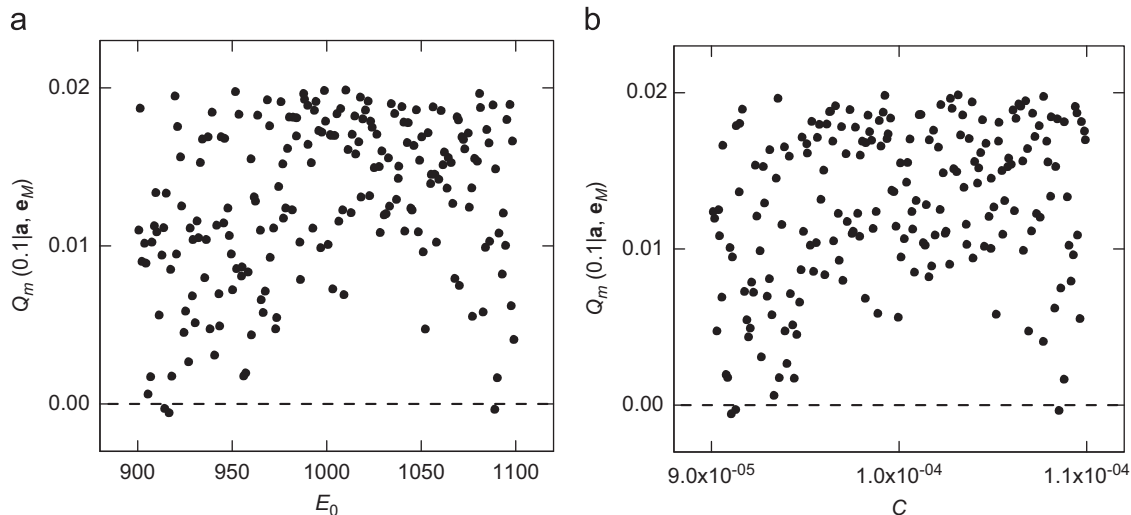


Fig. 4.8. Scatterplots for margin $Q_m(0.1|\mathbf{a}, \mathbf{e}_M)$ defined in Eq. (4.29): (a) $[E_{0i}, Q_m(0.1|\mathbf{a}, \mathbf{e}_{Mi})]$, $i = 1, 2, \dots, nSE = 200$, and (b) $[C_i, Q_m(0.1|\mathbf{a}, \mathbf{e}_{Mi})]$, $i = 1, 2, \dots, nSE = 200$.

Formally stated, the requirement is that the inequalities

$$\underline{Q}_b \leq Q(t|\mathbf{a}, \mathbf{e}_M) \leq \bar{Q}_b \quad (4.34)$$

be satisfied for $\mathbf{e}_M \in \mathcal{EM}$ and $t_{mn} \leq t \leq t_{mx}$.

Uncertainty in compliance with the indicated requirement can be represented with use of the indicator function

$$\delta[Q(t|\mathbf{a}, \mathbf{e}_M) : t_{mn} \leq t \leq t_{mx}] = \begin{cases} 1 & \text{if } \underline{Q}_b \leq Q(t|\mathbf{a}, \mathbf{e}_M) \leq \bar{Q}_b \text{ for } t_{mn} \leq t \leq t_{mx} \\ 0 & \text{otherwise} \end{cases} \quad (4.35)$$

and the associated sets

$$\mathcal{X}^+ = \{ \mathbf{e}_M : \mathbf{e}_M \in \mathcal{EM} \text{ and } \delta[Q(t|\mathbf{a}, \mathbf{e}_M) : t_{mn} \leq t \leq t_{mx}] = 1 \} \quad (4.36)$$

and

$$\mathcal{X}^- = \{ \mathbf{e}_M : \mathbf{e}_M \in \mathcal{EM} \text{ and } \delta[Q(t|\mathbf{a}, \mathbf{e}_M) : t_{mn} \leq t \leq t_{mx}] = 0 \}. \quad (4.37)$$

Then, the probabilities of compliance and noncompliance are given by

$$p_{EM}(\mathcal{X}^+) \cong \sum_{i=1}^{nSE} \delta[Q(t|\mathbf{a}, \mathbf{e}_{Mi}) : t_{mn} \leq t \leq t_{mx}] / nSE = 0.82 \quad (4.38)$$

and

$$p_{EM}(\mathcal{X}^-) = 1 - p_{EM}(\mathcal{X}^+) \cong 1 - 0.82 = 0.18, \quad (4.39)$$

respectively.

The preceding representation summarizes the uncertainty in whether or not compliance with the specified bounding interval over time will be satisfied. However, this representation does not display the associated margins. These margins can be defined by

$$Q_m(t|\mathbf{a}, \mathbf{e}_M, [t_{mn}, t_{mx}]) = \min \left\{ \frac{Q_{mn}(t|\mathbf{a}, \mathbf{e}_M, [t_{mn}, t_{mx}]) - \underline{Q}_b}{\bar{Q}_b - Q_{mx}(t|\mathbf{a}, \mathbf{e}_M, [t_{mn}, t_{mx}])}, \right. \quad (4.40)$$

where

$$Q_{mn}(t|\mathbf{a}, \mathbf{e}_M, [t_{mn}, t_{mx}]) = \min\{Q(t|\mathbf{a}, \mathbf{e}_M) : t_{mn} \leq t \leq t_{mx}\}$$

and

$$Q_{mx}(t|\mathbf{a}, \mathbf{e}_M, [t_{mn}, t_{mx}]) = \max\{Q(t|\mathbf{a}, \mathbf{e}_M) : t_{mn} \leq t \leq t_{mx}\}.$$

In turn, $Q_m(t|\mathbf{a}, \mathbf{e}_M, [t_{mn}, t_{mx}])$ has an uncertainty structure that derives from the uncertainty structure imposed on \mathbf{e}_M (Fig. 4.10).

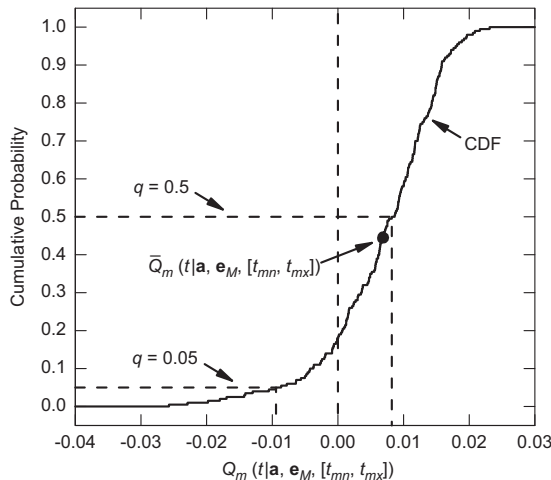


Fig. 4.10. Estimated CDF summarizing uncertainty in margin $Q_m(t|\mathbf{a}, \mathbf{e}_M, [t_{mn}, t_{mx}])$ defined in Eq. (4.40) for bounding interval $[\underline{Q}_b, \bar{Q}_b] = [0.07, 0.14]$ and time interval $[t_{mn}, t_{mx}] = [0.02, 0.18]$ s.

The probability $p_{EM}(\mathcal{X}^-) = 0.18$ in Eq. (4.39) corresponds to the cumulative probability associated with $Q_m(0.1|\mathbf{a}, \mathbf{e}_M, [t_{mn}, t_{mx}]) = 0$ in Fig. 4.10.

An alternative representation is to use normalized margins. Specifically, the margin $Q_m(t|\mathbf{a}, \mathbf{e}_M, [t_{mn}, t_{mx}])$ defined in Eq. (4.40) can be replaced by a normalized margin $Q_n(t|\mathbf{a}, \mathbf{e}_M, [t_{mn}, t_{mx}])$ defined by

$$Q_n(t|\mathbf{a}, \mathbf{e}_M, [t_{mn}, t_{mx}]) = \min \left\{ \frac{Q_{mn}(t|\mathbf{a}, \mathbf{e}_M, [t_{mn}, t_{mx}]) - \underline{Q}_b}{\bar{Q}_b - Q_{mx}(t|\mathbf{a}, \mathbf{e}_M, [t_{mn}, t_{mx}])}, \right. \quad (4.41)$$

which expresses margin as a fraction of the bounding value from which $Q(t|\mathbf{a}, \mathbf{e}_M)$ has the smallest fractional deviation (Fig. 4.11).

If desired, “margin/uncertainty” summary measures of the form defined in Eqs. (4.7), (4.8), (4.13) and (4.14) can be defined for the distribution of $Q(0.1|\mathbf{a}, \mathbf{e}_M, [t_{mn}, t_{mx}])$ in Fig. 4.10. Specifically,

$$\begin{aligned} Q_{m/u}(t|\mathbf{a}, \mathbf{e}_M, [t_{mn}, t_{mx}]) &= \frac{Q_{m,0.5}(t|\mathbf{a}, \mathbf{e}_M, [t_{mn}, t_{mx}])}{Q_{m,0.5}(t|\mathbf{a}, \mathbf{e}_M, [t_{mn}, t_{mx}]) - Q_{m,q}(t|\mathbf{a}, \mathbf{e}_M, [t_{mn}, t_{mx}])} \\ &= \begin{cases} 0.0082 / [0.0082 - (-0.0094)] = 0.47 & \text{for } q = 0.05 \\ 0.0082 / [0.0082 - (-0.0257)] = 0.24 & \text{for } q = 0.00 \end{cases} \end{aligned} \quad (4.42)$$

and

$$\begin{aligned} \bar{Q}_{m/u}(t|\mathbf{a}, \mathbf{e}_M, [t_{mn}, t_{mx}]) &= \frac{\bar{Q}_m(t|\mathbf{a}, \mathbf{e}_M, [t_{mn}, t_{mx}])}{\bar{Q}_m(t|\mathbf{a}, \mathbf{e}_M, [t_{mn}, t_{mx}]) - Q_{m,q}(t|\mathbf{a}, \mathbf{e}_M, [t_{mn}, t_{mx}])} \\ &= \begin{cases} 0.0069 / [0.0069 - (-0.0094)] = 0.42 & \text{for } q = 0.05 \\ 0.0069 / [0.0069 - (-0.0257)] = 0.21 & \text{for } q = 0.00. \end{cases} \end{aligned} \quad (4.43)$$

However, as is always the case, a significant amount of information is lost when the results in Figs. 4.9 and 4.10 are reduced to a single number (see Section 4.5 for additional discussion).

Sensitivity analysis can also be performed for $Q(t|\mathbf{a}, \mathbf{e}_M)$ and the results summarized by $Q_m(t|\mathbf{a}, \mathbf{e}_M, [t_{mn}, t_{mx}])$. A natural starting point is to investigate the variables affecting $Q(t|\mathbf{a}, \mathbf{e}_M)$ over the time interval $[t_{mn}, t_{mx}]$ (Fig. 4.12). To this end, partial correlation coefficients (PCCs) and SRCs for $Q(t|\mathbf{a}, \mathbf{e}_M)$ and the elements of \mathbf{e}_M are presented in Fig. 4.12.

Related, but not identical information is provided by PCCs and SRCs. Specifically, a PCC provides a measure of the strength of the

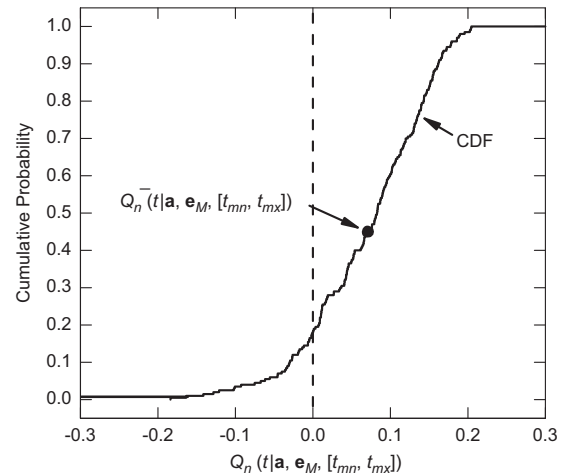


Fig. 4.11. Estimated CDF summarizing uncertainty in normalized margin $Q_n(t|\mathbf{a}, \mathbf{e}_M, [t_{mn}, t_{mx}])$ defined in Eq. (4.41) for bounding interval $[\underline{Q}_b, \bar{Q}_b] = [0.07, 0.14]$ and time interval $[t_{mn}, t_{mx}] = [0.02, 0.18]$ s.

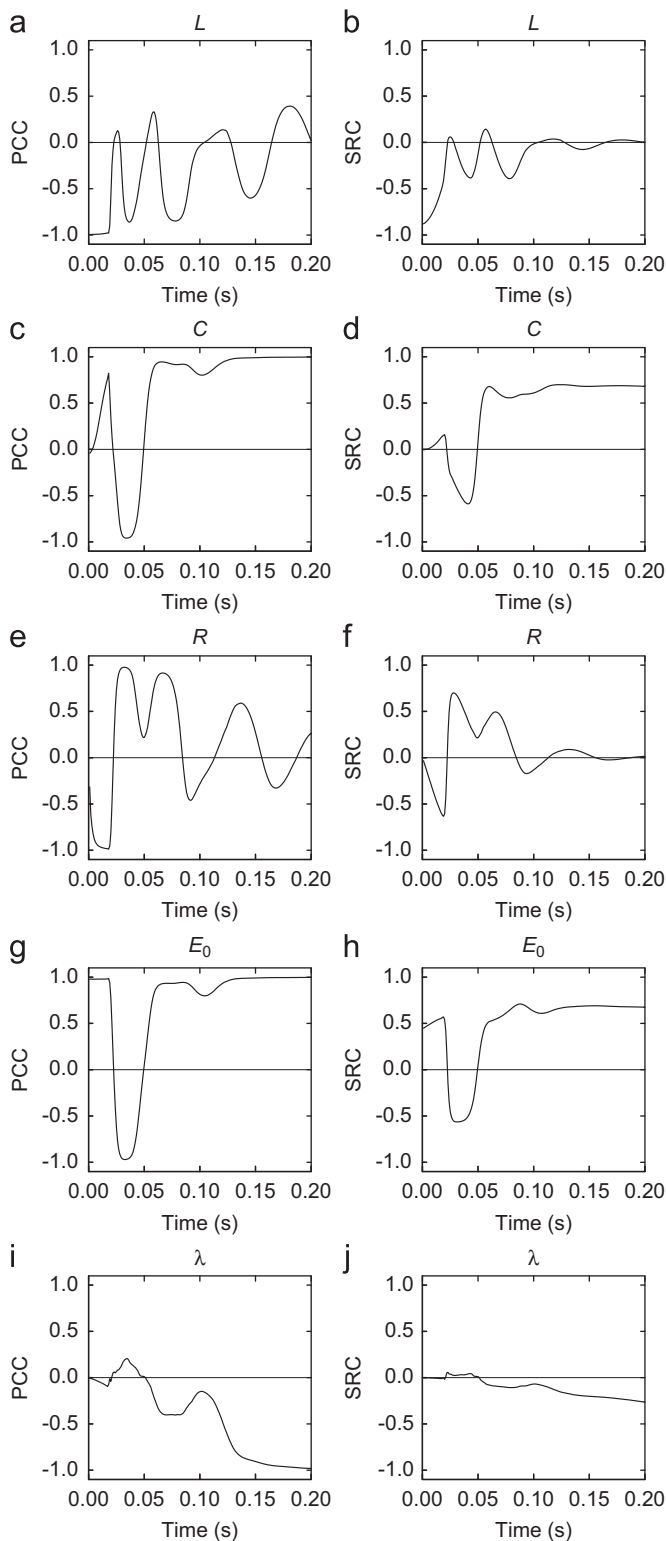


Fig. 4.12. Sensitivity analysis for $Q(t|\mathbf{a}, \mathbf{e}_M)$ for $0 < t < 0.2$ s with PCCs (left column) and SRCs (right column).

linear relationship between two variables after the linear effects of all other variables have been removed, and a SRC provides a measure of the fraction of the uncertainty in a dependent variable that can be accounted for by the independent variable under consideration (see Refs. [53,56] for additional discussion of PCCs and SRCs). Although their numeric values differ, the absolute values of PCCs and SRCs provide the same orderings of variable

importance when no correlations between the independent variables (i.e., the elements of \mathbf{e}_M) are present. For comparison, both PCCs and SRCs are presented in Fig. 4.12. For presentation purposes, PCCs can be preferable to SRCs because PCCs tend to be more spread out in the interval $[-1, 1]$ than SRCs, with the result that a single plot frame containing multiple time-dependent PCCs is easier to read than a single plot frame containing multiple time-dependent SRCs.

As examination of Fig. 4.12 shows, the effects of the elements of \mathbf{e}_M tend to swing from positive to negative prior to approximately 0.1 s. This effect results because of the oscillatory behavior of $Q(t|\mathbf{a}, \mathbf{e}_M)$ that can be seen in Fig. 4.9 and derives from the sine and cosine terms in the closed-form representation for $Q(t|\mathbf{a}, \mathbf{e}_M)$ shown in Eq. (3.31). During this early time period, all variables except λ have appreciable effects on $Q(t|\mathbf{a}, \mathbf{e}_M)$. After approximately 0.1 s, the oscillatory behavior of $Q(t|\mathbf{a}, \mathbf{e}_M)$ has significantly decayed, and the uncertainty in $Q(t|\mathbf{a}, \mathbf{e}_M)$ is dominated by C and E_0 . As indicated by its PCCs and SRCs, λ has a strong negative partial correlation with $Q(t|\mathbf{a}, \mathbf{e}_M)$ beginning at about 0.1 s but the actual size of this effect on the uncertainty in $Q(t|\mathbf{a}, \mathbf{e}_M)$ is rather small.

In this example, the margin $Q_m(t|\mathbf{a}, \mathbf{e}_M, [t_{mn}, t_{mx}])$ is not an affine transformation of the underlying analysis result $Q(t|\mathbf{a}, \mathbf{e}_M)$. As a consequence, sensitivity analysis results for $Q(t|\mathbf{a}, \mathbf{e}_M)$ cannot be expected to be the same as sensitivity analysis results for $Q_m(t|\mathbf{a}, \mathbf{e}_M, [t_{mn}, t_{mx}])$. For this reason, a sensitivity analysis for $Q_m(t|\mathbf{a}, \mathbf{e}_M, [t_{mn}, t_{mx}])$ with stepwise regression analysis is presented in Table 4.3. This analysis indicates that R is the dominant variable affecting the uncertainty in $Q_m(t|\mathbf{a}, \mathbf{e}_M, [t_{mn}, t_{mx}])$, with $Q_m(t|\mathbf{a}, \mathbf{e}_M, [t_{mn}, t_{mx}])$ tending to increase as R increases. After R , smaller effects on $Q_m(t|\mathbf{a}, \mathbf{e}_M, [t_{mn}, t_{mx}])$ are indicated for E_0 , C and L , with $Q_m(t|\mathbf{a}, \mathbf{e}_M, [t_{mn}, t_{mx}])$ tending to decrease as each of these variables increases.

Additional insights on the effects of R , E_0 , C and L on $Q_m(t|\mathbf{a}, \mathbf{e}_M, [t_{mn}, t_{mx}])$ can be obtained by examining the scatterplots involving these variables and $Q_m(t|\mathbf{a}, \mathbf{e}_M, [t_{mn}, t_{mx}])$ (Fig. 4.13). Specifically, the strong positive effect of R on $Q_m(t|\mathbf{a}, \mathbf{e}_M, [t_{mn}, t_{mx}])$ can be clearly seen, with negative values for $Q_m(t|\mathbf{a}, \mathbf{e}_M, [t_{mn}, t_{mx}])$ occurring for small values for R . Further, the negative but less strong effects of E_0 , C and L on $Q_m(t|\mathbf{a}, \mathbf{e}_M, [t_{mn}, t_{mx}])$ can also be seen, with negative values for $Q_m(t|\mathbf{a}, \mathbf{e}_M, [t_{mn}, t_{mx}])$ tending to be associated with large values for E_0 , C and L .

Although not particularly high, the final R^2 value of 0.62 in Table 4.3 is significantly better than the almost meaningless final R^2 value of 0.16 in Table 4.2. This difference results because the margins associated with the problem in Section 4.3 have relationships with the elements of \mathbf{e}_M that have a monotonic character while the margins in Section 4.2 and their relationships with the elements of \mathbf{e}_M do not have this character (i.e., compare the scatterplots in Figs. 4.8 and 4.13).

4.4. Epistemic uncertainty with an uncertain bound

The QMU results presented in Sections 4.1–4.3 involve uniquely specified bounds. However, it is likely that this will not always be the case in QMU analyses. For example, a requirement might be that

Table 4.3

Stepwise regression analysis to identify uncertain variables affecting margin $Q_m(t|\mathbf{a}, \mathbf{e}_M, [t_{mn}, t_{mx}])$ defined in Eq. (4.40).

Step ^a	Variable	SRC	R^2
1	R	0.67	0.45
2	E_0	−0.26	0.53
3	C	−0.23	0.58
4	L	−0.20	0.62

^a Table structure same as in Table 4.1.

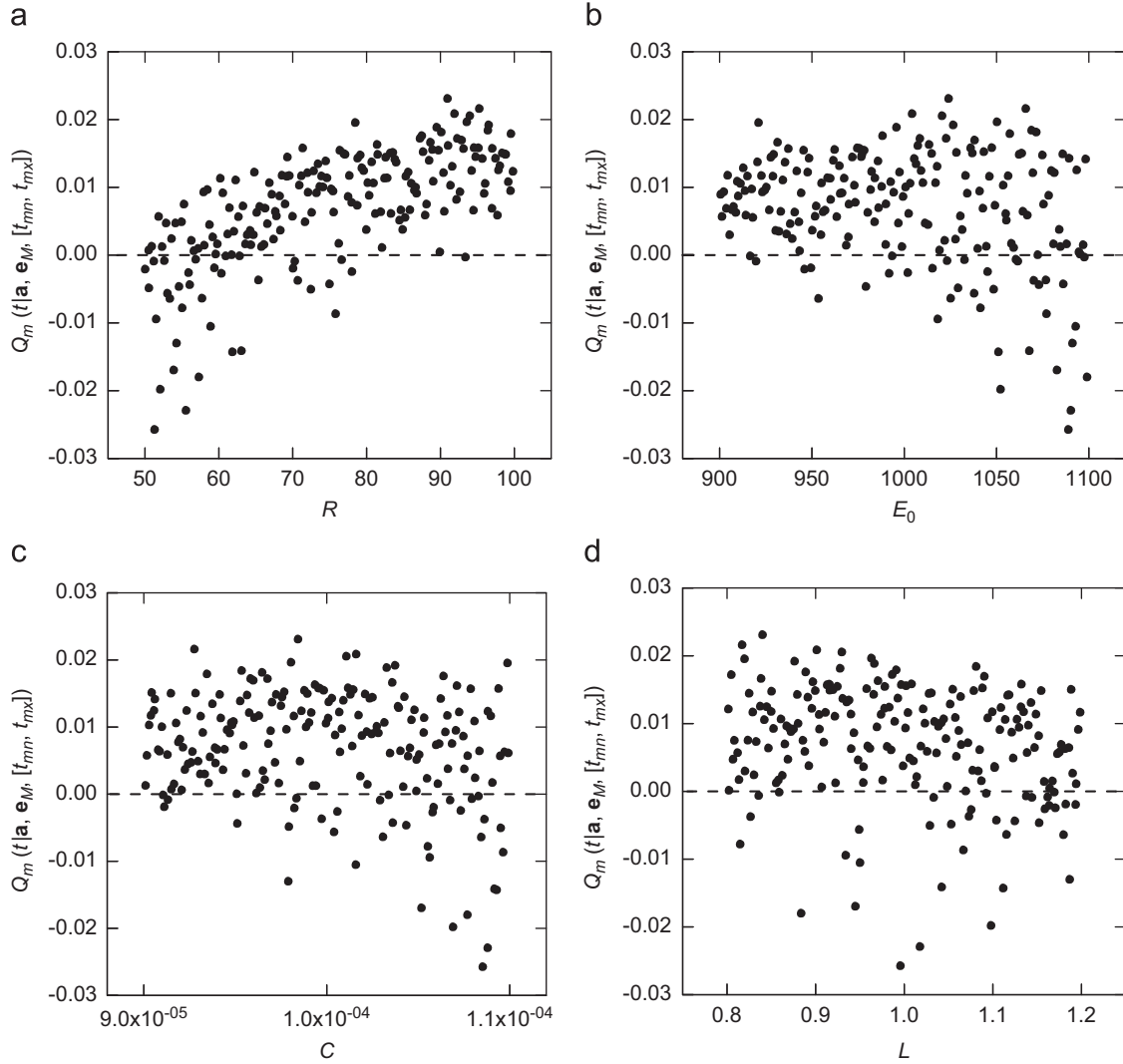


Fig. 4.13. Scatterplots for margin $Q_m(t|\mathbf{a}, \mathbf{e}_M, [t_{mn}, t_{mx}])$ defined in Eq. (4.40): (a) $[R_i, Q_m(t|\mathbf{a}, \mathbf{e}_{Mi}, [t_{mn}, t_{mx}])]$, $i=1,2, \dots, nSE=200$, (b) $[E_{0i}, Q_m(t|\mathbf{a}, \mathbf{e}_{Mi}, [t_{mn}, t_{mx}])]$, $i=1,2, \dots, nSE=200$, (c) $[C_i, Q_m(t|\mathbf{a}, \mathbf{e}_{Mi}, [t_{mn}, t_{mx}])]$, $i=1,2, \dots, nSE=200$, and (d) $[L_i, Q_m(t|\mathbf{a}, \mathbf{e}_{Mi}, [t_{mn}, t_{mx}])]$, $i=1,2, \dots, nSE=200$.

a certain system operates but the conditions that define when the system does and does not operate appropriately may not be specified. Then, it is the responsibility of the individuals (i.e., analysts) charged with carrying out the analysis to specify the conditions under which the system operates in the manner desired. However, there may be uncertainty with respect to exactly what conditions are necessary for the appropriate operation of the system. Then, in this situation, there is epistemic uncertainty as to the conditions that should be specified to define what constitutes appropriate operation of the system.

The example presented in Section 4.3 can be modified to illustrate this situation. As originally stated, the example in Section 4.3 involves a bounding interval $[Q_b, \bar{Q}_b]$ for $Q(t|\mathbf{a}, \mathbf{e}_M)$ over the time interval $[t_{mn}, t_{mx}]$. For the example of this section, it is assumed that the specified requirement is that the system be operational over the time interval $[t_{mn}, t_{mx}]$ but the requirement does not specify what conditions are necessary for the system to be operational. For purposes of illustration, it is assumed that the analysts involved conclude that the system being operational over $[t_{mn}, t_{mx}]$ corresponds to $Q(t|\mathbf{a}, \mathbf{e}_M)$ being within a bounding interval $[Q_b, \bar{Q}_b]$. However, they are uncertain with respect to the appropriate value for this bounding interval. Thus, there is epistemic uncertainty with respect to the values to use for Q_b

and \bar{Q}_b . As a result, the vector \mathbf{e}_M of epistemically uncertain inputs to the analysis now has the form

$$\mathbf{e}_M = [\mathbf{e}_R, \mathbf{e}_P] = [Q_b, \bar{Q}_b, L, R, C, E_0, \lambda], \quad (4.44)$$

where $\mathbf{e}_R = [Q_b, \bar{Q}_b]$ and $\mathbf{e}_P = [L, R, C, E_0, \lambda]$ as indicated in Eq. (3.21).

For purposes of illustration, it is assumed that the analysts conclude that (i) Q_b is contained in the interval $[0.06, 0.08]$, (ii) \bar{Q}_b is contained in the interval $[0.14, 0.16]$, (iii) Q_b and \bar{Q}_b have the same uncertainty structure specified for L, R_0, C, E and λ (see Eqs. (3.38)–(3.43) and associated discussion), and (iv) no dependency or correlation exists between Q_b and \bar{Q}_b (Fig. 4.14).

This problem can now be analyzed exactly as in Section 4.3. The only difference is that \mathbf{e}_M now contains 7 rather than 5 elements, with two of these elements being Q_b and \bar{Q}_b . Specifically, $\delta[Q(t|\mathbf{a}, \mathbf{e}_M): t_{mn} \leq t \leq t_{mx}]$, \mathcal{X}^+ and \mathcal{X}^- are defined as indicated in Eqs. (4.35)–(4.37) with the understanding that the indicator function $\delta[\sim]$ is now a function of Q_b and \bar{Q}_b . Given the dependency of $\delta[\sim]$ on Q_b and \bar{Q}_b , a more complete but rather cumbersome notation for $\delta[\sim]$ is $\delta[\sim, (Q_b, \bar{Q}_b)]$, which will be used below to make the dependence of $\delta[\sim]$ on Q_b and \bar{Q}_b explicit. In turn, the probabilities of compliance and

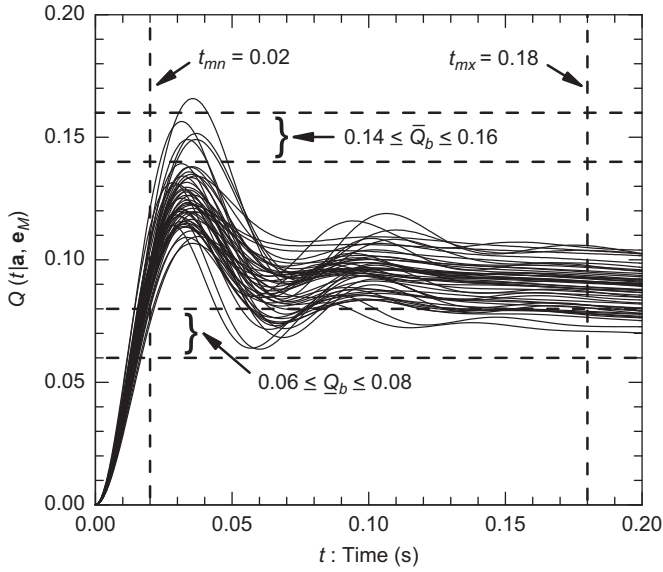


Fig. 4.14. Example uncertain bounding interval $[Q_b, \bar{Q}_b]$ with $0.06 \leq Q_b \leq 0.08$ and $0.14 \leq \bar{Q}_b \leq 0.16$ over the time interval $[t_{mn}, t_{mx}] = [0.02, 0.18 \text{ s}]$ for $Q(t|\mathbf{a}, \mathbf{e}_M)$.

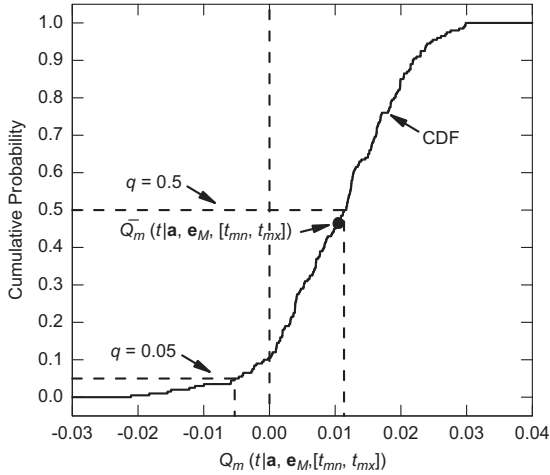


Fig. 4.15. Estimated CDF summarizing uncertainty in margin $Q_m(t|\mathbf{a}, \mathbf{e}_M, [t_{mn}, t_{mx}])$ defined in Eq. (4.40) for time interval $[t_{mn}, t_{mx}] = [0.02, 0.18 \text{ s}]$ and uncertain bounding interval $[Q_b, \bar{Q}_b]$ with $0.06 \leq Q_b \leq 0.08$ and $0.14 \leq \bar{Q}_b \leq 0.16$.

noncompliance are given by

$$p_{EM}(\mathcal{X}^+) \cong \sum_{i=1}^{nSE} \frac{\delta[Q(t|\mathbf{a}, \mathbf{e}_{Mi}) : t_{mn} \leq t \leq t_{mx}, (Q_{bi}, \bar{Q}_{bi})]}{nSE} = 0.895 \quad (4.45)$$

and

$$p_{EM}(\mathcal{X}^-) \cong 1 - p_{EM}(\mathcal{X}^+) = 1 - 0.895 = 0.105, \quad (4.46)$$

respectively, where

$$\mathbf{e}_{Mi} = [Q_{bi}, \bar{Q}_{bi}, L_i, R_i, C_i, E_{0i}, \lambda_i], \quad i = 1, 2, \dots, nSE,$$

is now an LHS of size $nSE = 200$ from vectors of the form defined in Eq. (4.44).

Margin analysis results $Q_m(t|\mathbf{a}, \mathbf{e}_M, [t_{mn}, t_{mx}])$ and normalized margin analysis results $\bar{Q}_m(t|\mathbf{a}, \mathbf{e}_M, [t_{mn}, t_{mx}])$ of the form defined in Eqs. (4.40) and (4.41), respectively, can also be obtained (Figs. 4.15 and 4.16).

Similarly to the results in Eqs. (4.42) and (4.43), “margin/uncertainty” ratios $Q_{m/u}(t|\mathbf{a}, \mathbf{e}_M, [t_{mn}, t_{mx}])$ and $\bar{Q}_{m/u}(t|\mathbf{a}, \mathbf{e}_M, [t_{mn}, t_{mx}])$ can be

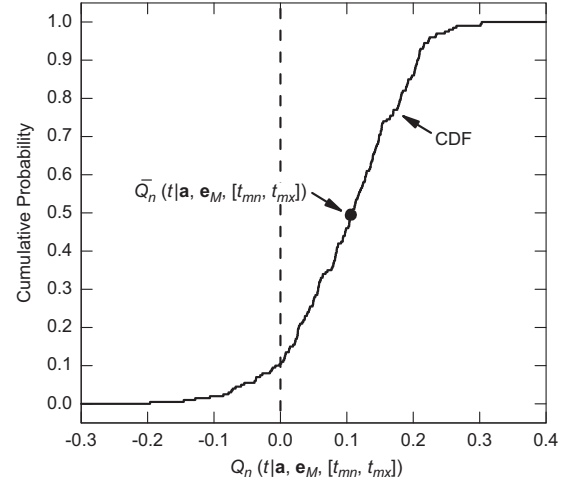


Fig. 4.16. Estimated CDF summarizing uncertainty in normalized margin $Q_n(t|\mathbf{a}, \mathbf{e}_M, [t_{mn}, t_{mx}])$ defined in Eq. (4.41) for time interval $[t_{mn}, t_{mx}] = [0.02, 0.18 \text{ s}]$ and uncertain bounding interval $[Q_b, \bar{Q}_b]$ with $0.06 \leq Q_b \leq 0.08$ and $0.14 \leq \bar{Q}_b \leq 0.16$.

Table 4.4

Stepwise regression analysis to identify uncertain variables affecting margin $Q_m(t|\mathbf{a}, \mathbf{e}_M, [t_{mn}, t_{mx}])$ defined in Eq. (4.40) for time interval $[t_{mn}, t_{mx}] = [0.02, 0.18 \text{ s}]$ and uncertain bounding interval $[Q_b, \bar{Q}_b]$ with $0.06 \leq Q_b \leq 0.08$ and $0.14 \leq \bar{Q}_b \leq 0.16$.

Step ^a	Variable	SRC	R ²
1	R	0.53	0.28
2	Q_b	−0.40	0.43
3	L	−0.32	0.54
4	\bar{Q}_b	0.23	0.59
5	E_0	0.13	0.61

^a Table structure same as in Table 4.1.

used to summarize the distribution for $Q_m(t|\mathbf{a}, \mathbf{e}_M, [t_{mn}, t_{mx}])$ in Fig. 4.15. Specifically,

$$Q_{m/u}(t|\mathbf{a}, \mathbf{e}_M, [t_{mn}, t_{mx}]) = \begin{cases} 0.011/[0.011 - (-0.005)] = 0.69 & \text{for } q = 0.05 \\ 0.011/[0.011 - (-0.021)] = 0.34 & \text{for } q = 0.00, \end{cases} \quad (4.47)$$

and similar values are obtained for $\bar{Q}_{m/u}(t|\mathbf{a}, \mathbf{e}_M, [t_{mn}, t_{mx}])$ as a consequence of the similarity of the mean and median values for $Q(t|\mathbf{a}, \mathbf{e}_M, [t_{mn}, t_{mx}])$ (see Fig. 4.15). However, as is always the case, a significant amount of information is lost when the results in Figs. 4.14 and 4.15 are reduced to a single number (see Section 4.5 for additional discussion).

A sensitivity analysis for $Q_m(t|\mathbf{a}, \mathbf{e}_M, [t_{mn}, t_{mx}])$ based on stepwise regression analysis is presented in Table 4.4. The two most important variables affecting the uncertainty in $Q_m(t|\mathbf{a}, \mathbf{e}_M, [t_{mn}, t_{mx}])$ are R and Q_b , with $Q_m(t|\mathbf{a}, \mathbf{e}_M, [t_{mn}, t_{mx}])$ tending to increase as R increases and tending to decrease as Q_b increases. In addition, a negative effect is indicated for L and positive effects are indicated for \bar{Q}_b and E_0 .

The effects of R , Q_b and \bar{Q}_b on $Q_m(t|\mathbf{a}, \mathbf{e}_M, [t_{mn}, t_{mx}])$ can be seen in the scatterplots in Fig. 4.17. In particular, negative values for $Q_m(t|\mathbf{a}, \mathbf{e}_M, [t_{mn}, t_{mx}])$ tend to be associated with small values for R that occur in conjunction with a large value for Q_b and a small value for \bar{Q}_b .

4.5. Information loss in a “margin/uncertainty” ratio

As already emphasized several times, results of the form “margin/uncertainty” involve a significant loss of information. This

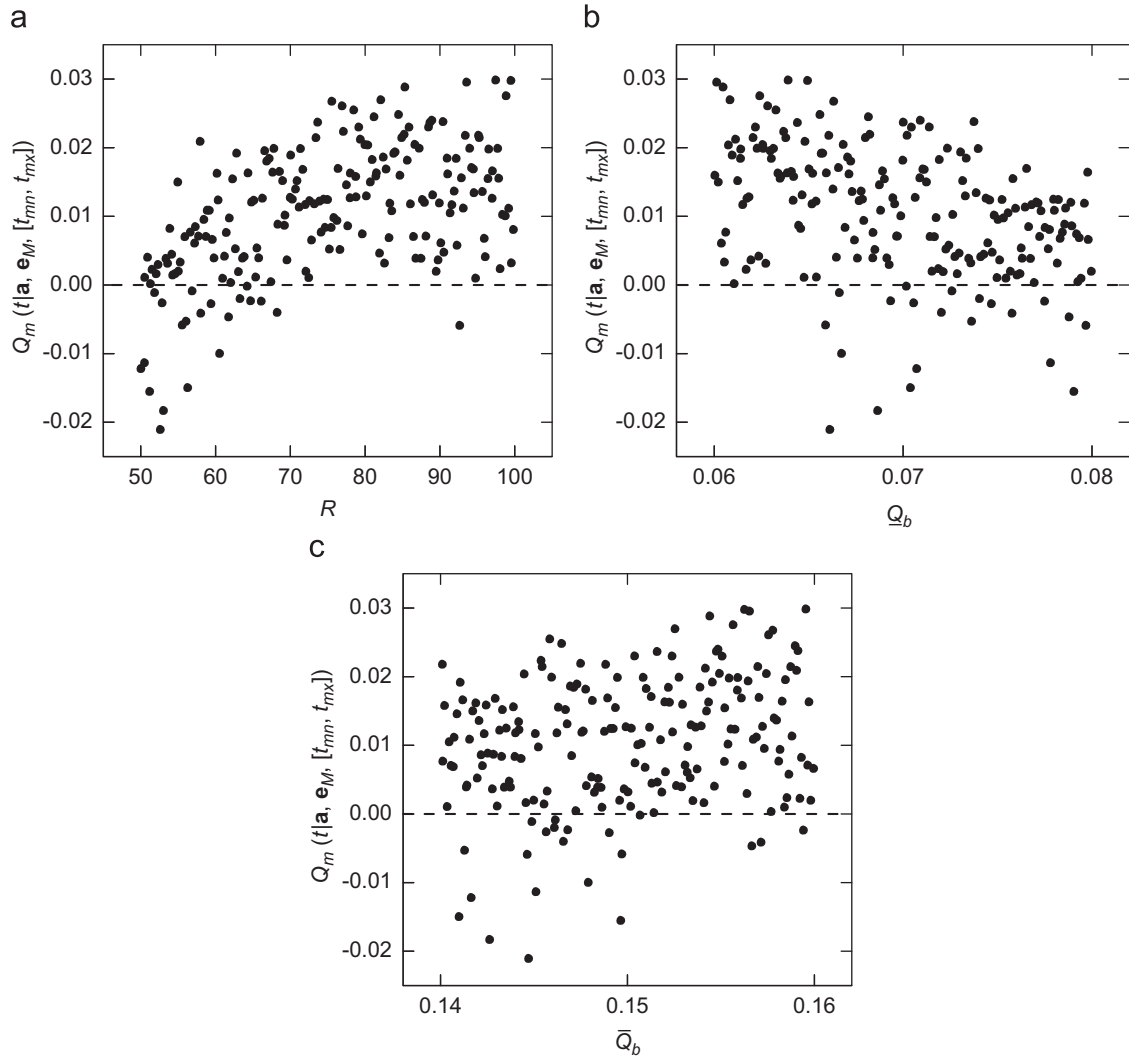


Fig. 4.17. Scatterplots for margin $Q_m(t|a, e_M, [t_{mn}, t_{mx}])$ defined in Eq. (4.40) for time interval $[t_{mn}, t_{mx}] = [0.02, 0.18]$ s and uncertain bounding interval $[Q_b, \bar{Q}_b]$ with $0.06 \leq Q_b \leq 0.08$ and $0.14 \leq \bar{Q}_b \leq 0.16$: (a) $[R_i, Q_m(t|a, e_{Mi}, [t_{mn}, t_{mx}])]$, $i=1, 2, \dots, nSE=200$, (b) $[Q_{bi}, Q_m(t|a, e_{Mi}, [t_{mn}, t_{mx}])]$, $i=1, 2, \dots, nSE=200$, and (c) $[\bar{Q}_{bi}, Q_m(t|a, e_{Mi}, [t_{mn}, t_{mx}])]$, $i=1, 2, \dots, nSE=200$.

loss is particularly acute because the actual magnitudes of the margins involved in the determination of “margin/uncertainty” are suppressed and cannot be determined from this ratio. Specifically, many different pairings of “margin” and “uncertainty” can result in the same “margin/uncertainty” ratio. In particular, it is impossible to determine from a “margin/uncertainty” ratio whether the underlying margins are large or small. Generally, large margins are preferable to small margins but insights into whether the margins underlying a “margin/uncertainty” ratio are large or small are not directly obtainable from this ratio.

The ambiguity of a “margin/uncertainty” ratio can be illustrated with a simple plot involving the ratio

$$k = m_b / (m_b - m_l), \quad (4.48)$$

where m_b is the best estimate for a margin (e.g., the mean or median of the epistemic uncertainty distribution for the margin under consideration), m_l is the lower estimate for a margin (e.g., the 0.05 or 0.00 quantile of the epistemic uncertainty distribution for the margin under consideration), and the difference $m_b - m_l$ defines the “uncertainty” in the margin under consideration. Then, as shown in Fig. 4.18, infinitely many pairs (m_b, m_l) of margin estimates result in the same “margin/uncertainty” ratio k . Specifically, each line segment in Fig. 4.18 defines pairs (m_b, m_l) of margin estimates that result in the same

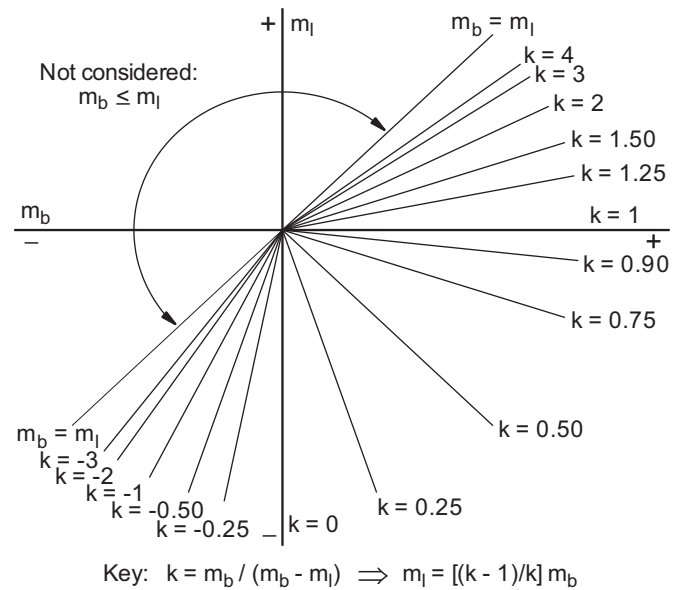


Fig. 4.18. Relationship of best estimate margin m_b and lower estimate margin m_l to “margin/uncertainty” ratio k defined by $k = m_b / (m_b - m_l)$.

“margin/uncertainty” ratio k . As a consequence, knowledge of the “margin/uncertainty” ratio k provides no information on whether the underlying margins involved in the definition of k are large or small.

Some additional properties of the “margin/uncertainty” ratio k are also illustrated by Fig. 4.18. Specifically, (i) $1 \leq k < \infty$ results for $0 \leq m_l < m_b$ with k approaching ∞ as m_l approaches m_b and k approaching 1 as m_l approaches 0, (ii) $0 < k < 1$ results for $m_l < 0 < m_b$ with k approaching 1 as m_l approaches 0 and k approaching 0 as m_l approaches $-\infty$, and (iii) $-\infty < k < 0$ results for $m_l < m_b < 0$ with k approaching 0 as m_l approaches $-\infty$ and k approaching $-\infty$ as m_l approaches m_b . However, as already discussed, knowledge of k provides no information on the underlying margins m_b and m_l . Presumably, the half plane to the left of the line $m_b = m_l$ in Fig. 4.18 is not of interest as the pairs (m_b, m_l) in this region correspond to the best estimate margin m_b being less than the lower margin estimate m_l . Also, the “margin/uncertainty” ratio k is not defined for points on the straight line $m_b = m_l$ as this situation involves an undefined division by $m_b - m_l = 0$.

Significant reservations about the use of “uncertainty/margin” ratios are also expressed in the NAS/NRC report on QMU (e.g., Finding 1–4, p. 25, Ref. [77]).

5. QMU with aleatory and epistemic uncertainty: characterization with probability

The use of probability to represent epistemic uncertainty in analyses that involve only epistemic uncertainty is discussed and illustrated in Sections 3.3, 3.4 and 4. Specifically, the formal discussion in Section 3.3 involves a generic real-valued quantity

$$y(t|\mathbf{a}, \mathbf{e}_M) = f(t|\mathbf{a}, \mathbf{e}_M) \quad (5.1)$$

conditional on a specific realization \mathbf{a} of aleatory uncertainty. The vector \mathbf{e}_M contains epistemically uncertain analysis inputs, with the uncertainty in these inputs characterized by a probability space $(\mathcal{E}_M, \mathbb{E}_M, p_{EM})$.

As discussed in Section 3.5, an increase in complexity is to include the aleatory uncertainty associated with \mathbf{a} in the analysis. Then, in addition to the probability space $(\mathcal{E}_M, \mathbb{E}_M, p_{EM})$ that characterizes the epistemic uncertainty associated with \mathbf{e}_M , there is also a probability space $(\mathcal{A}, \mathbb{A}, p_A)$ that characterizes the aleatory uncertainty associated with \mathbf{a} . Further, there can be, and often is, epistemic uncertainty with respect to a vector \mathbf{e}_A of quantities used in the definition of the probability space $(\mathcal{A}, \mathbb{A}, p_A)$. As a result, there is also a probability space $(\mathcal{E}_A, \mathbb{E}_A, p_{EA})$ that characterizes the epistemic uncertainty associated with \mathbf{e}_A . The vector $\mathbf{e} = [\mathbf{e}_A, \mathbf{e}_M]$ then contains the epistemically uncertain inputs to the analysis, with the uncertainty in \mathbf{e} characterized by a probability space $(\mathcal{E}, \mathbb{E}, p_E)$ that derives from the probability spaces $(\mathcal{E}_A, \mathbb{E}_A, p_{EA})$ and $(\mathcal{E}_M, \mathbb{E}_M, p_{EM})$. Conceptually, the resultant analysis involves the three basic analysis components discussed in Section 3.2: (i) EN1, a probabilistic characterization of aleatory uncertainty (i.e., a probability space $(\mathcal{A}, \mathbb{A}, p_A)$ that characterizes the aleatory uncertainty associated with the elements of \mathbf{a}), (ii) EN2, a model that predicts system behavior (i.e., a function $f(t|\mathbf{a}, \mathbf{e}_M)$), and (iii) EN3, a probabilistic characterization of epistemic uncertainty (i.e., a probability space $(\mathcal{E}, \mathbb{E}, p_E)$ that characterizes the epistemic uncertainty associated with the elements of $\mathbf{e} = [\mathbf{e}_A, \mathbf{e}_M]$).

The results of analyses involving aleatory and epistemic uncertainty are usually summarized with CDFs and CCDFs that display the effects of aleatory uncertainty conditional on specific realizations of epistemic uncertainty and also with various quantities derived from such CDFs and CCDFs (e.g., quantiles and expected values). In turn, margins can be defined in a variety

of ways for CDFs, CCDFs and associated derived quantities, and the presence of epistemic uncertainty results in a corresponding epistemic uncertainty in the resulting margins.

This section uses the function $A(t|\mathbf{a}, \mathbf{e}_M)$ introduced in Section 3.6 to illustrate two ways in which QMU analyses could arise and be carried out in the context of analyses that involve a generic result $y(t|\mathbf{a}, \mathbf{e}_M)$ of the form indicated in Eqs. (3.24) and (5.1). Further,

$$\mathbf{e} = [\mathbf{e}_A, \mathbf{e}_M] = [e_1, e_2, e_3, e_4, e_5] = [\lambda, a, m, b, r], \quad (5.2)$$

where (i) $\mathbf{e}_A = [\lambda, a, m, b]$ and $\mathbf{e}_M = [r]$ have the properties defined in conjunction with Eq. (3.59) and (ii) the corresponding probability space $(\mathcal{E}, \mathbb{E}, p_E)$ that characterizes the epistemic uncertainty associated with \mathbf{e} is defined in conjunction with Eqs. (3.60)–(3.65).

The time-dependent behavior of $A(t|\mathbf{a}, \mathbf{e}_M) = A(t|\mathbf{a}, r)$ is illustrated in Figs. 3.9 and 3.10, and the CDFs and CCDFs for $A(10|\mathbf{a}, \mathbf{e}_M) = A(10|\mathbf{a}, r)$ that result for different values of \mathbf{e} are illustrated in Figs. 3.11 and 3.12 and are defined by the probabilities $p_A[A(10|\mathbf{a}, r) \leq A|\mathbf{e}_A]$ and $p_A[A < A(10|\mathbf{a}, r)|\mathbf{e}_A]$, respectively. As indicated by the vertical line “|”, the value of $A(t|\mathbf{a}, r)$ is conditional on \mathbf{a} and r . As a result, \mathbf{e}_A does not affect the value of $A(t|\mathbf{a}, r)$ but does affect the distribution of $A(t|\mathbf{a}, r)$ arising from the distribution of possible values for \mathbf{a} . In contrast, probabilities of the form $p_A[A(t|\mathbf{a}, r) \leq A|\mathbf{e}_A]$ and $p_A[A < A(t|\mathbf{a}, r)|\mathbf{e}_A]$ are conditional on \mathbf{e}_A and hence on the probability space $(\mathcal{A}, \mathbb{A}, p_A)$ with associated density function $d_A(\mathbf{a}|\mathbf{e}_A)$.

The examples presented in this section use an LHS

$$\begin{aligned} \mathbf{e}_i &= [\mathbf{e}_{Ai}, \mathbf{e}_{Mi}] \\ &= [e_{i1}, e_{i2}, \dots, e_{i5}] \\ &= [\lambda_i, a_i, m_i, b_i, r_i], \quad i = 1, 2, \dots, nSE = 200, \end{aligned} \quad (5.3)$$

from \mathcal{E} generated in consistency with the distributions that define the probability space $(\mathcal{E}, \mathbb{E}, p_E)$. Further, results conditional on individual sample elements \mathbf{e}_i are generated with a random sample

$$\mathbf{a}_j, \quad j = 1, 2, \dots, nSA = 10,000, \quad (5.4)$$

from \mathcal{A} consistent with the probability space $(\mathcal{A}, \mathbb{A}, p_A)$. As a result of the values associated with $\mathbf{e}_{Ai} = [\lambda_i, a_i, m_i, b_i]$, the sample space $(\mathcal{A}, \mathbb{A}, p_A)$ underlying the generation of the sample in Eq. (5.4) changes for each sample element $\mathbf{e}_i = [\mathbf{e}_{Ai}, \mathbf{e}_{Mi}] = [\mathbf{e}_{Ai}, r_i]$. Evaluation of $A(t|\mathbf{a}_j, r_i)$ and results such as $p_A[A < A(t|\mathbf{a}, r_i)|\mathbf{e}_{Ai}]$ for elements of the preceding samples generates mappings of the form

$$[r_i, A(t|\mathbf{a}_j, r_i)], \quad i = 1, 2, \dots, nSE = 200, \quad j = 1, 2, \dots, nSA = 10,000 \quad (5.5)$$

and

$$\{\mathbf{e}_i, p_A[A < A(t|\mathbf{a}, r_i)|\mathbf{e}_{Ai}]\}, \quad i = 1, 2, \dots, nSE = 200, \quad (5.6)$$

that are used in the generation of the example results presented in this section.

The following topics related to QMU in the presence of aleatory and epistemic uncertainty are considered in this section: epistemic uncertainty in margins associated with a specified bound on a quantile deriving from aleatory uncertainty (Section 5.1), and epistemic uncertainty in margins associated with a specified bound on an expected value deriving from aleatory uncertainty (Section 5.2).

As indicated at the beginning of Section 3.5, the NAS/NRC report on QMU recommends the use of what it describes as the “probability of frequency approach” in QMU analyses (Recommendation 1–7, p. 33, and App. A, Ref. [77]). The examples presented in Sections 5.1 and 5.2 involve what the NAS/NRC report describes as the “probability of frequency approach” (i.e., an analysis that involves an explicit separation of aleatory and epistemic uncertainty).

5.1. Epistemic uncertainty with a specified bound on a quantile

For this example, it is assumed that $p_A[20 < A(10|\mathbf{a}, r)|\mathbf{e}_A]$ is required to be less than a bound (e.g., the possible bounds $p_{b1}=0.05$ and $p_{b2}=0.1$ in Fig. 5.1b). Specifically, the values for $p_A[20 < A(10|\mathbf{a}, r)|\mathbf{e}_A]$ in Fig. 5.1b correspond to the exceedance probabilities associated with the vertical line in Fig. 5.1a, and the corresponding distribution of these probabilities and the associated bounds p_{b1} and p_{b2} are shown in Fig. 5.1b. In particular, the probabilities that $p_A[20 < A(10|\mathbf{a}, r)|\mathbf{e}_A]$ will exceed $p_{b1}=0.05$ and $p_{b2}=0.1$ are 0.055 and 0.025, respectively. The indicated exceedance probabilities of 0.055 and 0.025 derive from epistemic uncertainty and thus characterize degrees of belief that $p_A[20 < A(10|\mathbf{a}, r)|\mathbf{e}_A]$ will exceed p_{b1} and p_{b2} , respectively.

In turn, the margins between $p_A[20 < A(10|\mathbf{a}, r)|\mathbf{e}_A]$ and the bounds p_{bk} , $k=1, 2$, indicated in Fig. 5.1b can be defined in the same manner as the margins in Eq. (4.5). Specifically, the margin $p_{mk}(10|\mathbf{e})$ is defined by

$$p_{mk}(10|\mathbf{e}) = p_{bk} - p_A[20 < A(10|\mathbf{a}, r)|\mathbf{e}_A], \quad (5.7)$$

with $p_{mk}(10|\mathbf{e}) > 0$ indicating that bound p_{bk} is satisfied and $p_{mk}(10|\mathbf{e}) < 0$ indicating that bound p_{bk} is not satisfied. As a result

of $p_A[20 < A(10|\mathbf{a}, r)|\mathbf{e}_A]$ being epistemically uncertain, the corresponding margins $p_{mk}(10|\mathbf{e})$ are also epistemically uncertain and have an uncertainty structure that derives from the corresponding uncertainty structure assumed for \mathbf{e} (Fig. 5.2).

As discussed in conjunction with Eq. (4.6), an alternative presentation involves the use of normalized margins. For the present example, normalized margins are defined by

$$p_{nk}(10|\mathbf{e}) = p_{mk}(10|\mathbf{e})/p_{bk} \quad (5.8)$$

for $k=1, 2$ and express margin as a fraction of the corresponding bounding value (Fig. 5.3).

If desired, the CDFs for margin in Fig. 5.2 can be converted into summary “margin/uncertainty” results as indicated in Eqs. (4.7) and (4.8) by the normalizations

$$p_{m/u}(10) = p_{m,0.5}(10)/[p_{m,0.5}(10) - p_{mq}(10)] \quad (5.9)$$

and

$$\bar{p}_{m/u}(10) = \bar{p}_m(10)/[\bar{p}_m(10) - p_{mq}(10)], \quad (5.10)$$

where $p_{mq}(10)$ is the q quantile (e.g., $q=0.0, 0.05$ or 0.5) for the margin $p_{mk}(10|\mathbf{e})$ corresponding to $p_{m1}(10|\mathbf{e})$ in Fig. 5.2a or $p_{m2}(10|\mathbf{e})$ in Fig. 5.2b and $\bar{p}_m(10)$ is the expected value for

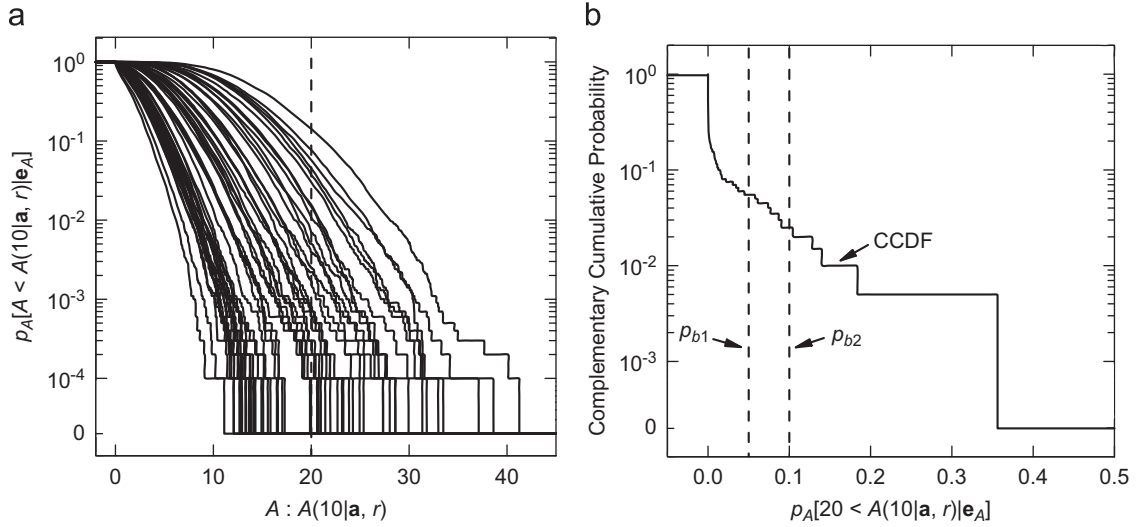


Fig. 5.1. Summary results for $A(10|\mathbf{a}, r)$: (a) CCDFs for $A(10|\mathbf{a}, r)$ obtained with the first 50 elements of the LHS in Eq. (5.3) shown with a vertical line indicating exceedance probabilities $p_A[20 < A(10|\mathbf{a}, r)|\mathbf{e}_A]$, and (b) Estimated CCDF for $p_A[20 < A(10|\mathbf{a}, r)|\mathbf{e}_A]$.

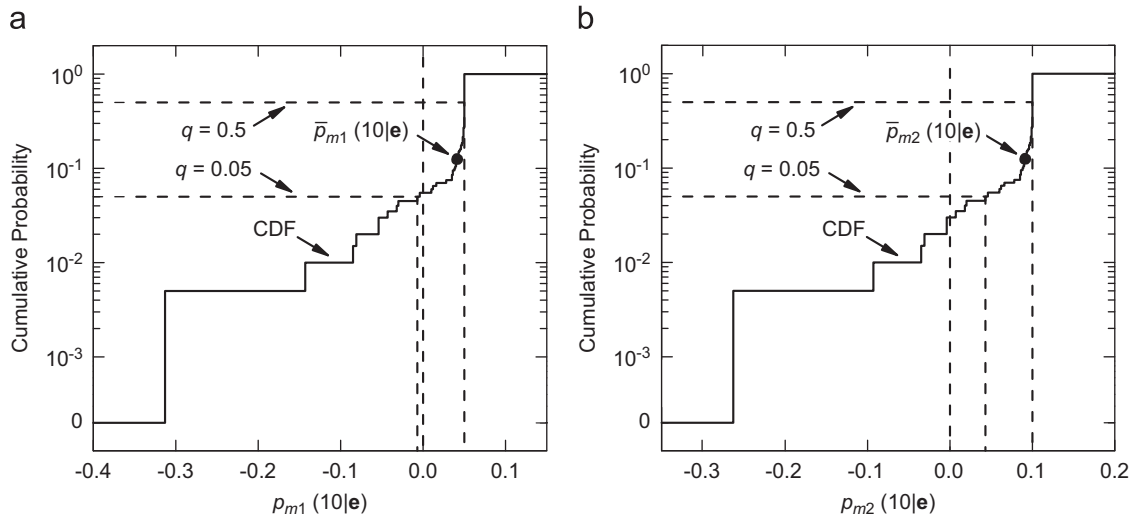


Fig. 5.2. Estimated CDFs for margins $p_{mk}(10|\mathbf{e})$ associated with bounds p_{bk} for $k=1, 2$: (a) $p_{m1}(10|\mathbf{e})$ for $p_{b1}=0.05$, and (b) $p_{m2}(10|\mathbf{e})$ for $p_{b2}=0.1$.

$p_{m1}(10|\mathbf{e})$. In turn,

$$p_{m/u,1}(10) = \begin{cases} 0.050/[0.050 - (-0.007)] = 0.88 & \text{for } q = 0.05 \\ 0.050/[0.050 - (-0.313)] = 0.14 & \text{for } q = 0.00 \end{cases} \quad (5.11)$$

and

$$\bar{p}_{m/u,1}(10) = \begin{cases} 0.041/[0.041 - (-0.007)] = 0.85 & \text{for } q = 0.05 \\ 0.041/[0.041 - (-0.313)] = 0.12 & \text{for } q = 0.00 \end{cases} \quad (5.12)$$

for $p_{m1}(10|\mathbf{e})$ in Fig. 5.2a, and

$$p_{m/u,2}(10) = \begin{cases} 0.100/[0.100 - 0.043] = 1.75 & \text{for } q = 0.05 \\ 0.100/[0.100 - (-0.263)] = 0.28 & \text{for } q = 0.00 \end{cases} \quad (5.13)$$

and

$$\bar{p}_{m/u,2}(10) = \begin{cases} 0.091/[0.091 - 0.043] = 1.90 & \text{for } q = 0.05 \\ 0.091/[0.091 - (-0.263)] = 0.26 & \text{for } q = 0.00 \end{cases} \quad (5.14)$$

for $p_{m1}(10|\mathbf{e})$ in Fig. 5.2b. The normalizations in Eqs. (5.11) and (5.12) are the outcomes of converting all the information in Figs. 5.1 and 5.2a into single numbers. Similarly, the normalizations in Eqs. (5.13) and (5.14) are the outcomes of converting all the information in Figs. 5.1 and 5.2b into single numbers. Because of the presence of both aleatory and epistemic uncertainty, the conversion of analysis results into a single “margin/uncertainty” ratio as illustrated in this section involves a greater loss of information than is the case when only epistemic uncertainty is present (see Section 4.5 for additional discussion).

Additional insights with respect to the uncertainty associated with the margins $p_{m1}(10|\mathbf{e})$ and $p_{m2}(10|\mathbf{e})$ in Fig. 5.2 can be obtained by performing a sensitivity analysis on the values for $p_A[20 < A(10|\mathbf{a}, r)|\mathbf{e}_A]$ summarized in Fig. 5.1 and used in the generation of $p_{m1}(10|\mathbf{e})$

Table 5.1

Stepwise regression analysis to identify uncertain variables affecting exceedance probability $p_A[20 < A(10|\mathbf{a}, r)|\mathbf{e}_A]$.

Step ^a	Variable	SRC	R ²
1	r	−0.36	0.14
2	λ	0.24	0.19

^a Table structure same as in Table 4.1.

and $p_{m2}(10|\mathbf{e})$ as indicated in Eq. (5.7). Because $p_{m1}(10|\mathbf{e})$ and $p_{m2}(10|\mathbf{e})$ are obtained from an affine transformation of $p_A[20 < A(10|\mathbf{a}, r)|\mathbf{e}_A]$, the analysis of $p_A[20 < A(10|\mathbf{a}, r)|\mathbf{e}_A]$ produces effectively the same results as an analysis of $p_{m1}(10|\mathbf{e})$ and $p_{m2}(10|\mathbf{e})$. The only difference is that the effects of individual variables are reversed owing to the subtraction of $p_A[20 < A(10|\mathbf{a}, r)|\mathbf{e}_A]$ in the definition of $p_{m1}(10|\mathbf{e})$ and $p_{m2}(10|\mathbf{e})$ in Eq. (5.7).

An initial sensitivity analysis for $p_A[20 < A(10|\mathbf{a}, r)|\mathbf{e}_A]$ based on stepwise regression analysis is presented in Table 5.1. This analysis is basically a failure as it produces a regression model containing the variables r and λ that has an R^2 value of only 0.19. As a result, this regression model provides little information on the variables that are affecting the uncertainty in $p_A[20 < A(10|\mathbf{a}, r)|\mathbf{e}_A]$ Fig. 5.3.

The natural next step at this point is to examine scatterplots involving $p_A[20 < A(10|\mathbf{a}, r)|\mathbf{e}_A]$ and the elements of \mathbf{e} (Fig. 5.4). A clearer picture of the effects of r and λ on $p_A[20 < A(10|\mathbf{a}, r)|\mathbf{e}_A]$ emerges from an examination of these plots. Specifically, $p_A[20 < A(10|\mathbf{a}, r)|\mathbf{e}_A]$ decreases as r increases and is almost always zero when r exceeds approximately 0.75. Further, zero values for $p_A[20 < A(10|\mathbf{a}, r)|\mathbf{e}_A]$ show a strong tendency to be associated with values for λ that are less than approximately 1.0.

The failure of the regression analysis in Table 5.1 results because the large number of zero values for $p_A[20 < A(10|\mathbf{a}, r)|\mathbf{e}_A]$ results in patterns that the linear regression model in use cannot match. In such situations, there are a number of additional techniques for sampling-based sensitivity analysis that can be tried. The examination of scatterplots as illustrated is certainly the simplest of these techniques. Other possibilities include rank regression, tests for patterns based on gridding, nonparametric regression, tests for patterns based on distance measures, tree-based searches, the two-dimensional Kolmogorov–Smirnov test, and the squared differences of ranks test [53,54,56].

5.2. Epistemic uncertainty with a specified bound on an expected value

For this example, it is assumed that the expected value $E_A[A(10|\mathbf{a}, r)|\mathbf{e}_A]$ summarized in Fig. 3.13 is required to be less than a bound (e.g., the bound $\bar{A}_b = 13$ in Fig. 5.5). At a conceptual level, this example is essentially the same as the example in Section 5.1 as the only difference is that (i) each CCDF in Section 5.1 is being reduced to an exceedance probability $p_A[20 < A(10|\mathbf{a}, r)|\mathbf{e}_A]$ associated with $A(10|\mathbf{a}, r) = 20$ and (ii) each CCDF in the present section is being reduced to an expected value $E_A[A(10|\mathbf{a}, r)|\mathbf{e}_A]$. In both cases, CCDFs summarizing aleatory uncertainty are being reduced to a single

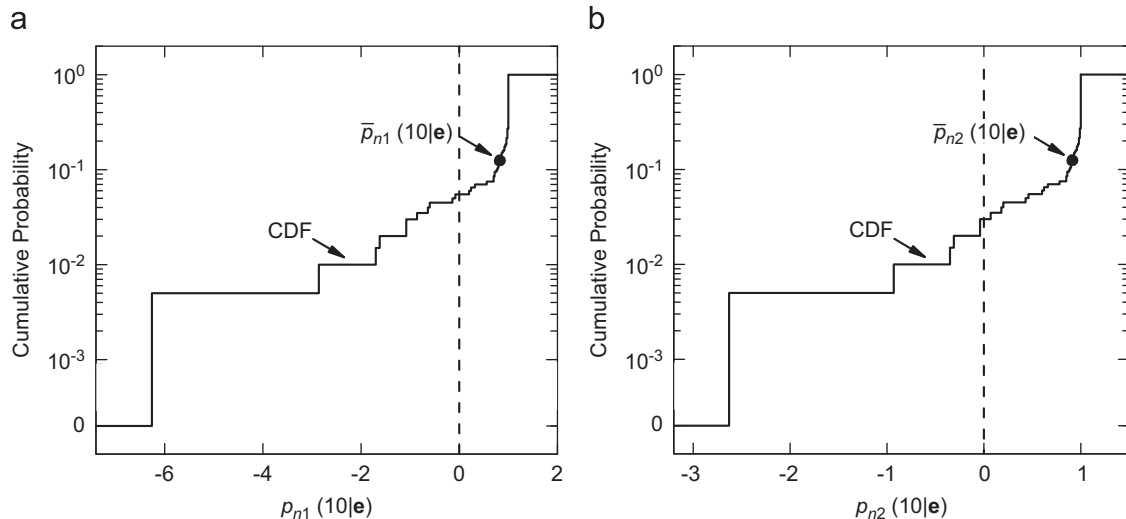


Fig. 5.3. Estimated CDFs for normalized margins $p_{nk}(10|\mathbf{e})$ associated with bounds p_{bk} for $k=1, 2$: (a) $p_{n1}(10|\mathbf{e})$ for $p_{b1}=0.05$, and (b) $p_{n2}(10|\mathbf{e})$ for $p_{b2}=0.1$.

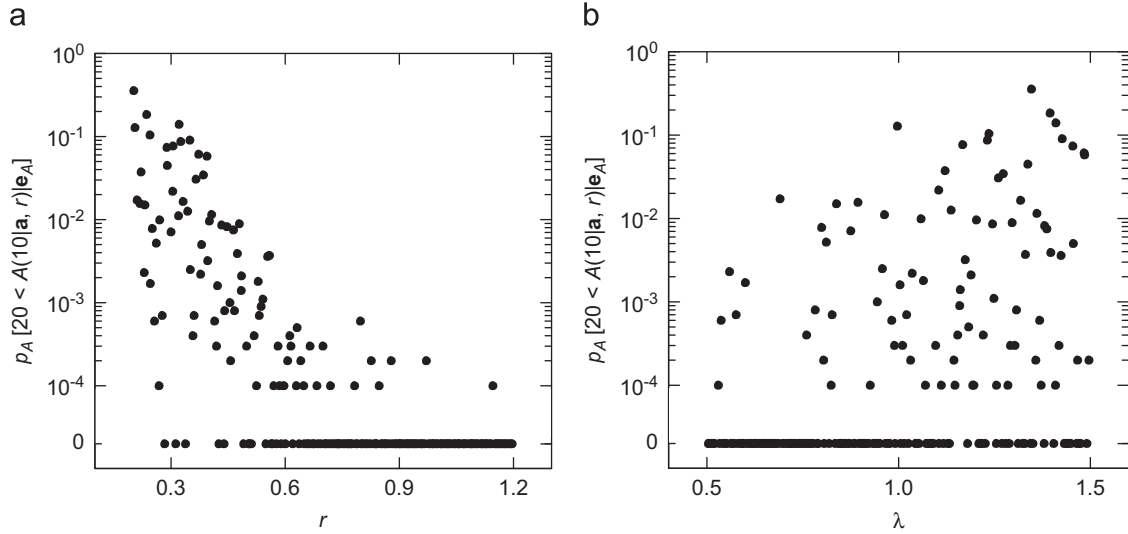


Fig. 5.4. Scatterplots for exceedance probability $p_A[20 < A(10|\mathbf{a}, r)|\mathbf{e}_A]$: (a) $(r_i, p_A[20 < A(10|\mathbf{a}, r_i)|\mathbf{e}_{Ai}])$, $i=1, 2, \dots, nSE=200$, and (b) $(\lambda_i, p_A[20 < A(10|\mathbf{a}, r_i)|\mathbf{e}_{Ai}])$, $i=1, 2, \dots, nSE=200$.

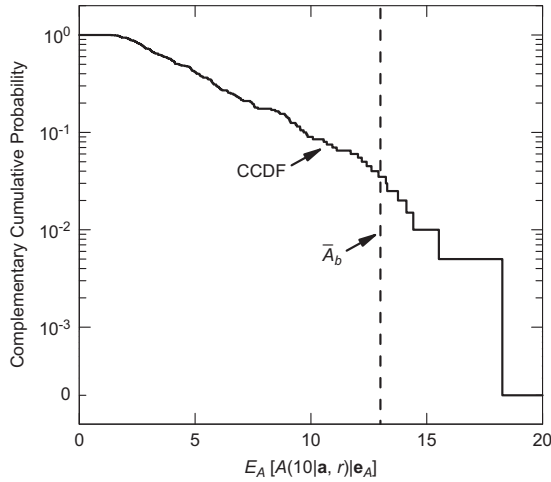


Fig. 5.5. Example bound $\bar{A}_b = 13$ on $E_A[A(10|\mathbf{a}, r)|\mathbf{e}_A]$.

number. However, it is easy to envision that each of these cases could arise in QMU analyses. Specifically, the results in Section 5.1 involve a situation in which a bound is being placed on the likelihood of extreme outcomes arising from aleatory uncertainty, and the results in the present section involve a situation in which a bound is being placed on the expected value of outcomes arising from aleatory uncertainty.

Margins and normalized margins for $E_A[A(10|\mathbf{a}, r)|\mathbf{e}_A]$ are defined by

$$\bar{A}_m(10|\mathbf{e}) = \bar{A}_b - E_A[A(10|\mathbf{a}, r)|\mathbf{e}_A] \quad (5.15)$$

and

$$\bar{A}_n(10|\mathbf{e}) = \bar{A}_m(10|\mathbf{e})/\bar{A}_b, \quad (5.16)$$

respectively, and summarized in Fig. 5.6.

Similarly to the results in Eqs. (5.9) and (5.10), the CDF for margin in Fig. 5.6a can be converted into summary “margin/uncertainty” results by the normalizations

$$\begin{aligned} \bar{A}_{m/u}(10) &= \bar{A}_{m,0.5}(10)/[\bar{A}_{m,0.5}(10) - \bar{A}_{mq}(10)] \\ &= \begin{cases} 8.7/(8.7 - 0.6) = 1.1 & \text{for } q = 0.05 \\ 8.7/8.7 - [(-5.3)] = 0.6 & \text{for } q = 0.00 \end{cases} \end{aligned} \quad (5.17)$$

and

$$\begin{aligned} \bar{A}_{m/u}(10) &= \bar{A}_m(10)/[\bar{A}_m(10) - \bar{A}_{mq}(10)] \\ &= \begin{cases} 7.8/(7.8 - 0.6) = 1.1 & \text{for } q = 0.05 \\ 7.8/[7.8 - (-5.3)] = 0.6 & \text{for } q = 0.00, \end{cases} \end{aligned} \quad (5.18)$$

where $\bar{A}_{mq}(10)$ is the q quantile for the margin $\bar{A}_m(10|\mathbf{e})$ and $\bar{A}_m(10)$ is the expected value for $\bar{A}_m(10|\mathbf{e})$. The preceding normalizations are the outcomes of converting all the information in Figs. 3.11, 3.12, 5.5 and 5.6a into single numbers (see Sections 4.5 for additional discussion).

A sensitivity analysis for $E_A[A(10|\mathbf{a}, r)|\mathbf{e}_A]$ based on stepwise regression analysis is presented in Table 5.2. As indicated, the uncertainty in $E_A[A(10|\mathbf{a}, r)|\mathbf{e}_A]$ is dominated by r and λ , with smaller effects indicated for m and a . Specifically, $E_A[A(10|\mathbf{a}, r)|\mathbf{e}_A]$ tends to decrease as r increases and tends to increase as each of λ , m and a increases. The final regression model has an R^2 value of 0.85, which indicates that most of the uncertainty in $E_A[A(10|\mathbf{a}, r)|\mathbf{e}_A]$ is being captured by the regression model. A regression-based sensitivity analysis for $\bar{A}_m(10|\mathbf{e})$ would produce the same results as shown in Table 5.2 with the exception that the signs on the SRCs would be reversed as a result of the subtraction of $E_A[A(10|\mathbf{a}, r)|\mathbf{e}_A]$ in the definition of $\bar{A}_m(10|\mathbf{e})$ in Eq. (5.15).

For perspective, the scatterplots for the two dominant variables affecting the uncertainty in $E_A[A(10|\mathbf{a}, r)|\mathbf{e}_A]$ identified in the regression analysis in Table 5.2 are shown in Fig. 5.7. Specifically, the negative effect of r and the positive effect of λ are easily seen in the two scatterplots in Fig. 5.7.

6. Summary discussion

As indicated by the name, QMU involves three concepts: quantification, margin and uncertainty. These concepts are discussed in the following sections: Margins (Section 6.1), uncertainty (Section 6.2), and quantification (Section 6.3). Then, the presentation of QMU results is discussed (Section 6.4).

6.1. Margins in QMU

Intuitively, a margin M is a measure of the difference between a requirement R placed on the performance of a system and the predicted performance P of the system, with $M \geq 0$ indicating that the requirement is met and $M < 0$ indicating that the requirement

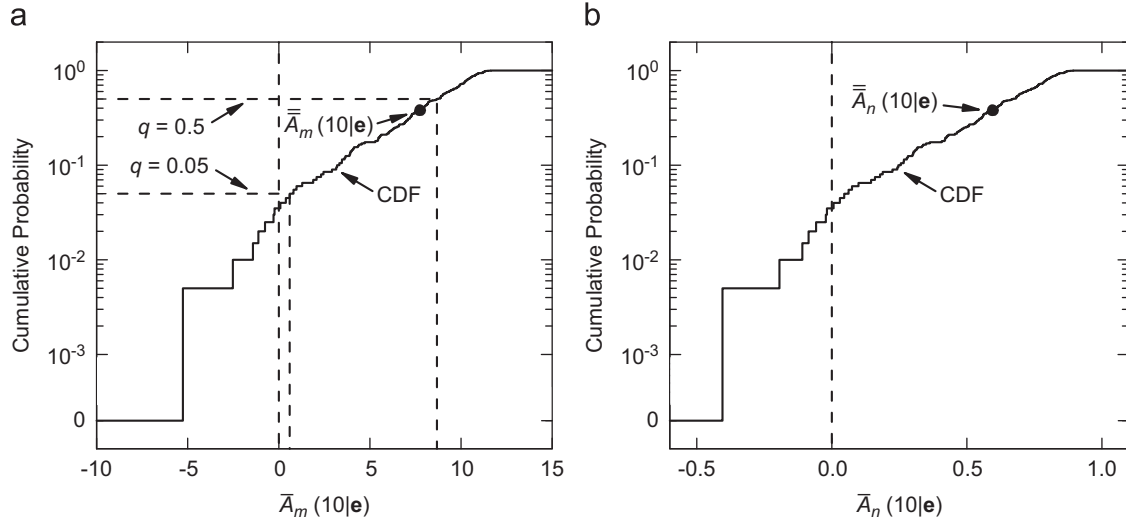


Fig. 5.6. Margins and normalized margins for $E_A[A(10|\mathbf{a}, r)|\mathbf{e}_A]$: (a) $\bar{A}_m(10|\mathbf{e})$, and (b) $\bar{A}_n(10|\mathbf{e})$.

Table 5.2

Stepwise regression analysis to identify uncertain variables affecting $E_A[A(10|\mathbf{a}, r)|\mathbf{e}_A]$.

Step ^a	Variable	SRC	R ²
1	r	−0.76	0.61
2	λ	0.47	0.82
3	m	0.13	0.84
4	a	0.08	0.85

^a Table structure same as in Table 4.1.

is not met. More explicitly, M is a function $M(R, P)$ of R and P with the properties that

$$M(R, P) \geq 0 \Rightarrow \text{compliance of performance } P \text{ with requirement } R \quad (6.1)$$

and

$$M(R, P) < 0 \Rightarrow \text{noncompliance of performance } P \text{ with requirement } R. \quad (6.2)$$

If R and P are single numerical values, then the definition of $M(R, P)$ could be as simple as

$$M(R, P) = R - P \quad (6.3)$$

if P is required to be less than or equal to R and

$$M(R, P) = P - R \quad (6.4)$$

if P is required to be greater than or equal to R . Margins of this type are extensively discussed and illustrated in Sections 4 and 5 and also in Refs. [79,80].

In many real analyses, it is unlikely that R and P will be single numbers. Rather, greater complexity in the definition of R and P is likely to be the case. For example, R might correspond to requirements on several subsystems of a larger system, and P , in turn, would correspond to the performance of these subsystems. As another example, R and P might be functions or vectors of functions. For this reason, the requirement R and performance P are more appropriately represented as the vectors \mathbf{R} and \mathbf{P} . The analyses presented in Ref. [79] are of this type with multiple requirements placed on system performance. Then, M is

a function $M(\mathbf{R}, \mathbf{P})$ with the properties that

$$M(\mathbf{R}, \mathbf{P}) \geq 0 \Rightarrow \text{compliance of performance } \mathbf{P} \text{ with requirement } \mathbf{R} \quad (6.5)$$

and

$$M(\mathbf{R}, \mathbf{P}) < 0 \Rightarrow \text{noncompliance of performance } \mathbf{P} \text{ with requirement } \mathbf{R}. \quad (6.6)$$

In this situation, the evaluation of $M(\mathbf{R}, \mathbf{P})$ involves a more complex calculation than the simple subtractions indicated in Eqs. (6.3) and (6.4).

In practice, it is also possible for $M(\mathbf{R}, \mathbf{P})$ itself to be a vector and thus appropriately denoted by $\mathbf{M}(\mathbf{R}, \mathbf{P})$. For example, if

$$\mathbf{R} = [R_1, R_2, \dots, R_{nR}], \quad (6.7)$$

$$\mathbf{P} = [P_1, P_2, \dots, P_{nP}] \quad (6.8)$$

and

$$M_r(R_r, P_r) = R_r - P_r \quad (6.9)$$

is the margin associated with requirement R_r for $r=1, 2, \dots, nR$, then $\mathbf{M}(\mathbf{R}, \mathbf{P})$ might be defined by

$$\mathbf{M}(\mathbf{R}, \mathbf{P}) = [M_1(R_1, P_1), M_2(R_2, P_2), \dots, M_{nR}(R_{nR}, P_{nP})] \\ = [R_1 - P_1, R_2 - P_2, \dots, R_{nR} - P_{nP}]. \quad (6.10)$$

In a situation of this type, one possibility is to (i) consider each of the margins $M_r(R_r, P_r)$ separately and (ii) define the corresponding real-valued margin $M(\mathbf{R}, \mathbf{P})$ to be the minimum of the values for the individual margins $M_r(R_r, P_r)$. This is the situation illustrated in Sections 4.2–4.4 and in Ref. [80] and also appears to be the intent of the regulatory requirements and associated margins illustrated in Ref. [79]. Another possibility is the use of some type of weighted average to reduce the margins $M_r(R_r, P_r)$ to a single number. In general, the reduction of $\mathbf{M}(\mathbf{R}, \mathbf{P})$ to a single real-valued margin

$$M(\mathbf{R}, \mathbf{P}) = f[\mathbf{M}(\mathbf{R}, \mathbf{P})] \quad (6.11)$$

through the application of a suitable function f is likely to be analysis specific and outside the scope of this discussion.

6.2. Uncertainty in QMU

If \mathbf{R} and \mathbf{P} were known with complete certainty and the function $M(\mathbf{R}, \mathbf{P})$ that defined the margin associated with \mathbf{R} and \mathbf{P} was unambiguously defined, then there is no uncertainty and

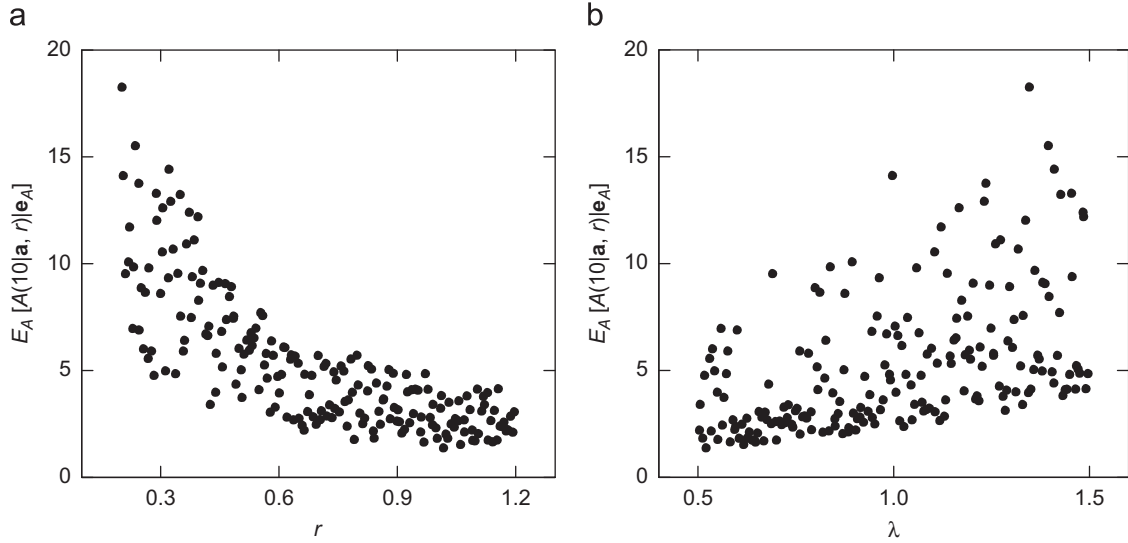


Fig. 5.7. Scatterplots for $E_A[A(10|\mathbf{a}, r)|\mathbf{e}_A]$: (a) $(r_i, E_A[A(10|\mathbf{a}, r_i)|\mathbf{e}_{Ai}])$, $i=1,2, \dots, nSE=200$, and (b) $(\lambda_i, E_A[A(10|\mathbf{a}, r_i)|\mathbf{e}_{Ai}])$, $i=1,2, \dots, nSE=200$.

the margin $M(\mathbf{R}, \mathbf{P})$ is uniquely defined. Unfortunately, this is unlikely to be the case in a real analysis. In the analyses of most systems, there is likely to be significant uncertainties associated with the determination of \mathbf{P} , and uncertainty with respect to the appropriate definition of \mathbf{R} is also possible. However, this discussion assumes there is no uncertainty in the definition of the function $M(\mathbf{R}, \mathbf{P})$ that converts \mathbf{R} and \mathbf{P} into a margin M . The examples in Ref. [79] illustrate analyses of real systems that involve significant uncertainties in the modeling of system performance \mathbf{P} . Further, the notional analyses in Section 4.4 and in Section 3.6 of Ref. [80] involve uncertainty in both \mathbf{R} and \mathbf{P} . The possibility of uncertainty in both \mathbf{R} and \mathbf{P} is recognized by the NNSA in Quote (NNSA-3).

The presence of uncertainty in the determination of $M(\mathbf{R}, \mathbf{P})$ can be acknowledged through the introduction of a vector

$$\mathbf{e}_M = [e_{M1}, e_{M2}, \dots, e_{M, nEM}] \quad (6.12)$$

of uncertain analysis inputs required in the evaluation of $M(\mathbf{R}, \mathbf{P})$. With this introduction, $M(\mathbf{R}, \mathbf{P})$ is appropriately represented by

$$M(\mathbf{R}, \mathbf{P}|\mathbf{e}_M) = \text{margin determined with value for } \mathbf{P} \text{ and possibly the value for } \mathbf{R} \text{ conditional on the values for } e_{M1}, e_{M2}, \dots, e_{M, nEM} \text{ contained in } \mathbf{e}_M. \quad (6.13)$$

More specifically,

$$M(\mathbf{R}, \mathbf{P}|\mathbf{e}_M) = M[\mathbf{R}, \mathbf{P}(\mathbf{e}_M)] \quad (6.14)$$

if only \mathbf{P} depends on \mathbf{e}_M ;

$$M(\mathbf{R}, \mathbf{P}|\mathbf{e}_M) = M[\mathbf{R}(\mathbf{e}_M), \mathbf{P}(\mathbf{e}_M)] \quad (6.15)$$

if \mathbf{R} and \mathbf{P} depend on \mathbf{e}_M ; and

$$M(\mathbf{R}, \mathbf{P}|\mathbf{e}_M) = M[\mathbf{R}(\mathbf{e}_R), \mathbf{P}(\mathbf{e}_P)], \quad \mathbf{e}_M = [\mathbf{e}_R, \mathbf{e}_P], \quad (6.16)$$

if \mathbf{e}_M can be decomposed into a vector \mathbf{e}_R that contains only variables affecting \mathbf{R} and a vector \mathbf{e}_P that contains only variables affecting \mathbf{P} . Section 4.4 and also Section 3.6 of Ref. [80] illustrate analyses in which \mathbf{e}_M can be decomposed into a vector \mathbf{e}_R and a vector \mathbf{e}_P ; specifically, \mathbf{e}_R and \mathbf{e}_P correspond to $[Q_b, \bar{Q}_b]$ and $[L, R, C, E_0, \lambda]$, respectively, in these sections.

The values for the variables contained in \mathbf{e}_M are assumed to be uncertain in the sense that the analysis leading to $M(\mathbf{R}, \mathbf{P})$ has been designed on the assumption that the appropriate value for $M(\mathbf{R}, \mathbf{P})$ will be obtained if the appropriate values for the elements of \mathbf{e}_M are used. Unfortunately, the appropriate value to use for \mathbf{e}_M

is not, and cannot be in most analyses, known with certainty. Rather, there is uncertainty with respect to the appropriate value to use for each element of \mathbf{e}_M . Uncertainty with respect to the value of a fixed, but poorly known, quantity is usually referred to as epistemic uncertainty, which is why \mathbf{e}_M is used as the designator for the vector of uncertain quantities in Eq. (6.12). Alternative descriptors used for epistemic uncertainty include subjective uncertainty, state of knowledge uncertainty, and reducible uncertainty (see Section 2 for additional discussion).

The epistemic uncertainty associated with the elements of \mathbf{e}_M is usually characterized with probability; however, alternative mathematical structures for the characterization of epistemic uncertainty such as possibility theory and evidence theory also exist [80,117]. With the use of probability to characterize epistemic uncertainty, the uncertainty associated with \mathbf{e}_M is defined by a sequence of distributions

$$D_1, D_2, \dots, D_{nEM}, \quad (6.17)$$

where the distribution D_r associated with element e_{Mr} of \mathbf{e}_M provides a mathematical characterization of the available information with respect to where the appropriate value for e_{Mr} is located for use in evaluation of $M(\mathbf{R}, \mathbf{P})$. Correlations and other restrictions involving relationships between individual elements of \mathbf{e}_M may also be present. Distributions of the form indicated in Eq. (6.17) are often developed, at least in part, through an expert review process [100–106]. In turn, the distribution for \mathbf{e}_M that results from the distributions in Eq. (6.17) and any associated restrictions leads to a resultant distribution of values for $M(\mathbf{R}, \mathbf{P}|\mathbf{e}_M)$ that characterizes the (epistemic) uncertainty with respect to the appropriate value for the margin $M(\mathbf{R}, \mathbf{P})$.

The distributions D_1, D_2, \dots, D_{nEM} indicated in Eq. (6.17) are, in essence, defining a probability space $(\mathcal{EM}, \mathbb{EM}, p_{EM})$ for epistemic uncertainty, where \mathcal{EM} is the set of possible values for \mathbf{e}_M , \mathbb{EM} is a suitably restricted set of subsets of \mathcal{EM} , and p_{EM} defines the probabilities for individual sets contained in \mathbb{EM} . In practice, the individual distributions D_r in Eq. (6.17) are usually defined by CDFs or CCDFs that, in effect, define \mathcal{EM} , \mathbb{EM} , p_{EM} and an associated density function $d_{EM}(\mathbf{e}_M)$ defined on \mathcal{EM} . Although \mathcal{EM} , \mathbb{EM} , p_{EM} and $d_{EM}(\mathbf{e}_M)$ are notationally useful and can be formally defined, actual calculations involving the probability space $(\mathcal{EM}, \mathbb{EM}, p_{EM})$ are usually carried out with direct use of the distributions D_1, D_2, \dots, D_{nEM} and any associated restrictions involving these distributions

(e.g., by using random or Latin hypercube sampling to generate values for \mathbf{e}_M consistent with the distributions D_1, D_2, \dots, D_{nEM}).

Once the distributions D_1, D_2, \dots, D_{nEM} in Eq. (6.17) are defined, and hence the probability space $(\mathcal{EM}, \mathbb{EM}, p_{EM})$ is also defined, the uncertainty in the margin $M(\mathbf{R}, \mathbf{P}|\mathbf{e}_M)$ can be formally represented by a CDF or a CCDF. Specifically, the CDF and CCDF for $M(\mathbf{R}, \mathbf{P}|\mathbf{e}_M)$ are formally defined by

$$p_{EM}[M(\mathbf{R}, \mathbf{P}|\mathbf{e}_M) \leq M] = \int_{\mathcal{EM}} \delta_M[M(\mathbf{R}, \mathbf{P}|\mathbf{e}_M)] d_{EM}(\mathbf{e}_M) d_{EM} \quad (6.18)$$

and

$$p_{EM}[M < M(\mathbf{R}, \mathbf{P}|\mathbf{e}_M)] = \int_{\mathcal{EM}} \bar{\delta}_M[M(\mathbf{R}, \mathbf{P}|\mathbf{e}_M)] d_{EM}(\mathbf{e}_M) d_{EM}, \quad (6.19)$$

respectively, where p_{EM} denotes epistemic probability, d_{EM} represents an increment of volume from \mathcal{EM} , and the indicator functions $\delta_M(\sim)$ and $\bar{\delta}_M(\sim)$ are defined by

$$\delta_M[M(\mathbf{R}, \mathbf{P}|\mathbf{e}_M)] = \begin{cases} 1 & \text{if } M(\mathbf{R}, \mathbf{P}|\mathbf{e}_M) \leq M \\ 0 & \text{otherwise} \end{cases}$$

and

$$\bar{\delta}_M[M(\mathbf{R}, \mathbf{P}|\mathbf{e}_M)] = \begin{cases} 1 & \text{if } M(\mathbf{R}, \mathbf{P}|\mathbf{e}_M) > M \\ 0 & \text{otherwise.} \end{cases}$$

In practice, the indicated probabilities are usually approximated by

$$p_{EM}[M(\mathbf{R}, \mathbf{P}|\mathbf{e}_M) \leq M] \cong \sum_{i=1}^{nS} \delta_M[M(\mathbf{R}, \mathbf{P}|\mathbf{e}_{Mi})] / nS \quad (6.20)$$

and

$$p_{EM}[M < M(\mathbf{R}, \mathbf{P}|\mathbf{e}_M)] \cong \sum_{i=1}^{nS} \bar{\delta}_M[M(\mathbf{R}, \mathbf{P}|\mathbf{e}_{Mi})] / nS, \quad (6.21)$$

where \mathbf{e}_{Mi} , $i=1, 2, \dots, nS$, is a random or Latin hypercube sample of size nS generated from \mathcal{EM} in consistency with the distributions D_1, D_2, \dots, D_{nEM} and any associated restrictions. Calculations of this type are discussed in Section 3.3 and illustrated in Sections 3.4 and 4. Related sampling-based computational procedures involving alternatives to probability for the representation of epistemic uncertainty are discussed and illustrated in Ref. [80].

To this point, only the effects of epistemic uncertainty on the margin $M(\mathbf{R}, \mathbf{P})$ have been considered. Specifically, $M(\mathbf{R}, \mathbf{P})$ has been assumed to be a function $M(\mathbf{R}, \mathbf{P}|\mathbf{e}_M)$ of a vector \mathbf{e}_M of epistemically uncertain analysis inputs. However, many analyses involve an additional class of uncertainty known as aleatory uncertainty (Section 2). Specifically, aleatory uncertainty corresponds to some form of random variability associated with the system under study. As examples, such variability might correspond to (i) variability in a population of manufactured devices, (ii) variability in the effects of aging processes, (iii) variability in the conditions associated with a particular class of accidents, or (iv) variability over time in the environmental conditions that a single device or a population of devices is subjected to. Alternative descriptors used for aleatory uncertainty include variability, stochastic uncertainty, and irreducible uncertainty.

Many analyses use probability to represent both aleatory uncertainty and epistemic uncertainty. The mathematics of probability is the same for both uncertainty representations; however, the concepts being represented are very different. The distinction between aleatory uncertainty and epistemic uncertainty is already present in the formal development of probability that began in the late sixteen hundreds. The distinction between aleatory uncertainty and epistemic uncertainty is fundamental to the design, implementation and interpretation of analyses for many complex systems.

If an analysis incorporates the effects of aleatory uncertainty, then underlying the analysis there must be a probability space $(\mathcal{A}, \mathbb{A}, p_A)$ for aleatory uncertainty. Each element \mathbf{a} of \mathcal{A} is a vector

$$\mathbf{a} = [a_1, a_2, \dots] \quad (6.22)$$

that characterizes one possible state of the system. For example, if the failures in a population of devices over a specified time interval $[u, v]$ are under consideration, then \mathbf{a} might have the form

$$\mathbf{a} = [n, t_1, t_2, \dots, t_n], \quad (6.23)$$

where n is the number of failed devices in time interval $[u, v]$ and t_i is the time of failure i with $u \leq t_1 \leq t_2 \leq \dots \leq t_n \leq v$.

A step up in complexity is for \mathbf{a} to have the form

$$\mathbf{a} = [n, t_1, \mathbf{p}_1, t_2, \mathbf{p}_2, \dots, t_n, \mathbf{p}_n], \quad (6.24)$$

where each \mathbf{p}_i is a vector of random properties associated with the failure at time t_i . In an actual analysis for a real system, the definition of \mathbf{a} , and hence the associated probability space $(\mathcal{A}, \mathbb{A}, p_A)$, can be very complicated. Notional analyses involving aleatory uncertainty are presented in Sections 3.6 and 5 and also in Ref. [80]. Further, three analyses for real systems involving aleatory uncertainty are presented in Ref. [79].

Similarly to the probability space $(\mathcal{EM}, \mathbb{EM}, p_{EM})$ for epistemic uncertainty, the probability space $(\mathcal{A}, \mathbb{A}, p_A)$ for aleatory uncertainty is usually defined by specifying conditions that define distributions for the elements of \mathbf{a} . For example, the probability space associated with vectors \mathbf{a} of the form indicated in Eq. (6.23) might be arrived at through the assumption that device failures are consistent with a Poisson process defined by a rate λ (yr^{-1}). Further, the probability space associated with vectors \mathbf{a} of the form indicated in Eq. (6.24) might be arrived at through the assumption again that device failures are consistent with a Poisson process defined by a rate λ and the additional specification of a joint probability distribution for the elements of the property vector \mathbf{p} conditional on the occurrence of a failure at a specific time t .

In practice, the probability space $(\mathcal{A}, \mathbb{A}, p_A)$ for aleatory uncertainty is unlikely to be precisely known. Specifically, many of the quantities employed in the definition of $(\mathcal{A}, \mathbb{A}, p_A)$ are likely to be uncertain in an epistemic sense. For example, the occurrence of a certain type of event might be assumed to follow a Poisson process with a rate λ that is imprecisely known. This lack of knowledge about λ is epistemic uncertainty and leads to uncertainty with respect to the appropriate values for probabilities that derive from λ . The very important point being made here is that there can be, and usually is, epistemic uncertainty present in the characterization of quantities used in the definition of the probability space $(\mathcal{A}, \mathbb{A}, p_A)$ for aleatory uncertainty. For notational purposes, these quantities can be represented by a vector \mathbf{e}_A in analogy to the vectors \mathbf{e}_R and \mathbf{e}_P introduced in conjunction with Eq. (6.16). With the introduction of \mathbf{e}_A , there is now a probability space $(\mathcal{EA}, \mathbb{EA}, p_{EA})$ that characterizes the uncertainty in \mathbf{e}_A and is developed in a manner similar to that previously described for the probability space $(\mathcal{EM}, \mathbb{EM}, p_{EM})$ associated with \mathbf{e}_M . For notational convenience, the effects of \mathbf{e}_A on $(\mathcal{A}, \mathbb{A}, p_A)$ can be indicated by representing the density function associated with $(\mathcal{A}, \mathbb{A}, p_A)$ by $d_A(\mathbf{a}|\mathbf{e}_A)$. In general, \mathbf{e}_A can affect the definition of the sample space \mathcal{A} but, for notational simplicity, this potential effect is typically not indicated.

The vector of epistemically uncertain analysis inputs now has the form

$$\mathbf{e} = [\mathbf{e}_A, \mathbf{e}_R, \mathbf{e}_P] = [\mathbf{e}_A, \mathbf{e}_M], \quad (6.25)$$

and the corresponding probability space $(\mathcal{E}, \mathbb{E}, p_E)$ derives from the properties of the probability spaces $(\mathcal{EA}, \mathbb{EA}, p_{EA})$ and $(\mathcal{EM}, \mathbb{EM}, p_{EM})$.

The consideration of the uncertainty in margins is now returned to. In concept, each possible realization \mathbf{a} of aleatory uncertainty could lead to a different performance of the system under consideration. Notationally, this performance can be represented by a vector

$$\mathbf{P}_A(\mathbf{a}|\mathbf{e}_p) = [P_{A1}(\mathbf{a}|\mathbf{e}_p), P_{A2}(\mathbf{a}|\mathbf{e}_p), \dots, P_{A,nO}(\mathbf{a}|\mathbf{e}_p)], \quad (6.26)$$

where $P_{Aj}(\mathbf{a}|\mathbf{e}_p)$, $j=1,2, \dots, nO$, are outcomes of an analysis given realization \mathbf{a} of aleatory uncertainty (i.e., $\mathbf{a} \in \mathcal{A}$) and conditional on realization \mathbf{e}_p of epistemic uncertainty (i.e., $\mathbf{e} = [\mathbf{e}_A, \mathbf{e}_R, \mathbf{e}_p] \in \mathcal{E}$). As an example from reactor risk assessment, $P_{A1}(\mathbf{a}|\mathbf{e}_p)$ could be the number of early fatalities, $P_{A2}(\mathbf{a}|\mathbf{e}_p)$ could be the number of latent cancer fatalities, and $P_{A3}(\mathbf{a}|\mathbf{e}_p)$ could be the economic cost for a reactor accident with properties defined by the vector \mathbf{a} and conditional on the values for the epistemically uncertain analysis inputs contained in \mathbf{e}_p . In the examples from reactor safety and radioactive waste disposal in Sections 2 and 3 of Ref. [79], nO equals 5 and 2, respectively.

In practice, performance measures used in comparisons with requirements are likely to be based on the distributions for the individual elements $P_{Aj}(\mathbf{a}|\mathbf{e}_p)$ of $\mathbf{P}_A(\mathbf{a}|\mathbf{e}_p)$ that derive from aleatory uncertainty. In this situation, the performance measures used in comparisons with requirements are defined by a functional relationship of the form

$$\mathbf{P}[\mathbf{P}_A(\mathbf{a}|\mathbf{e}_p)|\mathbf{e}_A] = [P_1(\mathbf{e}_A, \mathbf{e}_p), P_2(\mathbf{e}_A, \mathbf{e}_p), \dots, P_{nR}(\mathbf{e}_A, \mathbf{e}_p)], \quad (6.27)$$

where the conditionality on \mathbf{e}_A in $\mathbf{P}[\mathbf{P}_A(\mathbf{a}|\mathbf{e}_p)|\mathbf{e}_A]$ (i.e., “ $|\mathbf{e}_A$ ”) indicates that operations on the elements $P_{Aj}(\mathbf{a}|\mathbf{e}_p)$, $j=1,2, \dots, nO$, of $\mathbf{P}_A(\mathbf{a}|\mathbf{e}_p)$ to obtain the elements $P_j(\mathbf{e}_A, \mathbf{e}_p)$, $j=1,2, \dots, nR$, of $\mathbf{P}[\mathbf{P}_A(\mathbf{a}|\mathbf{e}_p)|\mathbf{e}_A]$ are conditional on the probability space $(\mathcal{A}, \mathbb{A}, p_A)$ associated with \mathbf{e}_A .

Three examples of possible definitions for $P_j(\mathbf{e}_A, \mathbf{e}_p)$ follow. First, $P_j(\mathbf{e}_A, \mathbf{e}_p)$ might be the expected value for $P_{Aj}(\mathbf{a}|\mathbf{e}_p)$ associated with the probability space $(\mathcal{A}, \mathbb{A}, p_A)$ that derives from \mathbf{e}_A . In this case,

$$P_j(\mathbf{e}_A, \mathbf{e}_p) = \int_{\mathcal{A}} P_{Aj}(\mathbf{a}|\mathbf{e}_p) d_A(\mathbf{a}|\mathbf{e}_A) d\mathbf{A}. \quad (6.28)$$

Second, $P_j(\mathbf{e}_A, \mathbf{e}_p)$ might be the q quantile (e.g., $q=0.05, 0.5, 0.95$) of the distribution of $P_{Aj}(\mathbf{a}|\mathbf{e}_p)$ associated with the probability space $(\mathcal{A}, \mathbb{A}, p_A)$ that derives from \mathbf{e}_A . In this case, $P_j(\mathbf{e}_A, \mathbf{e}_p)$ is the value of P such that

$$q = \int_{\mathcal{A}} \delta_P[P_{Aj}(\mathbf{a}|\mathbf{e}_p)] d_A(\mathbf{a}|\mathbf{e}_A) d\mathbf{A}. \quad (6.29)$$

Third, $P_j(\mathbf{e}_A, \mathbf{e}_p)$ might be the CCDF for $P_{Aj}(\mathbf{a}|\mathbf{e}_p)$ that derives from the probability space $(\mathcal{A}, \mathbb{A}, p_A)$ associated with \mathbf{e}_A . In this case, $P_j(\mathbf{e}_A, \mathbf{e}_p)$ is a function defined by the points

$$\left[P, \int_{\mathcal{A}} \bar{\delta}_P[P_{Aj}(\mathbf{a}|\mathbf{e}_p)] d_A(\mathbf{a}|\mathbf{e}_A) d\mathbf{A} \right], \quad (6.30)$$

with problem specific knowledge used to limit the range of P . The expressions in Eqs. (6.28)–(6.30) may seem complicated, but expressions of this type are routinely approximated in risk assessments for complex systems (e.g., see analyses in Ref. [79]). In practice, the definitions of the elements $P_j(\mathbf{e}_A, \mathbf{e}_p)$ of $\mathbf{P}[\mathbf{P}_A(\mathbf{a}|\mathbf{e}_p)|\mathbf{e}_A]$ could be more or less complex than indicated in Eqs. (6.28)–(6.30).

The determination of uncertainty in margins is now returned to. Once the determination $\mathbf{P}[\mathbf{P}_A(\mathbf{a}|\mathbf{e}_p)|\mathbf{e}_A]$ is completed, the determination and representation of the uncertainty in margins is the same as previously discussed in conjunction with Eqs. (6.13)–(6.16). Specifically, margin is defined by a function $M(\mathbf{R}, \mathbf{P}|\mathbf{e})$, which now has the form

$$M(\mathbf{R}, \mathbf{P}|\mathbf{e}) = M[\mathbf{R}(\mathbf{e}_R), \mathbf{P}[\mathbf{P}_A(\mathbf{a}|\mathbf{e}_p)|\mathbf{e}_A]], \mathbf{e} = [\mathbf{e}_A, \mathbf{e}_R, \mathbf{e}_p], \quad (6.31)$$

when stated in complete generality. In turn, the uncertainty in the margin $M(\mathbf{R}, \mathbf{P}|\mathbf{e})$ is defined as indicated in Eqs. (6.18) and (6.19)

and, in practice, is usually approximated as indicated in Eqs. (6.20) and (6.21). Examples of the uncertainty in margin results that derive from aleatory uncertainty are presented in Section 5 and in Ref. [80] for notional analyses and in Ref. [79] for three real analyses involving reactor safety and radioactive waste disposal.

As noted in conjunction with Eqs. (6.7)–(6.11), the meaning and analysis of margin is more complex when $M(\mathbf{R}, \mathbf{P}|\mathbf{e})$ is a vector rather than a scalar. Also, it is anticipated that \mathbf{e}_R will not be present in most analyses.

6.3. Quantification in QMU

Quantification in the context of QMU is now considered. Such quantification has two distinct and important parts. The first part is the definition of the mathematical components that underlie QMU in a particular analysis. The second part is the actual performance of the necessary calculations with these components to obtain a numerical representation for the uncertainty associated with the margin or margins of interest. Two cases are considered: (i) Analyses involving only epistemic uncertainty, and (ii) Analyses involving both aleatory and epistemic uncertainty.

Case 1: The case involving only epistemic uncertainty is considered first. For full generality, the vectors \mathbf{e}_R and \mathbf{e}_p of epistemically uncertain quantities are assumed to be present in the analysis under consideration, although this may not be the case for a specific analysis. In particular, \mathbf{e}_R is likely to be absent from many analyses, with the result that requirements placed on the system would be characterized by a single vector \mathbf{R} rather than by a vector function $\mathbf{R}(\mathbf{e}_R)$.

For this case, the first part of the quantification process entails the definition (i.e., mathematical characterization) of four analysis components: (i) a function $\mathbf{R}(\mathbf{e}_R)$ that defines the requirements that are to be met conditional on realization \mathbf{e}_R of epistemic uncertainty, (ii) a function $\mathbf{P}(\mathbf{e}_p)$ that defines system performance conditional on realization \mathbf{e}_p of epistemic uncertainty, (iii) a probability space $(\mathcal{EM}, \mathbb{EM}, p_{EM})$ that characterizes the epistemic uncertainty associated with $\mathbf{e}_M = [\mathbf{e}_R, \mathbf{e}_p]$, and (iv) a function $M(\mathbf{R}, \mathbf{P}|\mathbf{e}_M) = M[\mathbf{R}(\mathbf{e}_R), \mathbf{P}(\mathbf{e}_p)]$ that defines the margin associated with $\mathbf{R}(\mathbf{e}_R)$ and $\mathbf{P}(\mathbf{e}_p)$. In many analyses, $\mathbf{R}(\mathbf{e}_R)$ and $\mathbf{P}(\mathbf{e}_p)$ may be one dimensional (i.e., scalars); $(\mathcal{EM}, \mathbb{EM}, p_{EM})$ will probably be defined by specifying distributions for the individual elements of \mathbf{e}_M ; and $\mathbf{P}(\mathbf{e}_p)$ is likely to be a complex mathematical structure (e.g., a system of nonlinear partial differential equations) that requires a sophisticated computer program for evaluation. If the preceding quantities are not clearly defined, then the analysis is inadequately documented and, as a consequence, it is difficult to know what any QMU results obtained from the analysis really mean.

The second part of quantification in this case involves carrying out the calculations required to obtain an approximation to the distribution of $M[\mathbf{R}(\mathbf{e}_R), \mathbf{P}(\mathbf{e}_p)]$ that results from the epistemic uncertainty associated with $\mathbf{e}_M = [\mathbf{e}_R, \mathbf{e}_p]$ and characterized by the probability space $(\mathcal{EM}, \mathbb{EM}, p_{EM})$. For most analyses, it is anticipated that a sampling-based approach of the form indicated in conjunction with Eqs. (6.18)–(6.21) will be used to numerically approximate the distribution that characterizes the uncertainty in the margin $M(\mathbf{R}, \mathbf{P}|\mathbf{e}_M) = M[\mathbf{R}(\mathbf{e}_R), \mathbf{P}(\mathbf{e}_p)]$. The major computational cost in this quantification will most likely be the numerical evaluation of $\mathbf{P}(\mathbf{e}_p)$ in the sums indicated in Eqs. (6.20) and (6.21) as the evaluations of $\mathbf{R}(\mathbf{e}_{Ri})$ and $M[\mathbf{R}(\mathbf{e}_{Ri}), \mathbf{P}(\mathbf{e}_{pi})]$ are unlikely to be numerically demanding. However, it is important to recognize that human cost rather than computational cost will dominate the cost of most.

Case 2: The case involving both aleatory uncertainty and epistemic uncertainty is now considered. For full generality, the vectors \mathbf{e}_A , \mathbf{e}_R ,

and \mathbf{e}_p of epistemically uncertain quantities are assumed to be present in the analysis under consideration, although this may not be the situation for a specific analysis. As for Case 1, \mathbf{e}_R is likely to be absent from many analyses, with the result that the requirements placed on the system would be characterized by a single vector \mathbf{R} rather than by a vector function $\mathbf{R}(\mathbf{e}_R)$.

For this case, the first part of the quantification process entails the definition (i.e., mathematical characterization) of six analysis components: (i) a function $\mathbf{R}(\mathbf{e}_R)$ that defines the requirements that are to be met conditional on realization \mathbf{e}_R of epistemic uncertainty, (ii) a function $\mathbf{P}_A(\mathbf{a}|\mathbf{e}_p)$ that defines system performance given realization \mathbf{a} of aleatory uncertainty and conditional on realization \mathbf{e}_p of epistemic uncertainty (see Eq. (6.26)), (iii) a probability space $(\mathcal{A}, \mathbb{A}, p_A)$ that characterizes aleatory uncertainty conditional on realization \mathbf{e}_A of epistemic uncertainty (see Eqs. (6.22)–(6.24)), (iv) a probability space $(\mathcal{E}, \mathbb{E}, p_E)$ that characterizes the epistemic uncertainty associated with $\mathbf{e}=[\mathbf{e}_A, \mathbf{e}_R, \mathbf{e}_p]$ (see Eq. (6.25)), (v) a function $\mathbf{P}[\mathbf{P}_A(\mathbf{a}|\mathbf{e}_p)|\mathbf{e}_A]$ that determines summary measures of system behavior that derive from aleatory uncertainty for comparison with the requirements contained in $\mathbf{R}(\mathbf{e}_R)$ conditional on realizations \mathbf{e}_p and \mathbf{e}_A of epistemic uncertainty (see Eqs. (6.27)–(6.30)), and (vi) a function $M(\mathbf{R}(\mathbf{e}_R), \mathbf{P}[\mathbf{P}_A(\mathbf{a}|\mathbf{e}_p)|\mathbf{e}_A])$ that defines a margin based on requirement $\mathbf{R}(\mathbf{e}_R)$ and performance $\mathbf{P}[\mathbf{P}_A(\mathbf{a}|\mathbf{e}_p)|\mathbf{e}_A]$ conditional on realization $\mathbf{e}=[\mathbf{e}_A, \mathbf{e}_R, \mathbf{e}_p]$ of epistemic uncertainty (see Eq. (6.31)).

The second part of quantification for Case 2 involves carrying out the calculations required to obtain an approximation to the distribution of $M(\mathbf{R}, \mathbf{P}|\mathbf{e})=M(\mathbf{R}(\mathbf{e}_R), \mathbf{P}[\mathbf{P}_A(\mathbf{a}|\mathbf{e}_p)|\mathbf{e}_A])$ that results from the epistemic uncertainty associated with $\mathbf{e}=[\mathbf{e}_A, \mathbf{e}_R, \mathbf{e}_p]$ and characterized by the probability space $(\mathcal{E}, \mathbb{E}, p_E)$. As for Case 1, it is anticipated that most analyses will use a sampling-based approach of the form indicated in conjunction with Eqs. (6.18)–(6.21) to numerically approximate the distribution that characterizes the uncertainty in the margin $M(\mathbf{R}, \mathbf{P}|\mathbf{e})$. Interior to this calculation for a given sample element $\mathbf{e}_i=[\mathbf{e}_{Ai}, \mathbf{e}_{Ri}, \mathbf{e}_{pi}]$ of the form indicated in conjunction with Eqs. (6.20) and (6.21), it is necessary to estimate (i) $\mathbf{R}(\mathbf{e}_{Ri})$, (ii) $\mathbf{P}[\mathbf{P}_A(\mathbf{a}|\mathbf{e}_{pi})|\mathbf{e}_{Ai}]$, and (iii) $M(\mathbf{R}(\mathbf{e}_{Ri}), \mathbf{P}[\mathbf{P}_A(\mathbf{a}|\mathbf{e}_{pi})|\mathbf{e}_{Ai}])$. The estimation or, most likely, exact determination of the quantities in (i) and (iii) is anticipated to be straightforward in most analyses. In contrast, the determination of $\mathbf{P}[\mathbf{P}_A(\mathbf{a}|\mathbf{e}_{pi})|\mathbf{e}_{Ai}]$ could be a major computational challenge. This challenge exists because the determination of $\mathbf{P}[\mathbf{P}_A(\mathbf{a}|\mathbf{e}_{pi})|\mathbf{e}_{Ai}]$ must be preceded by an estimation of the distribution of $\mathbf{P}_A(\mathbf{a}|\mathbf{e}_{pi})$ conditional on the probability space $(\mathcal{A}, \mathbb{A}, p_A)$ for aleatory uncertainty associated with \mathbf{e}_{Ai} . In most large analyses, the major computational complexity and cost is associated with the determination of the distribution of $\mathbf{P}_A(\mathbf{a}|\mathbf{e}_{pi})$ for each pair $[\mathbf{e}_{Ai}, \mathbf{e}_{pi}]$ of sampled values for \mathbf{e}_p and \mathbf{e}_A . In many large analyses (e.g., probabilistic risk assessments for nuclear power plants; see Section 2, Ref. [79]) extensive use is made of fault trees and event trees in this determination. In addition, extensive modeling of physical processes is usually required.

As is the case for the example analyses in Ref. [79], a great deal of careful planning and computational organization is required to successfully carry out an analysis for a complex system that involves a separation of aleatory and epistemic uncertainty. However, without this separation, the results of the analysis are likely to provide limited and possibly misleading insights into the potential behavior of the system and extent of our knowledge with respect to this behavior.

6.4. Presentation of QMU results

Excessive simplification in the presentation of QMU results should be avoided. For analyses that involve only epistemic uncertainty, the best presentation format is provided by

cumulative or complementary cumulative summaries of the uncertainty in analysis results of interest (i.e., by CDFs or CCDFs if probability is used to characterize epistemic uncertainty) with a vertical line used to indicate the specified requirement on system performance (e.g., see Fig. 4.1 and, more generally, Fig. 3.2 in Ref. [80]). Specifically, cumulative summaries are appropriate when system performance has a specified lower bound (see Fig. 4.1a and also Fig. 3.2a in Ref. [80]), and complementary cumulative summaries are appropriate when system performance has a specified upper bound (see Fig. 4.1b and also Fig. 3.2b in Ref. [80]). This presentation format clearly shows the actual values for the performance measure of interest, the uncertainty in this measure, the specified bound on this measure, and the implications of uncertainty with respect to compliance with the specified bound.

A less informative presentation is provided by a cumulative summary of the uncertainty in the margin for the system performance measure and associated requirement under consideration (e.g., see Fig. 4.2 and also Fig. 3.3 in Ref. [80]). Cumulative summaries are appropriate for margins because small margins and, in particular, negative margins are undesirable. Margin summaries are less informative than performance summaries because they obscure the actual value of the performance measure and the relationship of this measure to its associated requirement. Of course, given the numerical value of the requirement, it is mathematically possible to convert from margin values to the values for the performance measure. However, this is not as easy as simply directly looking at the summary of the actual values for the performance measure and its associated requirement. If it is desired to show margin results as illustrated in Fig. 4.2 and in Fig. 3.3 in Ref. [80], it is recommended that actual performance results as illustrated in Fig. 4.1 and in Fig. 3.2 in Ref. [80] also be shown as this will help the reader recognize the nature of the performance results that give rise to the presented margins.

When margins arise from complex requirements (e.g., upper and lower bounds on performance over a time interval as illustrated in Section 4.3), the display of the actual performance is more complex than simply showing a cumulative or complementary cumulative summary for a single result. However, some way of showing the actual performance of the system should be sought. For the example system and associated requirements in Section 4.3, this is accomplished by displaying the time-dependent behavior of the system together with the required bounds on this behavior (Fig. 4.9) in addition to cumulative margin results (Fig. 4.10; also Fig. 3.8 in Ref. [80]). In general, the exact form of such displays will be analysis specific.

The statement is often made that the final outcome of a QMU analysis should be a summary measure of the form “margin/uncertainty”. For purposes of illustration, summary measures of this form are extensively presented in Sections 4 and 5 and also in Ref. [79]. However, these “margin/uncertainty” results provide a very poor representation of the outcome of a QMU analysis as too much meaningful information is lost when the results of a complex analysis are reduced to a single number. After all, the fundamental motivation for performing an uncertainty analysis derives from the recognition that it is not possible to use a single number to represent the existing knowledge about the behavior of a system. For example, the “margin/uncertainty” results in Eqs. (4.42) and (4.43) do not adequately capture the more detailed results in Figs. 4.9 and 4.10 that they are derived from and are intended to summarize. This same pattern of lost information with “margin/uncertainty” summaries for QMU analyses is repeated for all examples presented in Sections 4 and 5 and also in Ref. [79]. Bluntly put, “margin/uncertainty” results do not contain enough information to provide a basis for appropriately informed decisions (see Section 4.5 for additional discussion).

For analyses that involve aleatory and epistemic uncertainty, presentations of analysis results should include displays that

clearly show the separate effects of aleatory uncertainty and epistemic uncertainty. As an example, the analyses presented in Sections 5.1 and 4.3 of Ref. [80] involve aleatory and epistemic uncertainty, with (i) the effects of aleatory uncertainty conditional on specific realizations of epistemic uncertainty shown in Fig. 5.1a, (ii) the effects of epistemic uncertainty on the performance quantity of interest shown in Fig. 5.1b and in Fig. 4.2 of Ref. [80] and (iii) the effects of epistemic uncertainty on margin shown in Fig. 5.2 and in Fig. 4.3 of Ref. [80]. This presentation format provides a more informative transfer of information than the “margin/uncertainty” results shown in Eqs. (5.11)–(5.14) and intended to summarize the information contained in Fig. 5.1a and b. For complex analyses involving aleatory and epistemic uncertainty of the form illustrated in Ref. [79], single “margin/uncertainty” summaries simply cannot capture the information provided by the analysis about system behavior and the uncertainty present in our ability to predict this behavior.

In addition to uncertainty results, a QMU analysis should also present sensitivity analysis results [56]. Such results play a fundamental role in analyses of complex systems by providing (i) insights into system behavior, (ii) guidance on how to invest resources to reduce uncertainty in the assessment of system behavior, and (iii) a powerful tool for analysis verification. An uncertainty analysis without an associated sensitivity analysis is incomplete.

A fundamental part of the presentation of any QMU analysis should be quality documentation. Unfortunately, many large analyses are not well documented. This is probably due in part to a tendency to underestimate the time and resources required to produce quality documentation for a large analysis. The reality is that it can never be expected that everyone will agree with the manner in which a large analysis is conducted and consequently with the results of that analysis. However, everyone should be able to know exactly what was assumed and done in the analysis. This necessary knowledge can only result through quality documentation.

Acknowledgments

Work performed at Sandia National Laboratories (SNL), which is a multiprogram laboratory operated by Sandia Corporation, a Lockheed Martin Company, for the U.S. Department of Energy's National Nuclear Security Administration under Contract no. DE-AC04-94AL85000. The United States Government retains and the publisher, by accepting this article for publication, acknowledges that the United States Government retains a non-exclusive, paid-up, irrevocable, world-wide license to publish or reproduce the published form of this article, or allow others to do so, for United States Government purposes. Review provided by L.P. Swiler and T.G. Trucano at SNL and by K. Sentz at Los Alamos National Laboratory. Technical support on graphics provided by J.D. Johnson at ProStat. Editorial support provided by F. Puffer and J. Ripple of Tech Reps, a division of Ktech Corporation. This presentation is an independent product of the author and does not necessarily reflect views held by either SNL or the U.S. Department of Energy.

References

- [1] Goodwin BT, Juzaitis RJ. National certification methodology for the nuclear weapon stockpile. Draft working paper; 2003.
- [2] Sharp DH, Wood-Schultz MM. QMU and nuclear weapons certification: what's under the hood? Los Alamos Science 2003;28:47–53.
- [3] Abeyta H, et al. Report on the friendly reviews of QMU at the NNSA laboratories: Defense Programs Science Council; 2004.
- [4] Sharp DH, Wallstrom TC, Wood-Schultz MM. Physics package confidence: “One” vs. “1.0”. LA-UR-04-0496. Los Alamos, NM: Los Alamos National Laboratory; 2004.
- [5] JASON. Quantifications of margins and uncertainties (QMU). JSR-04-3330. McLean, VA: The Mitre Corporation; 2005.
- [6] U.S. GAO (U.S. Government Accountability Office). Nuclear weapons: NNSA needs to refine and more effectively manage its new approach for assessing and certifying nuclear weapons. GAO-06-261. Washington, DC: U.S. Government Accountability Office; 2006.
- [7] NNSA (National Nuclear Security Administration). Nuclear weapon assessments using quantification of margins and uncertainties methodologies. NNSA Policy Letter: NAP-XX, Draft 5/1/07. Washington, DC: National Nuclear Security Administration; 2007.
- [8] Rechard RP. Historical relationship between performance assessment for radioactive waste disposal and other types of risk assessment. Risk Analysis 1999;19(5):763–807.
- [9] U.S. NRC (U.S. Nuclear Regulatory Commission). Reactor safety study—an assessment of accident risks in U.S. commercial nuclear power plants. WASH-1400 (NUREG-75/014). Washington, DC: U.S. Nuclear Regulatory Commission; 1975.
- [10] U.S. NRC (U.S. Nuclear Regulatory Commission). Severe accident risks: an assessment for five U.S. nuclear power plants. NUREG-1150, vols. 1–3. Washington, DC: U.S. Nuclear Regulatory Commission, Office of Nuclear Regulatory Research, Division of Systems Research; 1990–1991.
- [11] Breeding RJ, Helton JC, Gorham ED, Harper FT. Summary description of the methods used in the probabilistic risk assessments for NUREG-1150. Nuclear Engineering and Design 1992;135(1):1–27.
- [12] Boyack BE, Catton I, Duffey RB, Griffith P, Katsma KR, Lellouche GS, et al. Quantifying reactor safety margins, Part 1: an overview of the code scaling, applicability, and uncertainty evaluation methodology. Nuclear Engineering and Design 1990;119(1):1–15.
- [13] Boyack BE, Catton I, Duffey RB, Griffith P, Katsma KR, Lellouche GS, et al. Quantifying reactor safety margins, Part 2: characterization of important contributors to uncertainty. Nuclear Engineering and Design 1990;119(1):17–31.
- [14] Wulff W, Boyack BE, Catton I, Duffey RB, Griffith P, Katsma KR, et al. Quantifying reactor safety margins, Part 3: assessment and ranging of parameters. Nuclear Engineering and Design 1990;119(1):33–65.
- [15] Lellouche GS, Levy PS, Boyack BE, Catton I, Duffey RB, Griffith P, et al. Quantifying reactor safety margins, Part 4: uncertainty evaluation of LBLOCA analysis based on TRAC-PF1/MOD 1. Nuclear Engineering and Design 1990;119(1):67–95.
- [16] Zuber N, Wilson GE, Boyack BE, Catton I, Duffey RB, Griffith P, et al. Quantifying reactor safety margins, Part 5: evaluation of scale-up capabilities of best estimate codes. Nuclear Engineering and Design 1990;119(1):97–107.
- [17] Catton I, Duffey RB, Shaw RA, Boyack BE, Griffith P, Katsma KR, et al. Quantifying reactor safety margins, Part 6: a physically based method of estimating PWR large break loss of coolant accident PCT. Nuclear Engineering and Design 1990;119(1):109–17.
- [18] Theofanous TG, et al. Discussion on quantifying reactor safety margins. Nuclear Engineering and Design 1992;132:403–47.
- [19] Payne AC Jr. Analysis of the LaSalle Unit 2 nuclear power plant: Risk Methods Integration and Evaluation Program (RMIEP). Summary. NUREG/CR-4832, SAND92-0537. Albuquerque, NM: Sandia National Laboratories; 1992.
- [20] U.S. DOE (U.S. Department of Energy). Title 40 CFR Part 191 compliance certification application for the Waste Isolation Pilot Plant. DOE/CAO-1996-2184, vols. I–XXI. Carlsbad, NM: U.S. Department of Energy, Carlsbad Area Office, Waste Isolation Pilot Plant; 1996.
- [21] Helton JC, Marietta MG, editors. Special issue: the 1996 performance assessment for the Waste Isolation Pilot Plant. Reliability Engineering and System Safety 2000;69(1–3):1–451.
- [22] SNL (Sandia National Laboratories). Total system performance assessment model/analysis for the license application. MDL-WIS-PA-000005 Rev 00, AD 01. Las Vegas, NV: U.S. Department of Energy Office of Civilian Radioactive Waste Management; 2008.
- [23] Lewis HW, Budnitz RJ, Kouts HJC, Loewenstein WB, Rowe WD, von Hippel F, et al. Risk assessment review group report to the U.S. Nuclear Regulatory Commission. NUREG/CR-0400. Washington, DC: U.S. Nuclear Regulatory Commission; 1978.
- [24] Iman RL, Conover WJ, Campbell JE. Risk methodology for geologic disposal of radioactive waste: small sample sensitivity analysis techniques for computer models, with an application to risk assessment. SAND80-0020, NUREG/CR-1397. Albuquerque, NM: Sandia National Laboratories; 1980.
- [25] Iman RL, Helton JC, Campbell JE. Risk methodology for geologic disposal of radioactive waste: sensitivity analysis techniques. SAND78-0912, NUREG/CR-0390. Albuquerque, NM: Sandia National Laboratories; 1978.
- [26] Cranwell RM, Campbell JE, Helton JC, Iman RL, Longsine DE, Ortiz NR, et al. Risk methodology for geologic disposal of radioactive waste: final report. SAND81-2573, NUREG/CR-2452. Albuquerque, NM: Sandia National Laboratories; 1987.
- [27] Sprung JL, Aldrich DC, Alpert DJ, Cunningham MA, Weigand GG. Overview of the MELCOR risk code development program. In: Proceedings of the international meeting on light water reactor severe accident evaluation. Cambridge, MA, August 28–September 1, 1983. Boston, MA: Stone and Webster Engineering Corporation; 1983. p. TS-10.11–11–18.
- [28] Iman RL, Helton JCA. Comparison of uncertainty and sensitivity analysis techniques for computer models. NUREG/CR-3904, SAND84-1461. Albuquerque, NM: Sandia National Laboratories; 1985.
- [29] Iman RL. Uncertainty and sensitivity analysis for computer modeling applications. In: Cruse TA, editor. Reliability technology—1992, The winter

- annual meeting of the American Society of Mechanical Engineers, Anaheim, California, November 8–13, 1992. New York, NY: American Society of Mechanical Engineers, Aerospace Division; 1992. p. 153–68.
- [30] Zio E. Reliability engineering: old problems and new challenges. *Reliability Engineering and System Safety* 2009;94:125–41.
 - [31] Bernstein PL. *Against the gods: the remarkable story of risk*. New York: John Wiley & Sons; 1996.
 - [32] Cacuci DG. *Sensitivity and uncertainty analysis, vol. 1: theory*. Boca Raton, FL: Chapman & Hall/CRC Press; 2003.
 - [33] Turányi T. Sensitivity analysis of complex kinetic systems: tools and applications. *Journal of Mathematical Chemistry* 1990;5(3):203–48.
 - [34] Rabitz H, Kramer M, Dacol D. Sensitivity analysis in chemical kinetics. *Annual Review of Physical Chemistry* 1983;34:419–61.
 - [35] Lewins J, Becker M, editors. *Sensitivity and uncertainty analysis of reactor performance parameters*. New York, NY: Plenum Press; 1982.
 - [36] Frank PM. *Introduction to system sensitivity theory*. New York, NY: Academic Press; 1978.
 - [37] Tomovic R, Vukobratovic M. *General sensitivity theory*. New York, NY: Elsevier; 1972.
 - [38] Myers RH. Response surface methodology—current status and future directions. *Journal of Quality Technology* 1999;31(1):30–44.
 - [39] Andres TH. Sampling methods and sensitivity analysis for large parameter sets. *Journal of Statistical Computation and Simulation* 1997;57(1–4):77–110.
 - [40] Kleijnen JPC. Sensitivity analysis and related analyses: a review of some statistical techniques. *Journal of Statistical Computation and Simulation* 1997;57(1–4):111–42.
 - [41] Kleijnen JPC. Sensitivity analysis of simulation experiments: regression analysis and statistical design. *Mathematics and Computers in Simulation* 1992;34(3–4):297–315.
 - [42] Morton RH. Response surface methodology. *Mathematical Scientist* 1983;8:31–52.
 - [43] Mead R, Pike DJ. A review of response surface methodology from a biometric viewpoint. *Biometrics* 1975;31:803–51.
 - [44] Myers RH. *Response surface methodology*. Boston, MA: Allyn and Bacon; 1971.
 - [45] McKay MD, Beckman RJ, Conover WJ. A comparison of three methods for selecting values of input variables in the analysis of output from a computer code. *Technometrics* 1979;21(2):239–45.
 - [46] Iman RL, Conover WJ. Small sample sensitivity analysis techniques for computer models, with an application to risk assessment. *Communications in Statistics: Theory and Methods* 1980;A9(17):1749–842.
 - [47] Iman RL, Helton JC, Campbell JE. An approach to sensitivity analysis of computer models, Part 1: introduction, input variable selection and preliminary variable assessment. *Journal of Quality Technology* 1981;13(3):174–83.
 - [48] Iman RL, Helton JC, Campbell JE. An approach to sensitivity analysis of computer models, Part 2: ranking of input variables, response surface validation, distribution effect and technique synopsis. *Journal of Quality Technology* 1981;13(4):232–40.
 - [49] Saltelli A, Marivoet J. Non-parametric statistics in sensitivity analysis for model output: a comparison of selected techniques. *Reliability Engineering and System Safety* 1990;28(2):229–53.
 - [50] Saltelli A, Andres TH, Homma T. Sensitivity analysis of model output. An investigation of new techniques. *Computational Statistics and Data Analysis* 1993;15(2):445–60.
 - [51] Blower SM, Dowlatbadi H. Sensitivity and uncertainty analysis of complex models of disease transmission: an HIV model, as an example. *International Statistical Review* 1994;62(2):229–43.
 - [52] Kleijnen JPC, Helton JC. Statistical analyses of scatterplots to identify important factors in large-scale simulations, 1: review and comparison of techniques. *Reliability Engineering and System Safety* 1999;65(2):147–85.
 - [53] Helton JC, Davis FJ. Sampling-based methods. In: Saltelli A, Chan K, Scott EM, editors. *Sensitivity analysis*. New York, NY: Wiley; 2000. p. 101–53.
 - [54] Helton JC, Davis FJ. Illustration of sampling-based methods for uncertainty and sensitivity analysis. *Risk Analysis* 2002;22(3):591–622.
 - [55] Helton JC, Davis FJ. Latin hypercube sampling and the propagation of uncertainty in analyses of complex systems. *Reliability Engineering and System Safety* 2003;81(1):23–69.
 - [56] Helton JC, Johnson JD, Sallaberry CJ, Storlie CB. Survey of sampling-based methods for uncertainty and sensitivity analysis. *Reliability Engineering and System Safety* 2006;91(10–11):1175–209.
 - [57] Li G, Rosenthal C, Rabitz H. High-dimensional model representations. *The Journal of Physical Chemistry* 2001;105(33):7765–77.
 - [58] Rabitz H, Alis OF. General foundations of high-dimensional model representations. *Journal of Mathematical Chemistry* 1999;25(2–3):197–233.
 - [59] Saltelli A, Tarantola S, Chan K. A quantitative model-independent method for global sensitivity analysis of model output. *Technometrics* 1999;41(1):39–56.
 - [60] Sobol' IM. Sensitivity estimates for nonlinear mathematical models. *Mathematical Modeling & Computational Experiment* 1993;1(4):407–14.
 - [61] Cukier RI, Levine HB, Shuler KE. Nonlinear sensitivity analysis of multi-parameter model systems. *Journal of Computational Physics* 1978;26(1):1–42.
 - [62] Iman RL, Helton JC. An investigation of uncertainty and sensitivity analysis techniques for computer models. *Risk Analysis* 1988;8(1):71–90.
 - [63] Ronen Y. *Uncertainty analysis*. Boca Raton, FL: CRC Press, Inc.; 1988.
 - [64] Helton JC. Uncertainty and sensitivity analysis techniques for use in performance assessment for radioactive waste disposal. *Reliability Engineering and System Safety* 1993;42(2–3):327–67.
 - [65] Hamby DM. A review of techniques for parameter sensitivity analysis of environmental models. *Environmental Monitoring and Assessment* 1994;32(2):135–54.
 - [66] Saltelli A, Chan K, Scott EM, editors. *Sensitivity analysis*. New York, NY: Wiley; 2000.
 - [67] Frey HC, Patil SR. Identification and review of sensitivity analysis methods. *Risk Analysis* 2002;22(3):553–78.
 - [68] Ionescu-Bujor M, Cacuci DGA. Comparative review of sensitivity and uncertainty analysis of large-scale systems—I: deterministic methods. *Nuclear Science and Engineering* 2004;147(3):189–2003.
 - [69] Cacuci DG, Ionescu-Bujor MA. Comparative review of sensitivity and uncertainty analysis of large-scale systems—II: statistical methods. *Nuclear Science and Engineering* 2004;147(3):204–17.
 - [70] Saltelli A, Ratto M, Tarantola S, Campolongo F. Sensitivity analysis for chemical models. *Chemical Reviews* 2005;105(7):2811–28.
 - [71] Saltelli A, Ratto M, Andres T, Campolongo F, Cariboni J, Gatelli D, et al. *Global sensitivity analysis: the primer*. New York, NY: Wiley; 2008.
 - [72] Booker JN, Ross T, Hamada M, Reardon R, Dolin R, Faust CL, et al. Engineering index: an engineering/certification metric. *Military Operations Research* 2006;11(2):27–44.
 - [73] Pilch M, Trucano TG, Helton JC. Ideas underlying the quantification of margins and uncertainties (QMU): a white paper. SAND2006-5001. Albuquerque, NM: Sandia National Laboratories; 2006.
 - [74] Diegert K, Klenke S, Novotny G, Paulsen R, Pilch M, Trucano T. Toward a more rigorous application of margins and uncertainties within the nuclear weapons life cycle—a Sandia perspective. SAND2007-6219. Albuquerque, NM: Sandia National Laboratories; 2007.
 - [75] Higdon DM, Anderson-Cook CM, Gattiker JR, Huzurbazar AP, Moore LM, Picard RR, et al. QMU for advanced certification: identifying existing limitations with discussion of solution strategies. LA-UR-08-06887. Los Alamos, NM: Los Alamos National Laboratory; 2008.
 - [76] Wallstrom TC. Quantification of margins and uncertainty: a Bayesian approach. LA-UR-08-4800. Los Alamos, NM: Los Alamos National Laboratory; 2008.
 - [77] NAS/NRC (National Academy of Science/National Research Council). Evaluation of quantification of margins and uncertainties for assessing and certifying the reliability of the nuclear stockpile. Washington, DC: National Academy Press; 2008.
 - [78] Helton JC. Conceptual and computational basis for the quantification of margins and uncertainty. SAND2009-3055. Albuquerque, NM: Sandia National Laboratories; 2009.
 - [79] Helton JC, Johnson JD, Sallaberry CJ. Quantification of margins and uncertainties: example analyses from reactor safety and radioactive waste disposal involving the separation of aleatory and epistemic uncertainty. *Reliability Engineering and System Safety*, this issue.
 - [80] Helton JC, Johnson JD. Quantification of margins and uncertainties: alternative representations of epistemic uncertainty. *Reliability Engineering and System Safety*, this issue.
 - [81] Helton JC. Uncertainty and sensitivity analysis in the presence of stochastic and subjective uncertainty. *Journal of Statistical Computation and Simulation* 1997;57(1–4):3–76.
 - [82] Helton JC, Burmaster DE. Guest editorial: treatment of aleatory and epistemic uncertainty in performance assessments for complex systems. *Reliability Engineering and System Safety* 1996;54(2–3):91–4.
 - [83] Paté-Cornell ME. Uncertainties in risk analysis: six levels of treatment. *Reliability Engineering and System Safety* 1996;54(2–3):95–111.
 - [84] Winkler RL. Uncertainty in probabilistic risk assessment. *Reliability Engineering and System Safety* 1996;54(2–3):127–32.
 - [85] Hofer E. When to separate uncertainties and when not to separate. *Reliability Engineering and System Safety* 1996;54(2–3):113–8.
 - [86] Parry GW, Winter PW. Characterization and evaluation of uncertainty in probabilistic risk analysis. *Nuclear Safety* 1981;22(1):28–42.
 - [87] Helton JC. Probability, conditional probability and complementary cumulative distribution functions in performance assessment for radioactive waste disposal. *Reliability Engineering and System Safety* 1996;54(2–3):145–63.
 - [88] Hoffman FO, Hammonds JS. Propagation of uncertainty in risk assessments: the need to distinguish between uncertainty due to lack of knowledge and uncertainty due to variability. *Risk Analysis* 1994;14(5):707–12.
 - [89] Helton JC. Treatment of uncertainty in performance assessments for complex systems. *Risk Analysis* 1994;14(4):483–511.
 - [90] Apostolakis G. The concept of probability in safety assessments of technological systems. *Science* 1990;250(4986):1359–64.
 - [91] Haan CT. Parametric uncertainty in hydrologic modeling. *Transactions of the ASAE* 1989;32(1):137–46.
 - [92] Kaplan S, Garrick BJ. On the quantitative definition of risk. *Risk Analysis* 1981;1(1):11–27.
 - [93] Der Kiureghian A, Ditlevsen O. Aleatory or epistemic? Does It matter? *Structural Safety* 2009;31:105–12.
 - [94] Hacking I. *The emergence of probability: a philosophical study of early ideas about probability, induction and statistical inference*. London; New York: Cambridge University Press; 1975.
 - [95] Shafer G. Non-additive probabilities in work of Bernoulli and Lambert. *Archive for History of Exact Sciences* 1978;19(4):309–70.

- [96] Feller W. An introduction to probability theory and its applications. 2nd ed. vol. 2. New York, NY: John Wiley & Sons; 1971.
- [97] Ash RB, Doléans-Dade CA. Probability and measure theory. 2nd ed. New York, NY: Harcourt/Academic Press; 2000.
- [98] Helton JC. Mathematical and numerical approaches in performance assessment for radioactive waste disposal: dealing with uncertainty. In: Scott EM, editor. Modelling radioactivity in the environment. New York, NY: Elsevier Science; 2003. p. 353–90.
- [99] Helton JC, Anderson DR, Jow H-N, Marietta MG, Basabilvazo G. Conceptual structure of the 1996 Performance assessment for the Waste Isolation Pilot Plant. Reliability Engineering and System Safety 2000;69(1–3):151–65.
- [100] Hora SC, Iman RL. Expert opinion in risk analysis: the NUREG-1150 methodology. Nuclear Science and Engineering 1989;102(4):323–31.
- [101] Thorne MC, Williams MMR. A review of expert judgement techniques with reference to nuclear safety. Progress in Nuclear Safety 1992;27(2–3):83–254.
- [102] Budnitz RJ, Apostolakis G, Boore DM, Cluff LS, Coppersmith KJ, Cornell CA, et al. Use of technical expert panels: applications to probabilistic seismic hazard analysis. Risk Analysis 1998;18(4):463–9.
- [103] McKay M, Meyer M. Critique of and limitations on the use of expert judgements in accident consequence uncertainty analysis. Radiation Protection Dosimetry 2000;90(3):325–30.
- [104] Ayyub BM. Elicitation of expert opinions for uncertainty and risks. Boca Raton, FL: CRC Press; 2001.
- [105] Cooke RM, Goossens LHJ. Expert judgement elicitation for risk assessment of critical infrastructures. Journal of Risk Research 2004;7(6):643–56.
- [106] Garthwaite PH, Kadane JB, O'Hagan A. Statistical methods for eliciting probability distributions. Journal of the American Statistical Association 2005;100(470):680–700.
- [107] American Institute of Aeronautics and Astronautics. AIAA guide for the verification and validation of computational fluid dynamics simulations. AIAA G-077-1998. Reston, VA: American Institute of Aeronautics and Astronautics; 1998.
- [108] Roache PJ. Verification and validation in computational science and engineering. Albuquerque, NM: Hermosa Publishers; 1998.
- [109] Oberkampf WL, Trucano TG. Verification and validation in computational fluid dynamics. Progress in Aerospace Sciences 2002;38(3):209–72.
- [110] Oberkampf WL, Trucano TG, Hirsch C. Verification, validation, and predictive capability in computational engineering and physics. Applied Mechanics Review 2004;57(5):345–84.
- [111] Roache PJ. Building PDE codes to be verifiable and validatable. Computing in Science & Engineering 2004;6(5):30–8.
- [112] Babuska I, Oden JT. Verification and validation in computational engineering and science: basic concepts. Computer Methods in Applied Mechanics and Engineering 2004;193(36–38):4057–66.
- [113] Trucano TG, Swiler LP, Igusa T, Oberkampf WL, Pilch M. Calibration, validation, and sensitivity analysis: what's what. Reliability Engineering and System Safety 2006;91(10–11):1331–57.
- [114] Storlie CB, Helton JC. Multiple predictor smoothing methods for sensitivity analysis: description of techniques. Reliability Engineering and System Safety 2008;93(1):28–54.
- [115] Storlie CB, Helton JC. Multiple predictor smoothing methods for sensitivity analysis: example results. Reliability Engineering and System Safety 2008;93(1):55–77.
- [116] Storlie CB, Swiler LP, Helton JC, Sallaberry CJ. Implementation and evaluation of nonparametric regression procedures for sensitivity analysis of computationally demanding models. Reliability Engineering and System Safety 2009;94(11):1735–63.
- [117] Helton JC, Johnson JD, Oberkampf WL. An exploration of alternative approaches to the representation of uncertainty in model predictions. Reliability Engineering and System Safety 2004;85(1–3):39–71.